Formation of Secondary $PM_{2.5}$ in the Capital Region Study

Final Report

Prepared for:
Maxwell Mazur
Environmental and Sustainable Resource Development
Main Floor Twin Atria Bldg.
4999-98 Avenue
Edmonton, AB T6B 2X3

Prepared by:
Uarporn Nopmongcol, Jeremiah Johnson, Bart Brashers, DJ Rasmussen, Tejas Shah, Justin Zagunis, Zhen Liu, and Ralph Morris
ENVIRON International Corporation
773 San Marin Drive, Suite 2115
Novato, California, 94998
and
Ted Pollock and William Allan
ENVIRON (EC) Canada Inc.
7070 Mississauga Road, Suite 140
Mississauga, ON, LFN 7G2
www.environcorp.com
P-415-899-0700
F-415-899-0707

March 2015

ENVIRON

CONTENTS

APPENDICES

TABLES

FIGURES

1.0 INTRODUCTION

1.1 Background

Alberta's Capital Region consists of many municipalities that surround and include the City of Edmonton. Air quality issues within the Capital Region are summarized in the Capital Region Air Quality Management Framework for Nitrogen Dioxide (NO_2), Sulphur Dioxide (SO_2), Fine Particulate Matter ($PM_{2.5}$) and Ozone (O_3)[1]. The Clean Air Strategic Alliance Particulate Matter and Ozone Management Framework defines a series of action trigger levels for fine particulate matter and ozone to help assure that the Canada Wide Standards (CWS) are not exceeded. For $PM_{2.5}$, the CWS has a threshold of 30 µg/m^3 to be achieved by 2010 based on the 98th percentile of the 24-hour $PM_{2.5}$ concentrations averaged over three consecutive years. Based on 2008-2010 $PM_{2.5}$ measurements, the Edmonton Central and Edmonton East monitoring sites exceed the Mandatory Plan trigger level (30 µg/m^3) and the Province is required to develop a plan for reducing the $PM_{2.5}$ concentrations to below the CWS threshold. On May 25, 2013 Environment Canada adopted new Canadian Ambient Air Quality Standards[2] that are more stringent than the CWS. The objectives of the new standards for 24-hour $PM_{2.5}$ objectives are to achieve thresholds of 28 and 27 µg/m^3 by 2015 and 2020, respectively.

ENVIRON International Corporation and Stantec (ENVIRON/Stantec) performed the Formation of Secondary $PM_{2.5}$ in the Capital Region during winter months study forAlberta Environmental and Sustainable Resources Development (ESRD). The objective of the study is to develop a Photochemical Grid Model (PGM) modelling database for the Capital Region, which includes Edmonton and surrounding communities, that reproduces the observed winter elevated $PM_{2.5}$ concentrations sufficiently well that it can be a reliable tool for analyzing source contributions to elevated $PM_{2.5}$ concentrations. This is a follow-on study to the Capital Region Particulate Matter Air Modelling Assessment study led by ENVIRON (Phase I) and is based in a large part on the Phase I modelling database and the recommendations in the final report (Nopmongcol et al., 2014).

1.1.1 Phase I Modelling Study

A team led by ENVIRON developed model input files for the Community Multiscale Air Quality (CMAQ) modelling system for the 2010 winter months to address high winter daily particulate matter observations in Capital Region (Nopmongcol et al., 2014). The study involved development of a comprehensive 2010 emission inventory, WRF meteorological modelling, and CMAQ air quality modelling for multiple sensitivity scenarios. Source apportionment modelling was performed for major source sectors.

The PM model performance in the Phase I study exhibited a systematic high PM biases in all species but NO_3 that was underestimated. In particular, sulphate was overestimated and the modeled sulphate to nitrate ratios were much higher than observed. The results of the source apportionment simulations suggested that ccontributions to primary PM including elemental

[1] http://environment.gov.ab.ca/info/library/8593.pdf
[2] http://www.ec.gc.ca/default.asp?lang=En&n=56D4043B-1&news=A4B2C28A-2DFB-4BF4-8777-ADF29B4360BD

and organic carbons (EC and OC) were mainly from non-point primary PM emitters including commercial/residential heating and off-road sources.

Sensitivity tests suggested that under-estimation of nitrate was related to HNO_3-limited not NH_3-limited formation condition. More radicals are needed to aid HNO_3 formation leading to improved nitrate performance. Ozone is one of the important radical sources and higher ozone transported through boundary helped improve the nitrate performance. Another pathway of HNO_3 formation is through heterogeneous N_2O_5 chemistry and the CMAQ parameters for this reaction may need to be revised for Capital Region. The meteorological conditions that occur during the Capital Region winter $PM_{2.5}$ episodes occur outside the range of conditions that the CMAQ heterogeneous N_2O_5 chemistry module was developed for (i.e., much colder and more humid).

Over-estimation of sulfate was dominated by secondary sulfate (conversion of SO_2). Limited vertical diffusion only worsened the sulfate model performance. Removal of fugitive dust emissions helped improve model performance for most species and total $PM_{2.5}$.

1.1.2 This Study (Phase II)

The work in the current study was to be conducted in two Steps:

> Task 1: Revisit the emissions inventory, meteorology and photochemical model for the time period January 1-February 28, 2010.
>
> Task 2: Expand the modelling period to the entire 2010 winter and perform source apportionment modelling for up to six source sectors.

In Step 1, we updated point source emissions, conducted additional WRF simulations, and modified heterogeneous chemistry in CMAQ. We performed several sensitivity tests to determine the optimal modelling configuration by evaluating the results against measurement data. A comparison against the speciated $PM_{2.5}$ data at the McIntyre monitoring site suggested that primary PM (e.g., EC and OC) were over-estimated; while the secondary PM (sulphate and nitrate) were under-estimated. The new WRF simulations offer significant improvement to sulphate predictions due to lower cloud water content. Nitrate performance shows slight improvement but still exhibits under-estimation bias. After discussing with ESRD, we revised the scope of work to focus primarily on the model performance based on the January-February, 2010, period that included the most days with exceedances of the $PM_{2.5}$ CWS (Task 1).

1.2 Overview of Approach

The Capital Region PM Modelling Study (Phase II) used three main models:

- The Sparse Matrix Operator Kernel Emissions (SMOKE) model to generate the hourly gridded speciated emission inputs needed by the PGM.
- The Weather Research Forecast (WRF) meteorological model used to generate the PGM meteorological inputs.
- The Community Multiscale Air Quality (CMAQ) PGM modelling system.

The modelling domains used are the same 36 km southwestern Canada (SWCAN) and northwest U.S., and 4 km North Saskatchewan Region (NSR) modelling domains (see Figure 1-1) as used in the Phase I Modelling Study (Nopmongcol et al., 2014). The 12 km domain is slightly smaller than the Phase I 12 km but covers the entire Alberta Province. A 1.33 km CMAQ modelling domain focused on the Capital Region used in Phase I was not used in this study due to time constraints. These domains use a Lambert Conformal Projection using the projection parameters given in Table 1-1. Note that the WRF meteorological modelling domains were defined slightly larger than the CMAQ/SMOKE modelling domains defined in Table 1-1 and shown in Figure 1-1.

Table 1-1. Definition of the Lambert Conformal Projection (LCP) 36/12/4 km domains used in the CMAQ photochemical and SMOKE emissions modelling of the Capital Region.

LCP Projection Parameters	
Central Longitude Meridian	-121.0 degrees
Latitude Origin	49.0 degrees
1st Standard Parallel	30.0 degrees
2nd Standard Parallel	60.0 degrees
36 km SWCAN Domain	
SW Corner (-828 km, -936 km)	59 x 74
12 km Alberta Domain	
SW Corner (12 km, -12 km)	70 x 110
4 km NSR Domain	
SW Corner (84 km, 168 km)	162 x 123

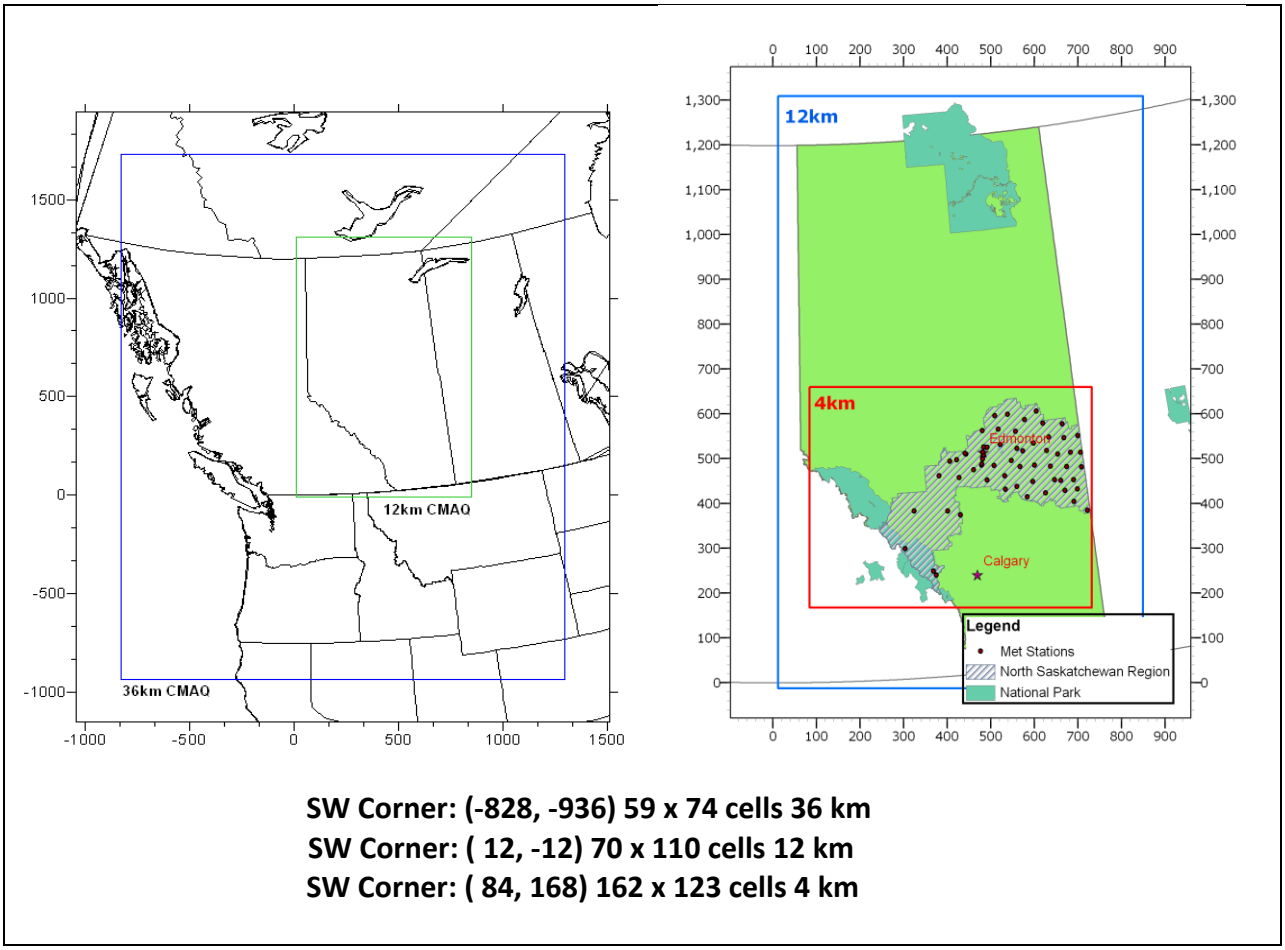

Figure 1-1. 36/12/4 km CMAQ modelling domains.

The overall approach for achieving the project objectives are summarized by task below.

1.2.1 Task 1.a: Base Case Emission Inputs

Base Case Emission Inputs were developed in Phase I by harmonizing multiple emissions inventories used in recent Alberta modelling including the ESRD North Saskatchewan Regional Plan (NSRP), South Saskatchewan Regional Plan (SSRP) and South Athabasca Oil Sands Area (SAOS) studies enhanced with additional data (e.g., Industrial Survey data, new Environmental Assessments and City of Edmonton mobile source emissions). However, emissions for several point sources in the Capital Region (e.g., Imperial Oil Strathcona Refinery and Suncor Energy Edmonton Refinery) were still based on the 2008 ESRD Industrial Survey. We revisited emission rates in the current inventory and compared them to the recent Environment Canada 2010 (EC 2010) inventory. Several emission sensitivity analyses through CMAQ modeling were also conducted. The revised 2010 Base Case emissions include the following improvements:

- Updated emissions from top industrial SO_2 and NOx emitters
- Incorporated on-road mobile NH_3 emissions within the city boundaries from the City of Edmonton

- Revised spatial distribution of residential wood combustion emissions
- Removed emissions from off-road equipment that are not relevant to winter season

The SMOKE emissions modelling system was used to generate the hourly, gridded, speciated CMAQ model-ready emissions inputs for the January-February, 2010 modelling period.

1.2.2 Task 1.b: Meteorological Inputs

The Phase I study applied the Weather Research Forecast (WRF) meteorological model (Version 3.5.1 released September 23, 2013) for meteorological modelling using the NCEP Climate Forecast System Reanalysis (CFSR) as input data. Upper air and surface observational data were used to "nudge" the WRF fields to obtain a better representation of the observed meteorological conditions. The WRF model performance was characterized by too high moisture content from the initial and boundary (IC/BC) gridded reanalysis inputs.

The Phase II study had a main focus on improving the wintertime meteorological conditions that have strong impacts on the high $PM_{2.5}$ ambient levels in the Capital Region, particularly the moisture content. We applied the latest version of WRF (Version 3.6.1) using several alternative WRF physics configurations (e.g., domain revision, objective analysis of IC/BC fields, nudging scheme, planetary boundary layer scheme, and data sources of IC/BC). After inspecting WRF model performance, all of the WRF simulation outputs were converted to CMAQ input format using the MCIP program.

1.2.3 Task 1.c: Photochemical Grid Modelling and Model Performance Evaluation

An initial CMAQ V5.0.2 simulation was performed for high $PM_{2.5}$ episodic periods in January and February, 2010. Based on these results, we performed a series of sensitivity tests designed to better simulate the winter elevated $PM_{2.5}$ concentrations in the Capital Region with particular emphasis on secondary PM model performance. The model performance evaluation procedures follow the recommendations in USEPA's (USEPA, 2007) and Alberta's (Idriss and Spurrell, 2009) air quality modelling guidance.

Our sensitivity tests were limited by the project schedule. Our proposal suggested that Task 1a, b and c be performed using an incremental approach. After consulting with ESRD, we were advised that these tasks be performed concurrently. Several CMAQ sensitivity tests were conducted for the January-February 2010 winter period, focusing on the high episode days.

1.3 Report Organization

This report provides detailed air quality modelling for the Capital Region. Chapter 2 describes winter PM issues in the Capital Region. Chapter 3 describes the base case emissions development. Chapter 4 presents WRF modelling setup and model performance evaluation at the monitoring stations within the Capital Region. Chapter 5 presents CMAQ modelling setup, sensitivity analyses, and model performance evaluation at the monitoring stations in the 4 km modelling domain. Chapter 6 provides the project recommendations with respect to improving model performance evaluation and summarizes the remaining project tasks to be considered in future work.

2.0 REVISITING PM ISSUES IN THE CAPITAL REGION

This chapter provided a brief review of the $PM_{2.5}$ issues based on available observational data in the Capital Region as documented in the Phase I final report (Nopmongcol et al., 2014).

2.1 Measurement Data

Continuous hourly $PM_{2.5}$ measurements have been collected in the Capital Region using the Tapered Element Oscillating Microbalance (TEOM) measurement technology as a well as several other technologies for several years. The hourly $PM_{2.5}$ measurement data for the year 2008-2010 is available from the Alberta Clean Air Strategic Alliance (CASA) data warehouse[3]. One issue associated with measuring $PM_{2.5}$ is that it is defined by the measurement technology used. Each measurement technology has its own artifacts, including evaporation of some volatile compounds, inclusion or exclusion of water mass, the use of blank corrections and other issues. Using different measurement technologies can produce very different $PM_{2.5}$ observations. Over the years, monitoring sites in the Capital Region have been migrating to the TEOM with a filter dynamics measurement system (TEOM FDMS) technology, which has resulted in higher observed $PM_{2.5}$ concentrations in the Capital Region for the more recent years just due to changes in measurement techniques. The TEOM FDMS overcomes some of the semi-volatile $PM_{2.5}$ loss of previous TEOM instruments through a self-referencing system and becomes a preferred technology. Within the Capital Region; there are four monitoring sites that use TEOM FDMS technology and they are all within vicinity of Edmonton City (Table 2-1). Only these four sites are included in our analyses of total $PM_{2.5}$ model performance. Given the loss of semi-volatile $PM_{2.5}$ species of the other $PM_{2.5}$ measurement technologies, their inclusion in the model performance evaluation could lead to misleading results. Figure 2-1 displays the locations of the $PM_{2.5}$ monitoring sites in the Capital Region with Table 2-1 identifying the four sites that use the TEOM FDMS measurement technology.

The McIntyre monitoring site also uses other sample technologies including a Dichot and $PM_{2.5}$ speciation 24-hour average filter based monitoring sites. The speciated $PM_{2.5}$ measurements are summed to obtain Reconstructed Fine Mass (RCFM) total $PM_{2.5}$ concentrations that are compared against the Dichot total $PM_{2.5}$ mass concentrations as part of the quality assurance (QA) process. When the speciated $PM_{2.5}$ RCFM deviates more than 5 percent from the Dichot total $PM_{2.5}$ mass concentration, the speciated $PM_{2.5}$ data are deemed invalid and not used in our modeling analysis. The speciated $PM_{2.5}$ measurements at McIntyre are critically important in understanding $PM_{2.5}$ formation and evaluating $PM_{2.5}$ models in the Capital Region. Evaluating models using just total $PM_{2.5}$ mass (e.g., TEOM FDMS data) is insufficient as compensatory errors could exit that produce good $PM_{2.5}$ model performance for a poorly performing model (e.g., a sulphate overestimation bias compensating for a nitrate underestimation bias).

[3] http://www.casadata.org/

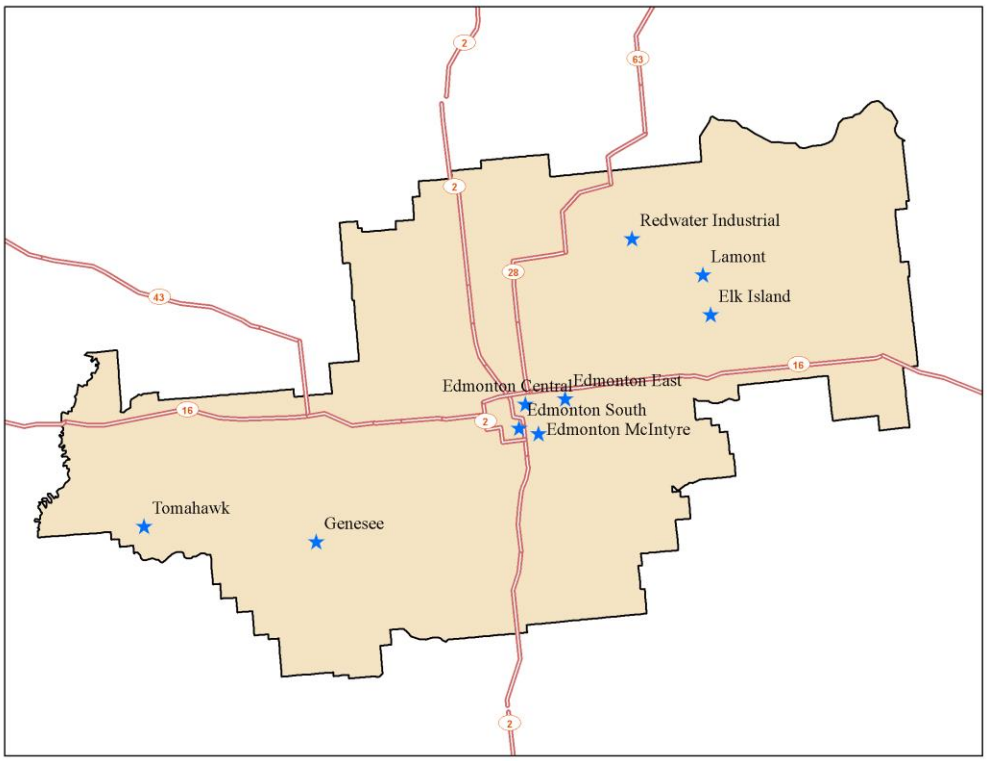

Figure 2-1. Locations of CASA $PM_{2.5}$ monitoring sites within the Capital Region.

Table 2-1. Capital Regional continuous $PM_{2.5}$ TEOM FDMS monitoring sites.

Stn ID	Name	Method
EDMC FDMS	Edmonton Central	TEOM @ 30C with FDMS (self-referencing)
EDME FDMS	Edmonton East	TEOM @ 30C with FDMS (self-referencing)
MCIN FDMS	Edmonton McIntyre	TEOM @ 30C with FDMS (self-referencing)
EDMS FDMS	Edmonton South	TEOM @ 30C with FDMS (self-referencing)

2.2 $PM_{2.5}$ Episodes in the Capital Region

A majority (58% to 72%) of the $PM_{2.5}$ mass on these CWS exceedance days come from nitrate (NO_3), ammonium (NH_4) and sulphate (SO_4) that is mainly secondary in nature (i.e., it is formed in the atmosphere from emissions of gaseous NO_X, NH_3 and SO_2). And of these species, ammonium nitrate [NH_3NO_3] makes up the largest component of the secondary $PM_{2.5}$ on these high $PM_{2.5}$ days contributing 36 to 62 percent of the total $PM_{2.5}$ mass. Note that some Organic Carbon (OC) may also be secondary in nature (i.e., Secondary Organic Aerosol or SOA). However, there is also a lot of primary organic carbon (POC) emitted by many sources (e.g., mobile sources, biomass burning, etc.) and we would expect a vast majority of the OC in Edmonton during the winter to be POC. The elevated $PM_{2.5}$ days in Edmonton from 2008-2010 are associated with very slow to stagnant wind speeds (< 2 m/s). Thus, to reproduce these winter PM events in Edmonton the meteorological modelling will be critically important to

simulate the buildup of ammonium nitrate precursors as well as the thermodynamic conditions that favor ammonium nitrate formation (i.e., cooler and wetter).

Phase I modelling study identified two $PM_{2.5}$ episodes during January-February, 2010, period:

- Episode #1: January 17-21, 2010 whose 3-5 days were CWS exceedance days including one day at McIntyre (Table 2-2).

Table 2-2. Maximum at any monitoring site and McIntyre daily $PM_{2.5}$ concentrations in the 2nd highest ranked 2010 episode for the Capital Region (Episode#1 – January 17 – 21, 2010).

JDay	Year	Month	Day	Max	McIntyre
17	2010	Jan	17	7.5	3.2
18	2010	Jan	18	37.5	
19	2010	Jan	19	57.0	
20	2010	Jan	20	51.0	40.6
21	2010	Jan	21	17.0	

- Episode #2: January 26 through February 4, 2010. This 10-day period covers five CWS exceedance days including one day at the McIntyre speciated PM monitoring site (Table 2-3).

Table 2-3. Maximum at any monitoring site and McIntyre daily $PM_{2.5}$ concentrations in the 1st highest ranked 2010 episode for the Capital Region (Episode#2 – January 26 – February 4, 2010).

JDay	Year	Month	Day	Max	McIntyre
26	2010	Jan	26	9.7	11.5
27	2010	Jan	27	24.6	
28	2010	Jan	28	58.0	
29	2010	Jan	29	74.4	61.4
30	2010	Jan	30	25.3	
31	2010	Jan	31	8.7	
32	2010	Feb	1	30.7	25.4
33	2010	Feb	2	40.5	
34	2010	Feb	3	37.9	
35	2010	Feb	4	24.8	18.9

During these two episodes, $PM_{2.5}$ mass time series correlate well with NO_X measurement (Figure 2-2). NO_X during high PM events was high reaching 400 ppb in Episode#1 and 200 ppb in Episode#2. Ozone shows a reverse trend, mostly lower than 10 ppb and settling around 0-2 ppb on peak days. Excess NO_X and scarce VOC in winter allow NO_X-ozone titration, which usually occurs at night, progresses even during daytime. SO_2 appeared lower than 10 ppb during both episodes and showed no diurnal correlation to $PM_{2.5}$ mass.

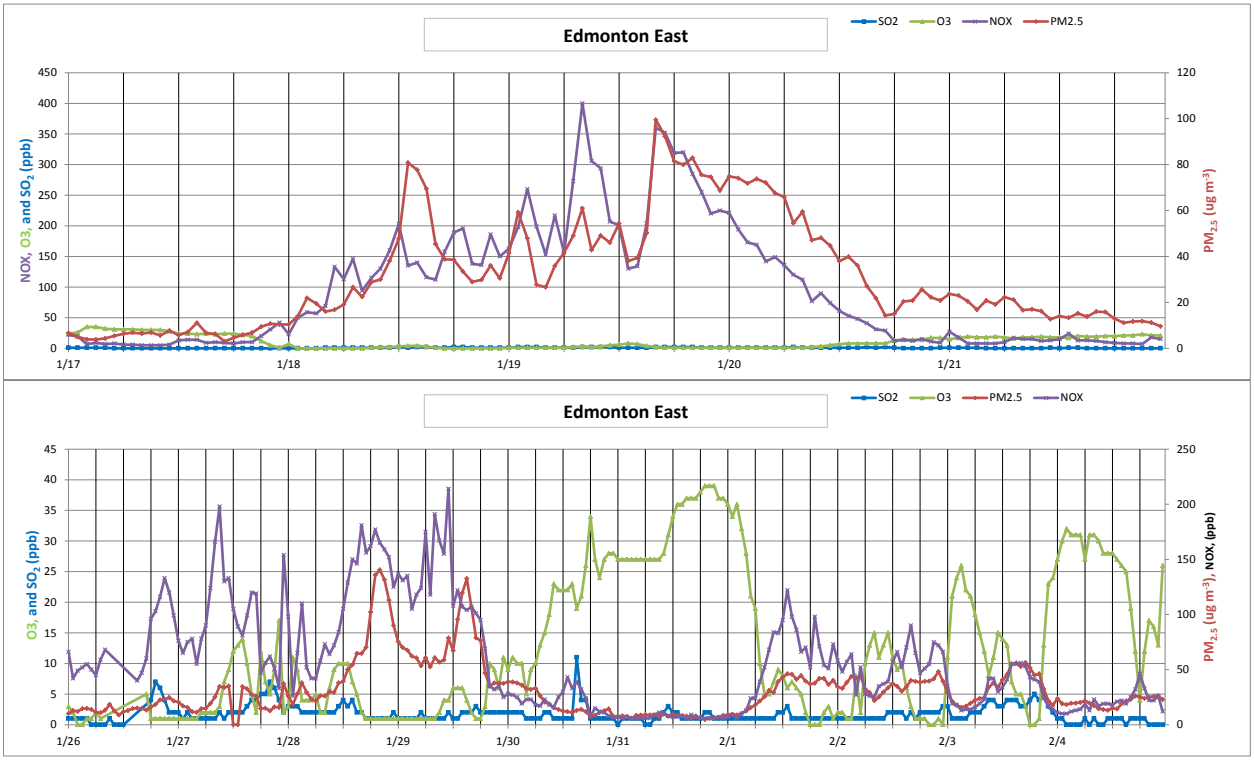

Figure 2-2. Time series plots of $PM_{2.5}$ mass, SO_2, O_3, and NO_X measurements at Edmonton East site during Episode #1 (top) and Episode #2 (bottom).

2.3 Modelling Winter Secondary $PM_{2.5}$

Elevated secondary $PM_{2.5}$ concentrations can also occur in the winter or cooler seasons when the colder temperatures result in aerosol thermodynamics that favors particulate nitrate formation over gaseous nitric acid and there is less competition by sulphate for the ammonia so that particulate ammonium nitrate can form. Because sulphate is a stronger acid than nitrate, ammonia will preferentially bond with sulphate over nitric acid. The formation of elevated particulate ammonium nitrate concentrations in the Capital Regions requires the following chemical processes to occur:

- Conversion of the primary emitted NO_X (NO and NO_2) to gaseous nitric acid (HNO_3);
- Availability of ammonia (NH_3 or other basic compound) to bind with gaseous HNO_3 to form particulate nitrate (NO_3); and
- Meteorological conditions (i.e., cooler and moister) so that the thermodynamic equilibrium favors particulate ammonium nitrate (NO_3NH_4) over gaseous HNO_3 and NH_3.

Thus, keys to simulating the Capital Region high winter $PM_{2.5}$ episodes will be simulating the conversion of NO_X to nitric acid, the availability of ammonia making the ammonia inventory critically important and the meteorological model simulation of winds, temperature and humidity.

2.3.1 Conversion of NO_X to HNO_3

The availability of NO_X emission to form HNO_3 is the first step for simulating elevated winter particulate NO_3 in the Capital Region. There are numerous sources of NO_X emissions within the Capital Region, including mobile sources, industrial sources and even power generating units to the west. Thus, there is ample availability of NO_X to be converted to HNO_3.

There are several pathways to convert NO_X to HNO_3. In this study we used the CB05 chemical mechanism (Yarwood et al., 2005[4]) within the CMAQ PGM model. Most NO_X is emitted as NO (Nitric Oxide) that gets converted to NO_2 (Nitrogen Dioxide), which in turn can form HNO_3 (Nitric Acid) or gets converted to NO_3^- (Nitrate Radical) or NTR (Organic Nitrate, RNO_3) that in turn can form HNO_3. Several of these reactions are as follows:

$NO_2 + OH \rightarrow HNO_3$

$NO_3 + HO_2 \rightarrow HNO_3$

$NTR + OH \rightarrow HNOS$ + other products

The three HNO_3 formation reactions above involve the hydroxyl (OH) or hydroperoxyl (HO_2) radicals that are produced by photochemistry. Photochemistry is the main source of ozone formation that involves VOC and NO_X precursors in the presence of sunlight. During the Capital Region winter $PM_{2.5}$ episodes, sunlight will be less available compared to summer months due to lower solar zenith angle and radical concentrations would be expected to be low and depend on the availability of incoming ozone concentrations.

Another gas-phase HNO_3 formation reaction is the reaction with aldehydes [formaldehyde (FORM) and acetaldehyde (ALD2)]:

$FORM + NO_3^- \rightarrow HNO_3 + HO_2 + CO$

$ALD2 + NO_3^- \rightarrow C2O3 + HNO_3$

One of the primary sources of aldehydes in the Capital Region will be from mobile sources, especially with the cold temperature conditions resulting in the catalysts taking longer to warm up and be more effective at reducing the mobile source VOC emissions. Another source of aldehydes is refineries and petrochemical plants, such as occur to the northeast of Edmonton.

At night, HNO_3 formation occurs through N_2O_5 (Dinitrogen Pentoxide), which will disassociate in the presence of sunlight. N_2O_5 is first formed through a reaction between NO_2 and NO_3^-, and then in the gas-phase forms HNO_3 through reaction with water vapor (H_2O):

$NO_2 + NO_3^- \rightarrow N_2O_5$

$N_2O_5 + H_2O \rightarrow HNO_3$

$N_2O_5 + H_2O + H_2O \rightarrow HNO_3$

[4] http://www.camx.com/publ/pdfs/cb05_final_report_120805.pdf

Thus, the correct simulation of water vapor concentrations by the meteorological model becomes important. If the WRF meteorological fields are too dry, that may inhibit HNO_3 formation.

The availability of NO_3^- radical is a key component in the nighttime HNO_3 formation pathway, as well as the pathway through aldehydes. NO_3^- radical is formed through reactions involving NO_2 and ozone. As we would not expect there to be very much ozone formation in the Capital Region during the winter $PM_{2.5}$ episodes, the simulation of ozone transport into the region and the ability to simulate the observed ozone concentrations is very important in simulating the elevated particulate NO_3 levels in the region.

Another HNO_3 formation pathway in the CMAQ chemistry modules is the heterogeneous reaction probability (Y) of N_2O_5 that is a function of temperature, relative humidity (RH), particle composition and phase state. As described by Davis, Bhave and Foley (2008), the reaction probabilities are used for defining aqueous ammonium sulphate and ammonium nitrate formation. In the Phase I study, a CMAQ sensitivity test increasing Y reaction probability by a factor of 3 has a small effect to nitrate concentrations.

The final HNO_3 formation pathway is the heterogeneous reaction of NO_2 that is a function of surface availability (Kurtenbach et al. (2001):

$$NO_2 \quad \text{-->} \quad 0.5\ HONO + 0.5\ HNO_3 \qquad k = 3.0e\text{-}3\ [min^{-1}] \times Surface/Volume$$

2.3.2 Availability of NH_3 Concentrations to form Particulate NO_3

CMAQ sensitivity tests in the Phase I study suggested that there is very little leftover gaseous HNO_3 that has not been converted to particulate NO_3. The average modeled total ammonia (NH_4+NH_3; 15.2 µg/m^3) is 4.5 µg/m^3higher than the NH_4 (10.7 µg/m^3) indicating that there is left over ammonia concentrations (~6 ppb). NO_3 formation in the CMAQ model during the high PM episodes is nitric acid limited and not ammonia limited.

2.3.3 Equilibrium between Particulate NO_3 and Gaseous HNO_3

As noted above, the WRF simulation of the temperature and absolute humidity conditions during the Capital Region $PM_{2.5}$ episodes will be important for both the gas-phase and heterogeneous-phase particulate nitrate formation pathways, as well as the equilibrium between particulate NO_3 and gaseous HNO_3.

3.0 BASE CASE EMISSIONS INPUT

We revisited emission rates in the current inventory and compared them to the recent Environment Canada 2010 (EC 2010) inventory. This chapter documents various updates to the emissions inventory and modelling system. Summary tables of the final emission inventories are also provided.

3.1 Comparison to EC 2010 Emission Inventory

EC has recently prepared detailed 2010 Canadian Inventory and provided to the US EPA for incorporation in their 2011 modelling database. The EC 2010 inventory introduced several improvements (EC, 2014) that are relevant to modelling winter PM concentrations:

- Use of facility-specific temporal profiles[5]
- Treating off-road emissions related to oil-sands activities as virtual point sources to avoid the need to use province-level spatial surrogates to allocate these emissions in space
- Use of detailed spatial-surrogates for agricultural ammonia
- Application of US EPA's MOVES model for heavy-duty vehicles
- Account for emissions from all other sources not reported to NPRI

Emissions comparison (Table 3-1) suggests that the province-wide NO_X emissions are higher and SO_2 emissions are lower in the 2010 EC inventory compared to the Phase I inventory for Alberta. The 2010 EC has more than twice the VOC emissions compared to the Phase I inventory. Higher VOC emissions in the 2010 EC inventory would likely promote radical availability that facilitates nitrate formation. The discrepancy in VOC emissions is mainly from the industrial point sector (e.g., UOG, refineries, etc.) accounting a total of 229, 029 tonne/year with 46% of the difference from UOG sources that are not reporting to NPRI (i.e., small emitters). These sources are mostly held at 2006 level in the Phase I inventory; whereas they are presented at 2010 level in the 2010 EC inventory. VOC components from UOG sources are mostly paraffins, but are also comprised of more reactive compounds such as olefins. VOC emissions and the component weight profiles from the top three SCCs in the UOG sector are shown in Table 3-2. There are also large discrepancies of VOC emissions from oilsands related sources in the Lower Athabasca Region. Emissions from non-industrial point sources are comparable between the two inventories.

Stantec further reviewed industrial emissions and recommended several updates to the EC 2010 (more information is available in Appendix A). Although the updated EC 2010 inventory was not selected as the preferred emissions inventory in this study, it was used in CMAQ emission sensitivity tests.

[5] Not available in time for this study

Table 3-1. Province-wide emissions comparison between the EC 2010 and Capital Region PM Modeling Study (Phase I) inventory.

Source Category	Inventory	Pollutants [tonne/yr]						
		CO	NH_3	NO_X	PM_{10}	$PM_{2.5}$	SO_2	VOC*
Agriculture	Phase I	0	107,584	0	0	0	0	0
	EC 2010	0	105,055	0	0	0	0	0
AIRCRAFT + RAIL	Phase I	6,055	14	13,265	471	435	200	1,346
	EC 2010	6,284	15	14,555	558	515	443	1,513
Other Area	Phase I	47,919	784	19,823	14,252	6,104	5,410	182,948
	EC 2010	71,212	573	21,381	13,197	5,600	2,623	157,522
OFFROAD	Phase I	303,080	223	109,961	8,655	8,286	407	25,694
	EC 2010	209,647	85	91,855	8,665	8,480	128	23,013
ONROAD	Phase I	636,504	2,701	71,733	2,196	1,543	1,062	35,666
	EC 2010	597,364	2,731	85,348	4,000	3,281	362	43,921
RWC	Phase I	21,197	29	319	3,444	3,432	46	4,085
	EC 2010	20,809	28	312	3,380	3,369	45	4,011
Industrial Point	Phase I	353,667	6,651	479,149	15,614	14,449	394,299	188,527
	EC 2010	450,684	9,232	522,521	39,364	16,137	360,844	448,582
Total	Phase I	371,469	6,651	517,983	16,658	15,493	395,044	219,513
	EC 2010	450,684	9,232	522,521	39,364	16,137	360,844	448,582
% Difference	EC2010-Phasel	-2%	-0.2%	0.4%	51%	6%	-9%	45%

Table 3-2. VOC emissions from UOG sources (top three SCCs).

SCC	Description	Alberta 2010 UOG VOC Emissions *(tonne/yr)*		CB05 weight profiles	
		EC 2010	Phase I		
49000201	Solvent Evap /Waste Solvent Recovery Ops /Storage Tank Vent	99,616	61,918	PAR	66%
				TOL	9%
				OLE	9%
				UNR	8%
				XYL	5%
				TERP	1%
				ETHA	1%
				ALDX	1%
				IOLE	0%
				FORM	0%
31000220	Natural Gas Production /All Equipt Leak Fugitives (Valves, Flanges, Connections, Seals, Drains	83,164	52,590	CH4	61%
				PAR	27%
				ETHA	8%
				UNR	4%
31000123	Crude Oil Production /Well Casing Vents	64,122	38,104	PAR	50%
				CH4	38%
				ETHA	6%
				UNR	6%

3.2 Emission Updates

This section describes specific updates to Phase I emissions inventory.

3.2.1 Industrial Point Sources

Phase I emission inputs were developed by harmonizing multiple emissions inventories used in other Alberta modelling studies (including ESRD SSRP, ESRD NSRP, and ESRD SAOS) with 2008 ESRD Industrial Survey data and updating emissions to 2010 for selected industrial facilities in the Capital Region. However, emissions for several point sources in the Capital Region (e.g., Imperial Oil Strathcona Refinery and Suncor Energy Edmonton Refinery) were still based on the 2008 ESRD Industrial Survey.

The EC 2010 point source inventory consists of emissions reported by facilities based on the National Pollutant Release Inventory (NPRI); whereas the current inventory consists of ESRD Industrial Survey data that are at unit level. We preserved the stack information in the current inventory and scale their emissions to match the 2010 NPRI facility-wide emissions. This update was applied to the top 100 emitting stacks in the Capital Region. Table 3-3 provides a summary of these updates for important CAC point source emissions.

Table 3-3. Summary of 2010 point sources emissions updates based on 2010 NPRI

	CO	NH_3	NO_X	PM_{10}	$PM_{2.5}$	SO_2	VOC
# of facilities updated	53	6	55	51	51	33	47
Phase I point source emissions (tonnes/yr)	21,864	2,458	72,614	4,692	2,374	81,799	1,894
2010 NPRI emissions (tonnes/yr)	23,125	2,409	77,327	4,972	2,336	88,671	3,184
Total emissions changes by NPRI updates to 2010 (tonnes/yr)	1,261	-49	4,712	280	-38	6,872	1,289
% Change	5.77%	-1.98%	6.49%	5.96%	-1.62%	8.40%	68.05%

3.2.2 Adding Ammonia Emissions from CALMOB6

The Phase I study incorporated on-road mobile emissions within the City of Edmonton boundary from the CALMOB6 model (Calibrated MOBILE6) as provided by the City of Edmonton's Transportation Operations division. CALMOB6 is a custom tool for the City of Edmonton that is based on the US EPA's MOBILE6 model. It uses real traffic counts from inside the city along with urban travel forecasting models, and local parameters such as road grade and ambient weather conditions. Previously, CALMOB6 included all criteria pollutants except ammonia. We incorporated the CALMOB6 emissions only in the 1 km domain.

In the Phase II study, the City of Edmonton provided the missing ammonia emissions from CALMOB6. We adopted the same approach used in Phase I to integrate CALMOB6 emissions with the rest of emissions, therefore spatial distributions of ammonia emissions from mobile sources are consistent with other pollutants. The total ammonia emissions from CALMOB6 are 2.2 tonnes per day in January and 2.12 tonnes per day in February. CALMOB6 emissions for all criteria pollutants were incorporated into the 4 km domain in this modelling round.

3.2.3 Exclusion of Emissions from some Off-Road Equipment

CMAQ model performance conducted in the Phase I study suggested over-estimation of primary PM components, such as EC and OC, which are emitted largely from surface combustion sources. Specifically, off-road equipment (for agriculture, lawn and garden, construction and mining) is the main source of EC in the Capital Region. Temporal profiles for these sources were based on US EPA's recommendations for US sources. Some of these profiles may be less appropriate for a colder climate. For example, 5% of the annual off-road emissions related to agricultural and construction activities are distributed to each winter month; however these activities are expected to be minimal in the Capital Region during January and February due to extensive snow coverage.

We identified off-road sources included in the inventory that are expected to have limited activities during January and February period (Table 3-4) and excluded their emissions. Examples of this equipment are agricultural tractors, lawn mowers and excavators. EC emissions from this equipment are 3.80 tonne per average winter day, about 90% of all off-road equipment sources.

Table 3-4. Source Category Code (SCC) of off-road sources that have limited activities in the Capital Region in winter

Agriculture and Lawn/Garden related sources		Construction and Mining related sources	
2260001010	2265004071	2260002006	2267002054
2260002021	2265004075	2260002009	2267002057
2260004015	2265004076	2260002039	2267002060
2260004016	2265005010	2260002054	2267002066
2260004020	2265005015	2265002003	2267002072
2260004021	2265005025	2265002006	2270002009
2260004025	2265005030	2265002009	2270002015
2260004026	2265005035	2265002015	2270002018
2260004030	2265005040	2265002027	2270002027
2260004031	2265005045	2265002030	2270002030
2260005035	2265005060	2265002033	2270002033
2265001010	2267002003	2265002039	2270002036
2265001050	2267002021	2265002042	2270002039
2265002021	2267002024	2265002045	2270002042
2265002024	2270002003	2265002054	2270002045
2265004010	2270002021	2265002057	2270002048
2265004011	2270002024	2265002060	2270002051
2265004015	2270004046	2265002066	2270002054
2265004016	2270004056	2265002072	2270002057
2265004025	2270004066	2265002078	2270002060
2265004026	2270004071	2267002015	2270002066
2265004030	2270005010	2267002030	2270002069
2265004031	2270005015	2267002033	2270002072
2265004040	2270005020	2267002039	2270002075
2265004041	2270005025	2267002045	2270002078
2265004046	2270005030		
2265004051	2270005035		
2265004055	2270005045		
2265004056	2270005060		
2265004066	2282005010		

3.2.4 Reallocation of Residential Wood Combustion Emissions

Heating accounts for more particulate carbon emissions than any other activity in the residential sector. Heating fuel options in Alberta included in the Phase I emissions inventory are natural gas, fuel oil, kerosene, liquefied petroleum gas (LPG), and wood. Residential wood combustion (RWC) alone represents about 75% of annual $PM_{2.5}$ emissions from residential heating sector in the Phase I inventory. The $PM_{2.5}$ emission rate from RWC is about 1.5 tonne

per year per 1000 population, comparable to the US estimates in the range of 1.2-1.4 tonne per year per 1000 population[6].

Natural gas is the preferred fuel option for major cities like Edmonton, while wood is used mostly by rural residents. The Phase I emissions inventory, however, spatially distributed province-wide RWC emissions using total dwelling surrogate, placing much of the RWC emissions in the city center. We revised the RWC spatial allocation using rural dwelling surrogate. Figure 3-1 demonstrates the effect of the allocation of RWC emissions that moves some of the RWC emissions in the city center to more rural areas.

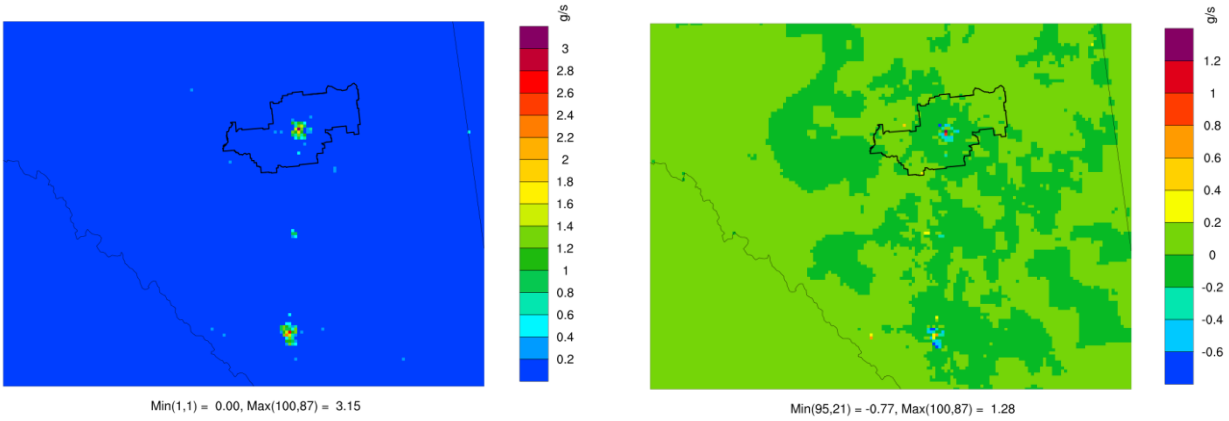

Original RWC emissions spatial allocation

Difference plot (Revised – Original)

Figure 3-1. Original RWC emissions in the 4 km domain using total dwelling spatial distribution (left) and differences with the revised RWC that used rural dwelling spatial distribution (right).

3.2.5 Emissions Summaries

Table 3-5 and Figure 3-2 summarize the updated Capital Region 2010 emissions by pollutant in tonnes per month (averaged for January-February period).

[6] Based on US EPA's 2011 National Emission Inventory and 2011 population for the state of Rhode Island, Montana, and Wyoming

Table 3-5. Emissions summary by pollutant and by source sector (tonnes per month).

	NOx	VOC	TOG	CO	NH_3	SO_2	PM_{25}	PM_{10}
Industrial – upstream oil and gas	399	393	913	560	0	109	7	7
Industrial – electric power generation	5,654	65	154	1,088	5	6,292	160	350
Industrial – others	789	2,225	2,879	1,764	221	1,182	111	208
Transportation: Onroad	984	1,119	1,328	13,526	150	12	19	65
Transportation: Offroad	532	247	281	3,776	0	4	20	21
Commercial and residential heating	391	272	300	1,413	5	67	247	250
Agriculture	0	265	408	4	332	0	16	44

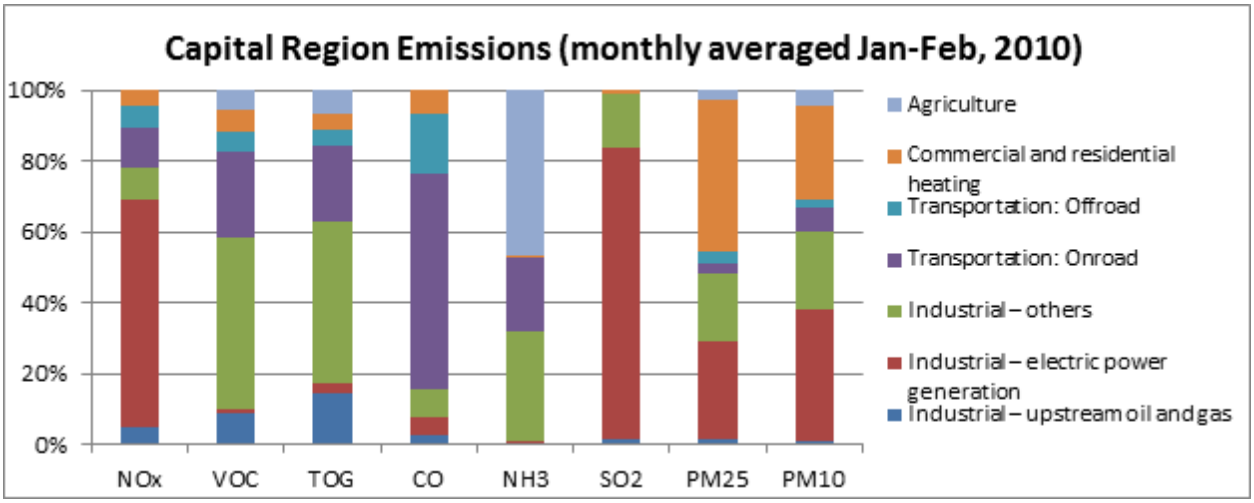

Figure 3-2. Emission contributions by source sector within the Capital Region.

4.0 METEOROLOGICAL INPUTS

We developed CMAQ meteorological inputs for the Capital Region using the latest version of the Weather Research Forecast (WRF; Skamarock et al., 2008) meteorological model (Version 3.6.1 released August 14, 2014). For clarity, we refer to the final WRF simulation performed for the previous phase of the project in 2014 as "Phase I". We refer to WRF simulations performed in January 2015 as "Phase II-A" and simulations performed in March 2015 as "Phase II-B". Together, we refer to Phase II-A and Phase II-B as "Phase II".

We describe the WRF model configuration, including modeling domains, vertical layer structure, and selected physics options for all WRF simulations in Section 4.1. We present model performance evaluations in Sections 4.2 (Phase I versus Phase II-A simulations) and 4.3 (Phase II-B simulations). Finally, we summarize the WRF simulations and model performance evaluation in Section 4.4.

4.1 WRF Model Configuration

4.1.1 Modeling Domains

Figure 4-1 shows the 36/12/4/1.33 km WRF domains. The 36 km domain was expanded from the Phase I modeling to include enough east-west extent to resolve a full synoptic scale (the distance between typical mid-latitude cyclones) and includes most of Canada and the contiguous United States. The 12 km domain was also expanded from Phase I in order to include more buffer cells to the west of the 4 km domain and now includes nearly all of the British Columbia and Saskatchewan provinces. This was done because the distance between the 12 km and 4 km domain edges must be large enough for 12 km "features" to develop, such as turbulent potential vorticity. The 4 km and 1.33 km domains are unchanged from Phase I, but we ultimately did not use the 1.33 km domain for WRF modeling. Because we needed to perform many simulations in a short amount of time, the cost of including the 1.33 km domain outweighed the benefit of the higher resolution fields. Results from Phase I showed very similar results from the two domains.

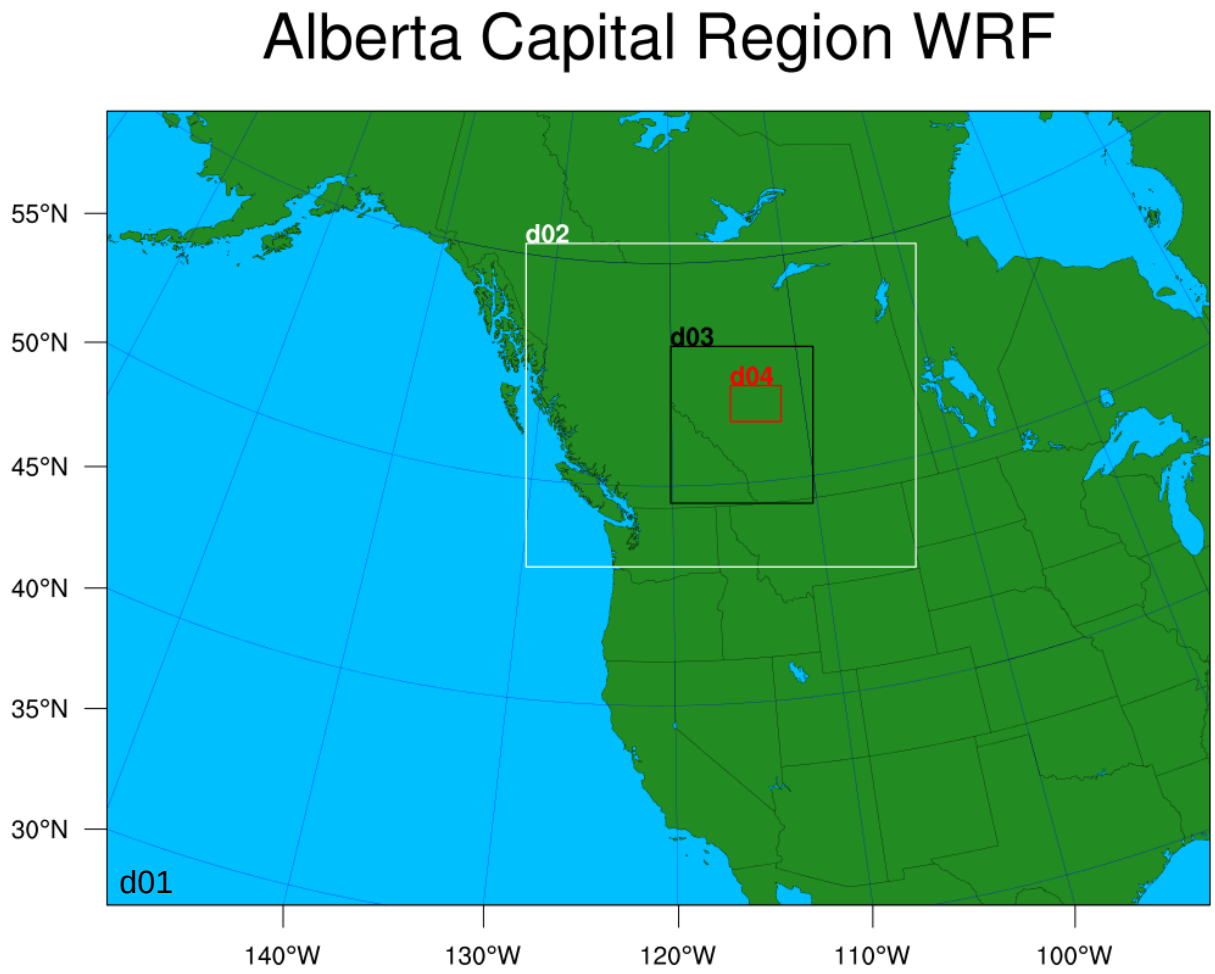

Figure 4-1. WRF domain extents for 36 km (d01), 12 km (d02), 4 km (d03) and 1.33 km (d04) domains.

4.1.2 Vertical Layer Structure

We provide the WRF vertical layer structure and mapping to corresponding CMAQ layers in **Table** 4-1. The vertical layer structure employed for Phase II modeling is unchanged from Phase I. As discussed in the Phase I final report, adequate simulation of the wintertime stable atmosphere guided the selection of WRF model layers.

Running CMAQ with 39 vertical layers would be computationally demanding, so the WRF vertical layers were collapsed for CMAQ modelling concentrating on air quality issues within the PBL. We collapse the 39 WRF vertical layers to 22 CMAQ layers. No layers are collapsed within the first 500 m AGL, and each CMAQ layer below ~2,000 m AGL comes from collapsing a maximum of two WRF layers.

Table 4-1. Definition of WRF 40 vertical levels (39 vertical layers) and mapping to the 22 vertical layers used in the CMAQ Chemical Transport Model. Heights (m) are geopotential heights above ground level, actual layer thicknesses will be shallower in areas above sea level.

WRF					CMAQ				
Layer	Sigma	Pressure (mb)	Height (m)	Depth (m)	Layer	Sigma	Pressure (mb)	Height (m)	Depth (m)
40	0.0000	100	15685	1190	22	0	100	15685	5206
39	0.0280	125.2	14495	1229					
38	0.0620	155.8	13266	1514					
37	0.1120	200.8	11752	1273					
36	0.1620	245.8	10479	1104	21	0.162	245.8	10479	2961
35	0.2120	290.8	9375	977					
34	0.2620	335.8	8397	879					
33	0.3120	380.8	7518	800	20	0.312	380.8	7518	2216
32	0.3620	425.8	6718	735					
31	0.4120	470.8	5983	681					
30	0.4620	515.8	5302	635	18	0.462	515.8	5302	1569
29	0.5120	560.8	4667	479					
28	0.5520	596.8	4189	456					
27	0.5920	632.8	3733	350	17	0.592	632.8	3733	933
26	0.6240	661.6	3383	317					
25	0.6540	688.6	3067	266					
24	0.6800	712.0	2800	259	16	0.68	712	2800	739
23	0.7060	735.4	2541	233					
22	0.7300	757.0	2308	247					
21	0.7560	780.4	2061	223	15	0.756	780.4	2061	440
20	0.7800	802.0	1838	218					
19	0.8040	823.6	1621	178	14	0.804	823.6	1621	353
18	0.8240	841.6	1443	175					
17	0.8440	859.6	1268	155	13	0.844	859.6	1268	307
16	0.8620	875.8	1113	152					
15	0.8800	892.0	961	125	12	0.88	892	961	241
14	0.8950	905.5	836	115					
13	0.9090	918.1	720	106	11	0.909	918.1	720	203
12	0.9220	929.8	614	97					
11	0.9340	940.6	517	88	10	0.934	940.6	517	88
10	0.9450	950.5	429	79	9	0.945	950.5	429	79
9	0.9550	959.5	350	71	8	0.955	959.5	350	71
8	0.9640	967.6	279	63	7	0.964	967.6	279	63
7	0.9720	974.8	216	62	6	0.972	974.8	216	62
6	0.9800	982.0	154	46	5	0.98	982	154	46
5	0.9860	987.4	108	46	4	0.986	987.4	108	46
4	0.9920	992.8	61	23	3	0.992	992.8	61	23
3	0.9950	995.5	38	19	2	0.995	995.5	38	19
2	0.9975	997.8	19	19	1	0.9975	997.8	19	19
1	1.0000	1000.0	0	0					

4.1.3 WRF Physics and Data Assimilation Configuration

4.1.3.1 Phase II-A Sensitivity Simulations

Table 4-2 compares the physics and data assimilation options used in the Phases I and IIA. Configuration differences are shown in bold text. Under Phase II-A, ENVIRON performed four sensitivity simulations resulting from all possible combinations of the two PBL schemes (YSU and MYJ) and reanalysis datasets (Climate Forecast System Reanalysis [CFSR] and ERA-Interim) and upgraded to the latest version of the WRF model available. The CFSR archive is maintained by the US National Centers for Environmental Prediction (NCEP) and ERA-Interim archive is maintained by the European Centre for Medium‐Range Weather Forecasts (ECMWF). Aside from the version of WRF used, the main configuration differences involve the application of analysis and observation nudging.

For Phase I, analysis nudging was applied to the 36 km domain only, while Phase II-A used analysis nudging on the 12 km domain as well. The Phase I modeling used a considerably larger analysis nudging moisture coefficient ($3x10^{-4}$) than Phase II-A ($1x10^{-4}$).

Phase I used observation nudging within all four domains. This practice is discouraged at large grid resolutions (e.g. 36 and 12 km). One reason for this concerns the placement of sensors, which tend to be located near where people live, where humidity is higher. When observation nudging is used at these large grid resolutions, high humidity can be artificially spread into the air above places where people do not live (e.g. mountainous areas). For Phase II-A, observation nudging was just applied to the 4 km domain.

Phase I employed observation nudging using data from Alberta's Clean Air Strategic Alliance (CASA) and Environment Canada (EC). ENVIRON did not have resources to process the CASA observations in time for the Phase II-A modeling and does not have access to the EC observations. So the Phase II-A modeling used observations from the Meteorological Assimilation Data Ingest System (MADIS) dataset, a global observational database. MADIS runs operationally at the United States National Weather Service (NWS) National Centers for Environmental Prediction (NCEP) Central Operations (NCO) as part of the Integrated Dissemination Project (IDP). Phase II-A used observation nudging for winds and temperature only, while Phase I also nudged to moisture observations.

The last configuration difference involves observation nudging coefficients. Phase I and IIA used the same coefficient for wind nudging ($6x10^{-4}$), but used different coefficients for temperature (Phase I: $1x10^{-3}$; Phase II-A: $6x10^{-4}$). As noted above, the Phase II-A simulations turned off observation nudging for moisture. The Phase I WRF simulation used a moisture nudging coefficient of $6x10^{-4}$.

Table 4-2. Comparison of WRF physics and data assimilation options used in Phase I and IIA of the Capital Region PM Modelling Study. Differences are shown in bold text.

WRF Treatment	Phase I	Phase II-A
Model Version	**3.5.1**	**3.6.1**
Microphysics	Thompson scheme	Thompson scheme
Longwave Radiation	RRTMG	RRTMG
Shortwave Radiation	RRTMG	RRTMG
Land Surface Model (LSM)	NOAH	NOAH
Planetary Boundary Layer (PBL) scheme	**YSU**	**2 configurations: YSU/MYJ**
Explicit Moisture Scheme	WSM6	WSM6
Grid Nesting	36/12/4/1.33 km run together with 1-way feedback only	36/12/4 km run together with 1-way feedback only
Analysis nudging	Nudging applied to winds, temperature and moisture in the **36 km domain only**	Nudging applied to winds, temperature and moisture in the **36 and 12 km domains**
Analysis Nudging Wind Coefficient	3x10-4	3x10-4
Analysis Nudging Temp Coefficient	3x10-4	3x10-4
Analysis Nudging Moisture Coefficient	**3x10-4**	**1x10-4**
IC/BC + Analysis nudging dataset	**CFSR**	**2 configurations: CFSR/ERA**
Observation Nudging	Nudging applied to both surface wind and temperature for **all four domains**	Nudging applied to both surface wind and temperature for **4 km domains only**
Observation Nudging Dataset	**CASA + EC**	**MADIS**
Observation Nudging Wind Coefficient	6x10-4	6x10-4
Observation Nudging Temp Coefficient	**1x10-3**	**6x10-4**
Observation Nudging Moisture Coefficient	**6x10-4**	**None**

4.1.3.2 Phase II-B WRF Sensitivity Simulations

Table 4-3 lists the WRF simulations performed for Phase II-B. Because we chose the ERA+MYJ configuration as the best performing WRF simulation, we used this configuration as a "baseline" configuration for the Phase II-B WRF sensitivity runs.

The first WRF sensitivity, ERA+MYJ+Noah_MP (short name: Noah_MP), replaces the Noah land surface model (LSM) with the newer Noah Multi-Parameterization (Noah-MP) LSM, which includes improvements for surface layer radiation balances, snow depth, soil moisture and heat fluxes, leaf area-rainfall interaction, vegetation and canopy temperature distinction, soil column and drainage of soil, and runoff.

Next, the GFS+MYJ (short name: GFS) simulation replaces ERA-Interim reanalysis archive for initial/boundary conditions and analysis nudging with 0.5 degree Global Forecast System (GFS) reanalysis data.

The ERA+MYJ+Opt_Nudge WRF sensitivity (short name: Opt_Nudge) is identical to the ERA+MYJ WRF configuration from Phase II-A, but uses "optimal" nudging strengths that were used by ENVIRON for modeling for a similar application in the US Intermountain West. These coefficients led to the best performance for this previous application.

ENVIRON designed the final three WRF sensitivities to be based on the Opt_Nudge configuration. The ERA+MYJ+Opt+Mois sensitivity (short name: Opt+Mois) turns on observation nudging to moisture to determine if more clouds could be generated in the model, with the aim of improving sulphate under-predictions in the CMAQ model. The ERA+MYJ+Opt+GF_Cu simulation (Opt+GF_Cu) replaces the Kain-Fritsch cumulus parameterization with the newer scale-aware Grell-Freitas scheme, which is designed to be used at higher horizontal resolutions. Finally, the ERA+MYJ+Opt+CASA simulation (short name: Opt+CASA) adds the Edmonton East, Edmonton South, and Edmonton McIntyre CASA monitors to the MADIS stations used for observation nudging, with the purpose of replicating the stagnant conditions observed at the Edmonton McIntyre monitor on January 28-29, 2010 (see Figure 4-7).

Table 4-3. WRF configuration options for Phase II-B sensitivity simulations. Differences from Phase IA ERA+MYJ configuration shown in bold.

Run	Short Name	Analysis Nudging (36/12 km)			Obs Nudging (4 km)			Notes
		Wind	Temp	Moisture	Wind	Temp	Moisture	
ERA+MYJ	ERA+MYJ	3x10-4	3x10-4	1x10-4	6x10-4	6x10-4	N/A	Baseline WRF simulation
ERA+MYJ+Noah_MP	Noah_MP	3x10-4	3x10-4	1x10-4	6x10-4	6x10-4	N/A	Use Noah MultiParamterization LSM
GFS+MYJ	GFS	3x10-4	3x10-4	1x10-4	6x10-4	6x10-4	N/A	Use 0.5 degree GFS instead of ERA for IC/BCs + analyses
ERA+MYJ+Opt_Nudge	Opt_Nudge	**5x10-4**	**5x10-4**	1x10-4	**9x10-4**	**9x10-4**	N/A	Use "optimal" nudging strengths + other tweaks
ERA+MYJ+Opt+Mois	Opt+Mois	**5x10-4**	**5x10-4**	**1x10-4**	**9x10-4**	**9x10-4**	**6x10-4**	Add moisture nudging
ERA+MYJ+Opt+GF_Cu	Opt+GF_Cu	**5x10-4**	**5x10-4**	**1x10-4**	**9x10-4**	**9x10-4**	N/A	Grell-Freitas cumulus parameterization
ERA+MYJ+Opt+CASA	Opt+CASA	**5x10-4**	**5x10-4**	**1x10-4**	**9x10-4**	**9x10-4**	N/A	Add obs nudging to CASA sites: East, South, McIntyre

4.2 Phase II-A WRF Model Performance Evaluation

In this section, we present the 4 km model performance evaluation for Phase I and Phase II-A WRF simulations for the January 28-February 3, 2010 period. The WRF surface meteorological model performance metrics were compared against the simple and complex terrain model performance goals using “soccer plots.” Soccer plots display two WRF performance metrics on the x-axis and y-axis (e.g., temperature bias and error), along with the performance benchmarks, such that the closer the symbols are to the zero origin, the better the model performance and it is easy to see when the two WRF performance metrics fall within the benchmark lines (i.e., score a goal). Below we present daily surface meteorological model performance across four sites in and near downtown Edmonton (map of sites given in Figure 4-2).

Figure 4-3 displays soccer plots for wind direction (top left), humidity (top right), wind speed (bottom left), and temperature (bottom right). Colors represent different WRF simulations and

symbols represent different days and both are shown in the legend of each plot. Stagnant conditions with very low wind speeds persist through much of the modeling period, when wind direction tends to be variable and difficult to measure. Therefore, wind direction soccer plots should not be used as a way to determine the best WRF configuration. The humidity soccer plot shows that all simulations fall within the simple terrain goal. In addition, there is little spread between the various WRF simulations. The wind speed soccer plot shows generally good performance, with most of the simulations within the simple goal for most of the days. The ERA+MYJ simulation shows particularly good performance, with all five days of the episode within the simple benchmarks. The temperature soccer plot shows poor performance for February 1-3, with the Phase II-A YSU-based runs (red: ERA+YSU; blue: CFSR+YSU) showing a large cold bias. We note that the Phase I WRF simulation (yellow) tends to deviate significantly from the Phase II-A simulations on most days. For February 1-3, the Phase I performance is much better than the Phase II-A simulations. We explore the reason for this deviation and why the soccer plots are misleading below.

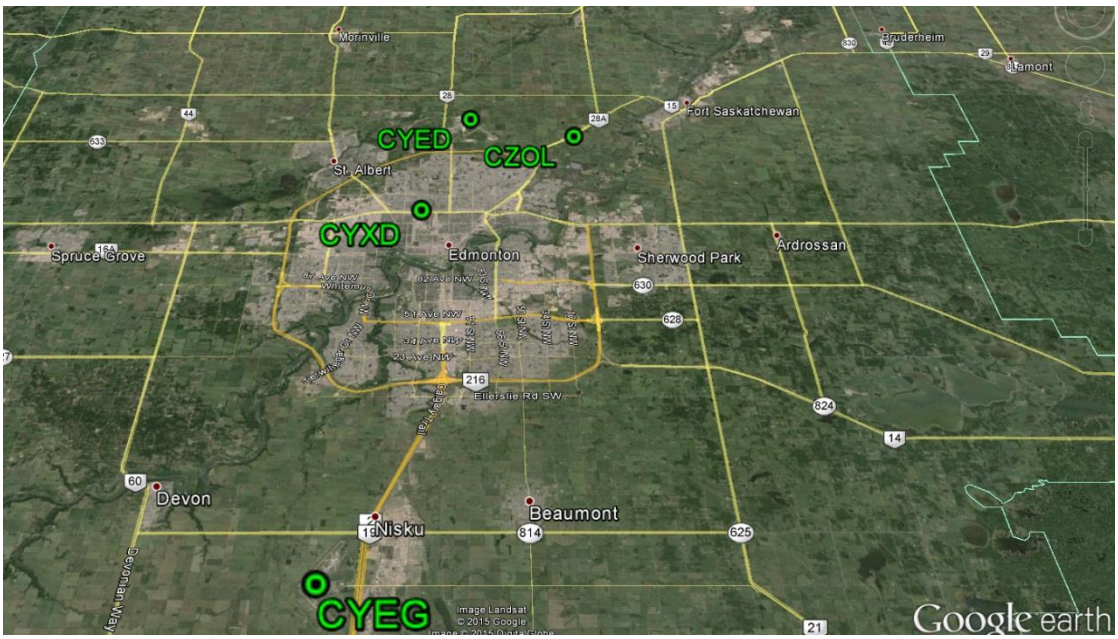

Figure 4-2. Map of the four sites in and near downtown Edmonton used for the soccer plot analysis.

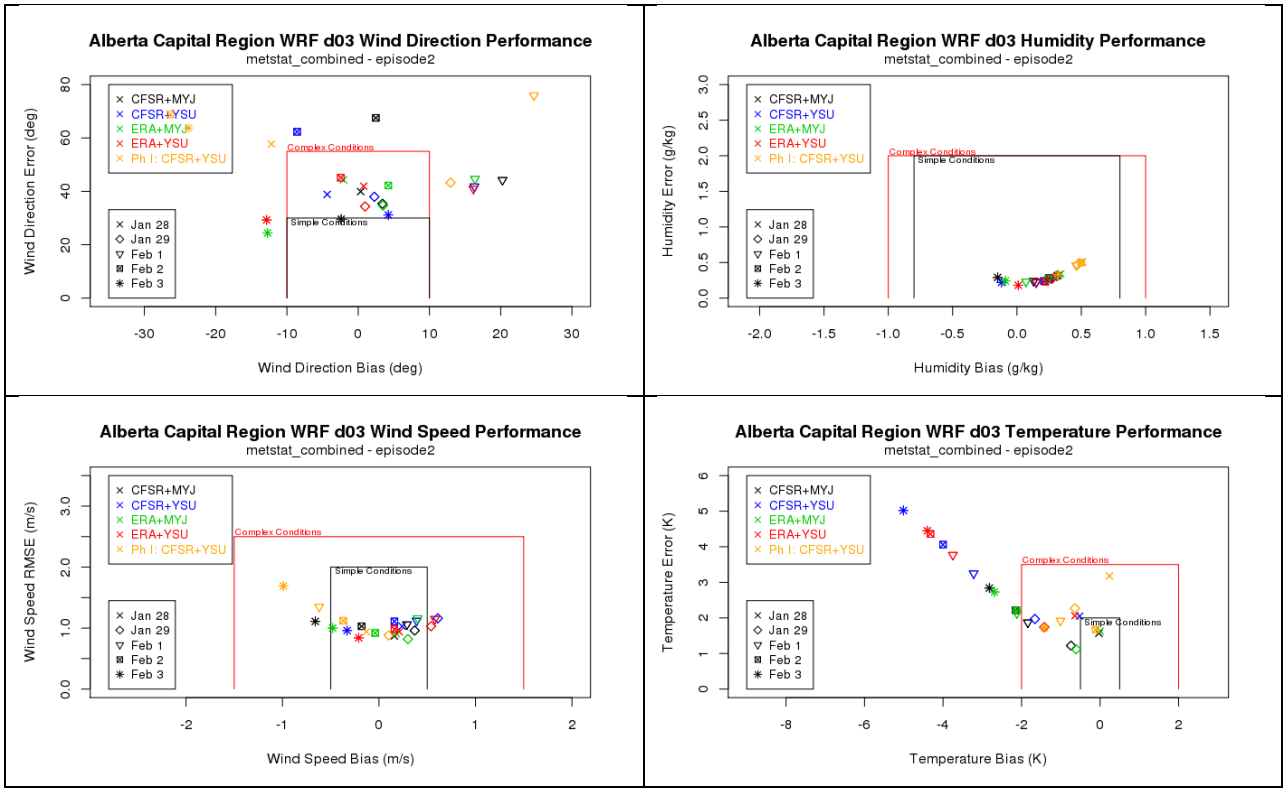

Figure 4-3. Daily statistics for wind direction (top left), humidity (top right), wind speed (bottom left), and temperature (bottom right) for the Phase I and Phase II-A WRF simulations covering Jan 28, 29 and Feb 1, 2, and 3, 2010.

Figure 4-4 shows CMAQ 4 km domain maps of 2-meter temperature (top) and 2-meter water vapor mixing ratio (bottom) for the Phase I run (left) and Phase II-A CFSR+YSU run (right) for January 29, 2010 10:00 MST. We chose this particular Phase II-A run for comparison because it has the most similar configuration to the Phase I simulation (identical PBL scheme and IC/BC/analysis dataset). We note "patchwork" patterns observed in both the temperature and moisture maps for the Phase I simulation that are not observed in the Phase II-A simulation. The irregular spacing indicates that the sharp horizontal gradients result from an observation nudging artifact. ENVIRON did not perform the Phase I modeling and did not have access to the complete WRF modeling database, so we do not know the exact cause of these patchwork fields. It is possible that an error was made in the OBSGRID program or some other issue related to the processing of the observation data before it was ingested into WRF.

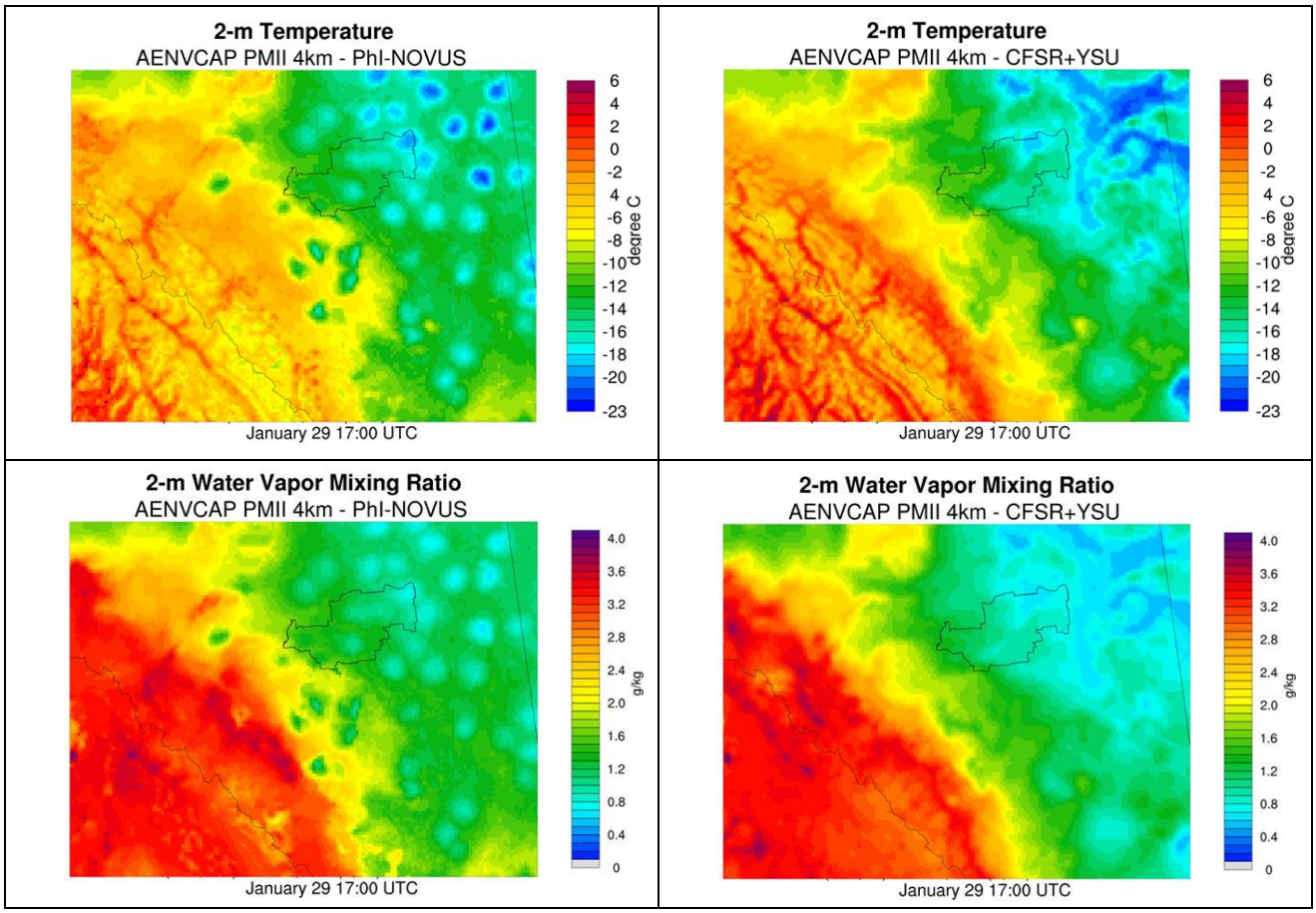

Figure 4-4. CMAQ 4 km spatial plots for 2-m temperature (top panel) and 2-m water vapor mixing ratio (bottom panel) for Phase I (left) and the Phase II-A CFSR+YSU WRF (right) simulations for January 29, 2010 10:00 MST.

The observation nudging artifacts found in the temperature and moisture maps guided us to examine low-level cloudiness. Figure 4-5 shows CMAQ 4 km domain maps of layer 1 cloud water content (CWC) for the Phase I run (left) and Phase II-A CFSR+YSU run (right) for the same time period as Figure 4-4, January 29, 2010 10:00 MST. The Phase I map indicates that the

moisture removed from the surface in the vicinity of observation sites (shown in Figure 4-4) has been displaced vertically and condensed into low-level clouds. As expected, we do not observe this overabundance of low-level cloudiness in the Phase II-A CFSR+YSU WRF simulation.

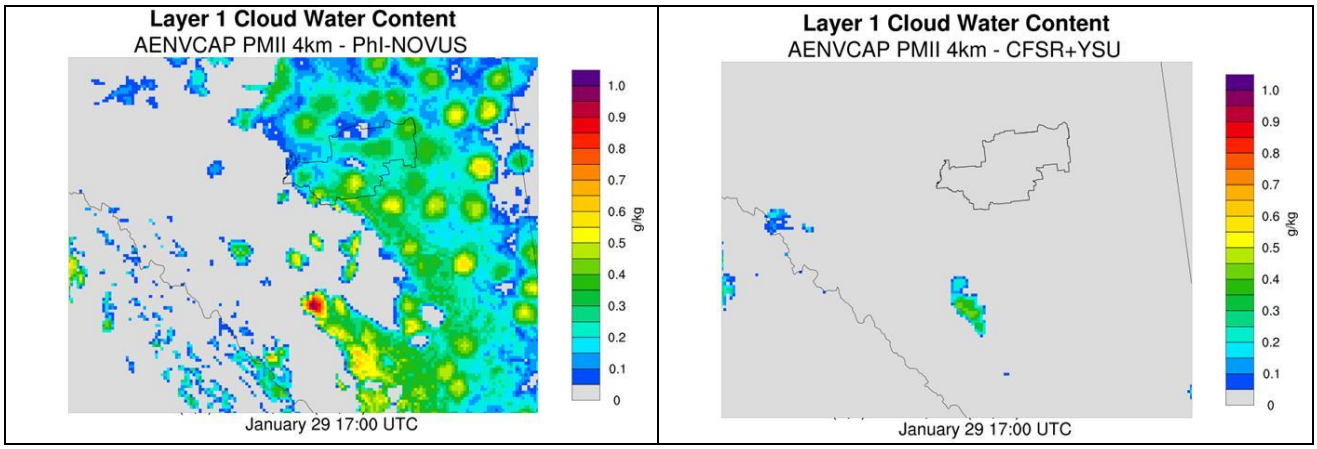

Figure 4-5. CMAQ 4 km spatial plots for layer 1 cloud water content for Phase I (left) and the Phase II-A CFSR+YSU (right) WRF simulations for January 29, 2010 10:00 MST.

In order to determine how the various WRF model configurations simulate the low wind speeds observed during the elevated $PM_{2.5}$ episode (January 26-February 3), we examine wind speed time series at the Edmonton East and Edmonton McIntyre CASA monitors (map shown in Figure 4-6).

In Figure 4-7, we present observed and modeled hourly wind speed (primary axis) for Phase I and IIA WRF simulations and observed $PM_{2.5}$ (secondary axis) time series at the Edmonton McIntyre CASA monitor for January 26-February 4, 2010. The green arrow highlights the period of elevated $PM_{2.5}$ concentrations that coincides with stagnant conditions. Generally, WRF (or any other meteorological model) cannot accurately simulate near-zero wind speeds as seen at the McIntyre monitor. The Phase I simulation matches the near-zero wind speeds observed on the morning of January 29, while the Phase II-A simulations all over-predict the wind speeds during this time. Because of this result, we designed a Phase II-B WRF sensitivity (Opt+CASA) to include observation nudging to the CASA sites to determine if wind speeds could be lowered at the McIntyre monitor (discussion in Section 4.3).

Figure 4-8 presents the same time series as in the previous figure, but for the Edmonton East monitor. As seen at McIntyre, elevated $PM_{2.5}$ concentrations coincide with stagnant conditions. The WRF simulations are better able to replicate the observations at Edmonton East on January 28-29 and observed wind speeds do not reach the near-zero values seen at McIntyre during this stagnant period.

Figure 4-6. Map of the two Edmonton CASA sites used for the wind speed/$PM_{2.5}$ time series analysis.

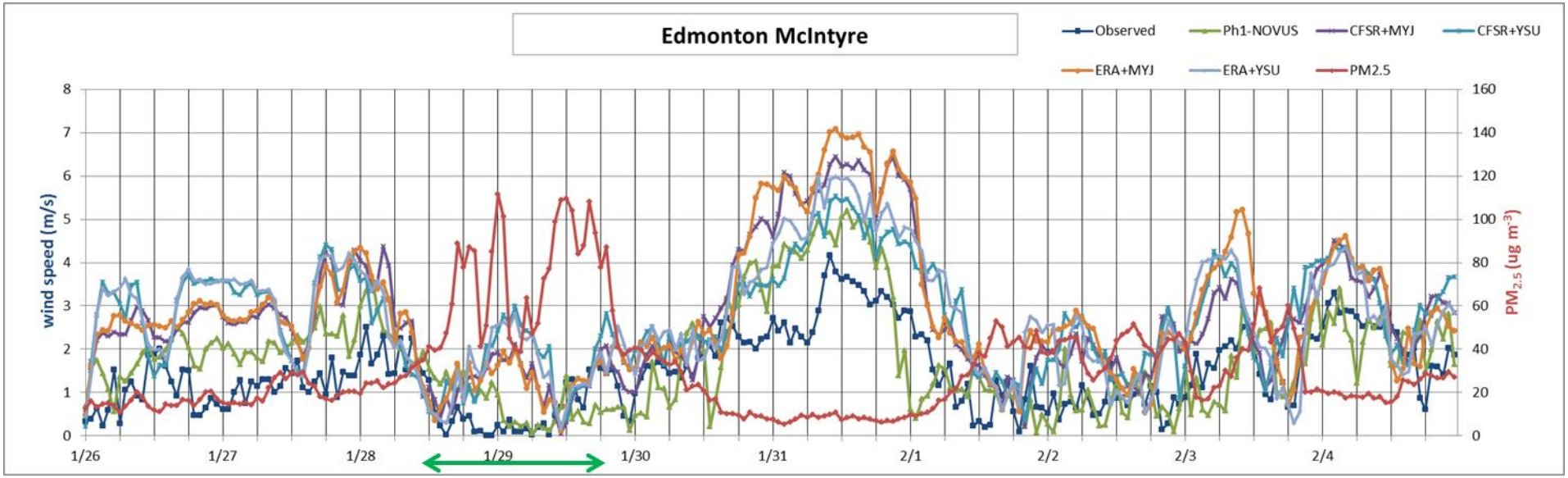

Figure 4-7. Observed and modeled hourly wind speed (primary axis) for Phase I and IIA WRF simulations and observed $PM_{2.5}$ (secondary axis) time series at the Edmonton McIntyre CASA monitor for January 26-February 4, 2010. Green arrow highlights period of elevated $PM_{2.5}$ concentrations that coincides with stagnant conditions.

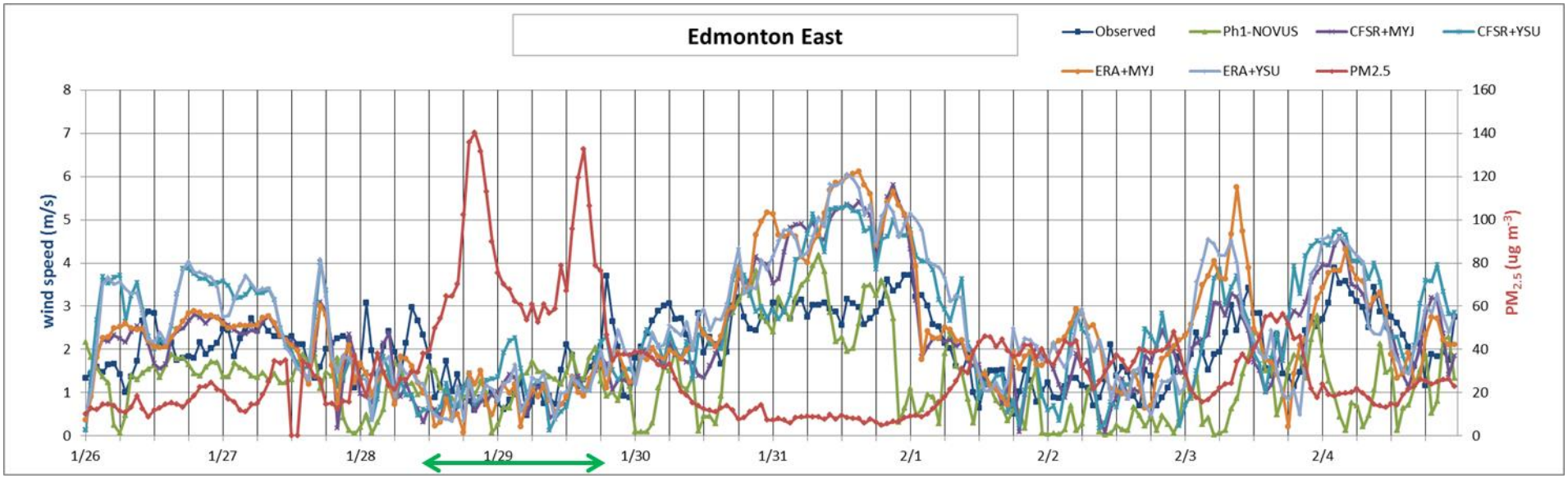

Figure 4-8. Observed and modeled hourly wind speed (primary axis) for Phase I and IIA WRF simulations and observed $PM_{2.5}$ (secondary axis) time series at the Edmonton East CASA monitor for January 26-February 4, 2010. Green arrow highlights period of elevated $PM_{2.5}$ concentrations that coincides with stagnant conditions.

The Phase II-A WRF simulations corrected the observational nudging artifacts discovered in the Phase I modeling. While performance among the four Phase II-A WRF simulations was quite similar, we observed that the MYJ-based runs performed slightly better overall in terms of less wind speed bias during the stagnant Jan 28-29 period and a smaller cold bias than the YSU-based runs during the Feb 1-3 period. Results from the CMAQ evaluation gave a slight edge to the ERA+MYJ simulation in terms of $PM_{2.5}$ composition at the McIntyre monitor and total $PM_{2.5}$ performance at all Edmonton monitors, so we chose that simulation to serve as a baseline for further sensitivity tests performed in Phase II-B.

4.3 Phase II-B WRF Model Performance Evaluation

We present the Phase II-B model performance evaluation in this section. The goal of this evaluation is to determine if performance is improved from the ERA+MYJ simulation, which we selected as the best performing Phase II-A run. Descriptions of the six Phase II-B simulations are given in Section 4.1.3.2.

Figure 4-9 shows soccer plots for the Phase II-A ERA+MYJ and Phase II-B WRF simulations. As noted previously, wind direction during this episode is highly variable and difficult to measure accurately, so it does not help differentiate model performance between the model runs. All simulations attain the simple model benchmarks for humidity and wind speed on all days and are all tightly grouped, indicating that the different WRF configurations are not leading to significantly different results. As shown in the Phase II-A soccer plots (Figure 4-3), the temperature soccer plots show a significant cold bias for February 1-3, but the runs are now more tightly clustered together.

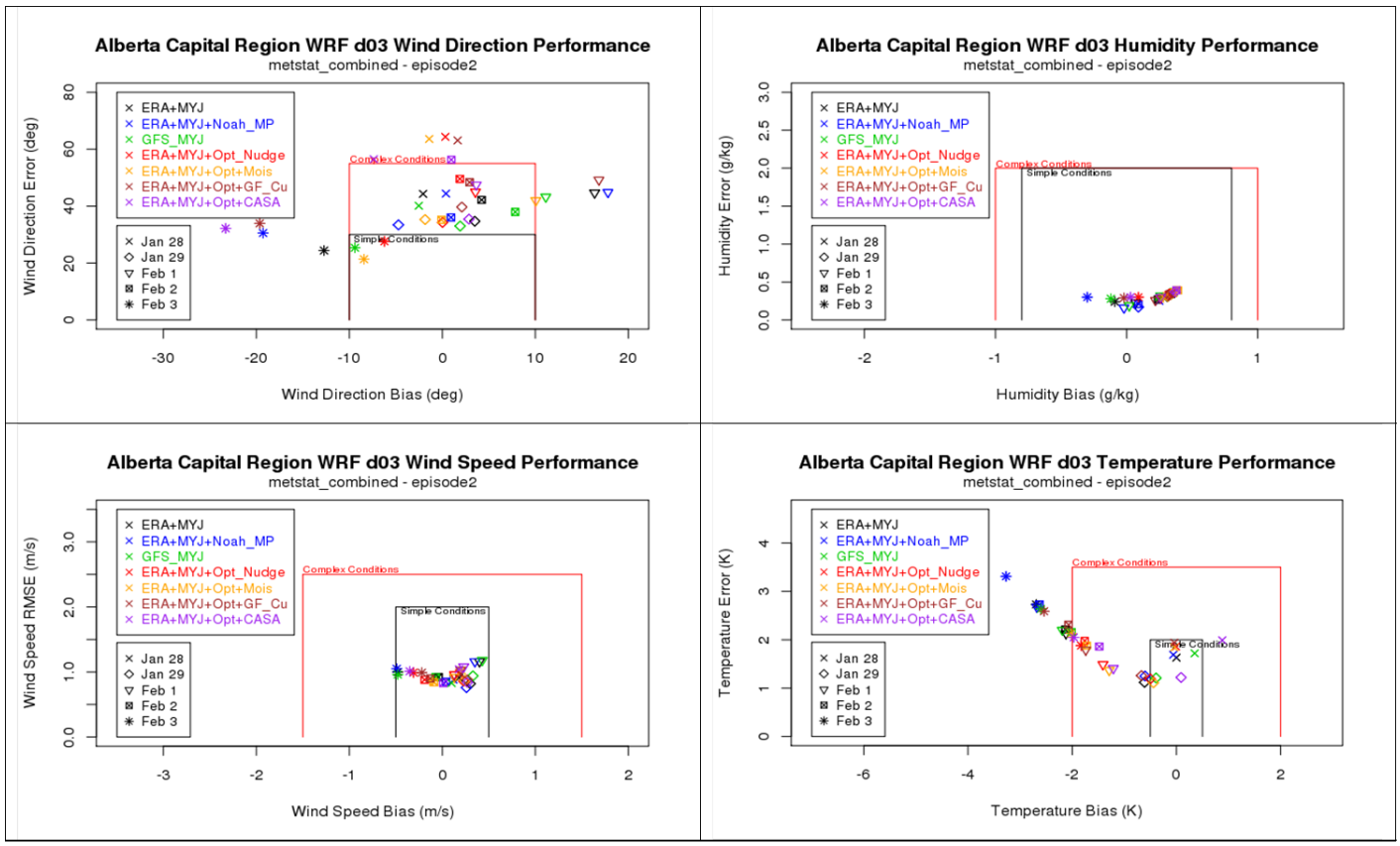

Figure 4-9. Daily statistics for wind direction (top left), humidity (top right), wind speed (bottom left), and temperature (bottom right) for the Phase II-A ERA+MYJ and Phase II-B WRF simulations covering Jan 28, 29 and Feb 1, 2, and 3, 2010.

In Figure 4-10, we present observed and modeled hourly wind speed (primary axis) for ERA+MYJ and Phase II-B WRF simulations and observed $PM_{2.5}$ (secondary axis) time series at the Edmonton McIntyre CASA monitor for January 26-February 3, 2010. The green arrow highlights the period of elevated $PM_{2.5}$ concentrations that coincides with stagnant conditions. As observed in the soccer plots, we note that simulations are now more tightly clustered. The GFS simulation matches the near-zero wind speeds observed late on January 28, but then moves back to the rest of the WRF simulations, over-predicting the wind speeds on January 29. We do not see a significant improvement in wind speeds from the CASA simulation, indicating that this is not the driving factor in reaching the very low wind speeds at McIntyre.

Figure 4-11 presents the same time series as in the previous figure, but for the Edmonton East monitor. As seen at McIntyre, there is not much spread in wind speed among the six WRF simulations. As seen with the Phase II-A results, the WRF simulations are better able to replicate the observations at Edmonton East on January 28-29.

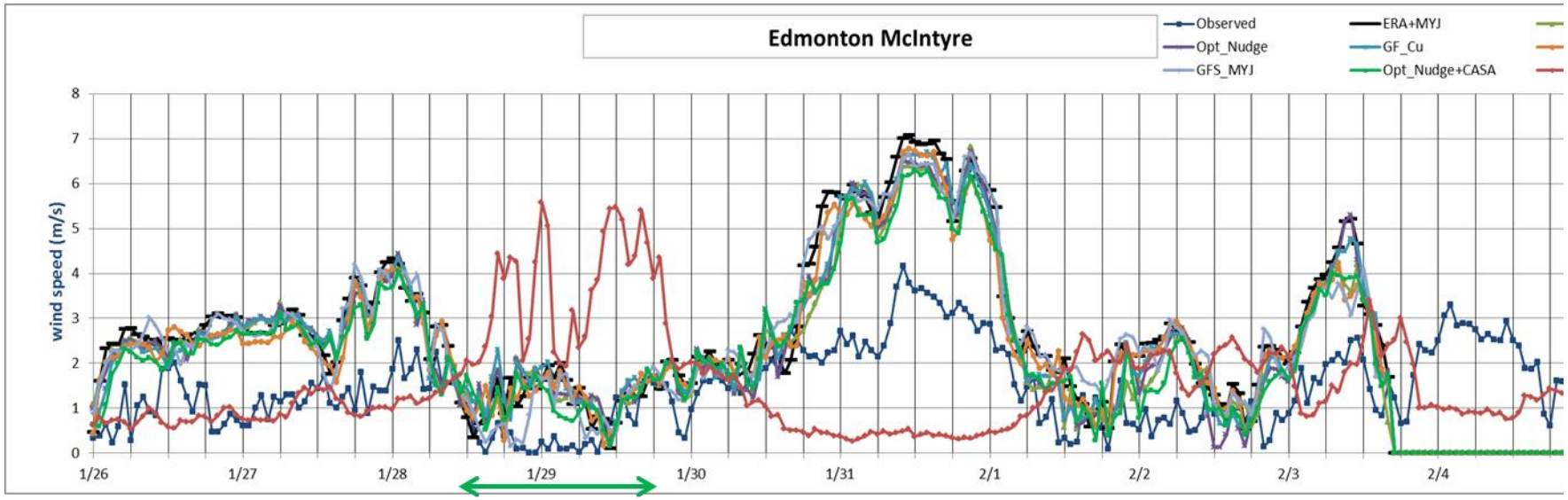

Figure 4-10. Observed and modeled hourly wind speed (primary axis) for ERA+MYJ and Phase II-B WRF simulations and observed $PM_{2.5}$ (secondary axis) time series at the Edmonton McIntyre CASA monitor for January 26-February 4, 2010. Green arrow highlights period of elevated $PM_{2.5}$ concentrations that coincides with stagnant conditions.

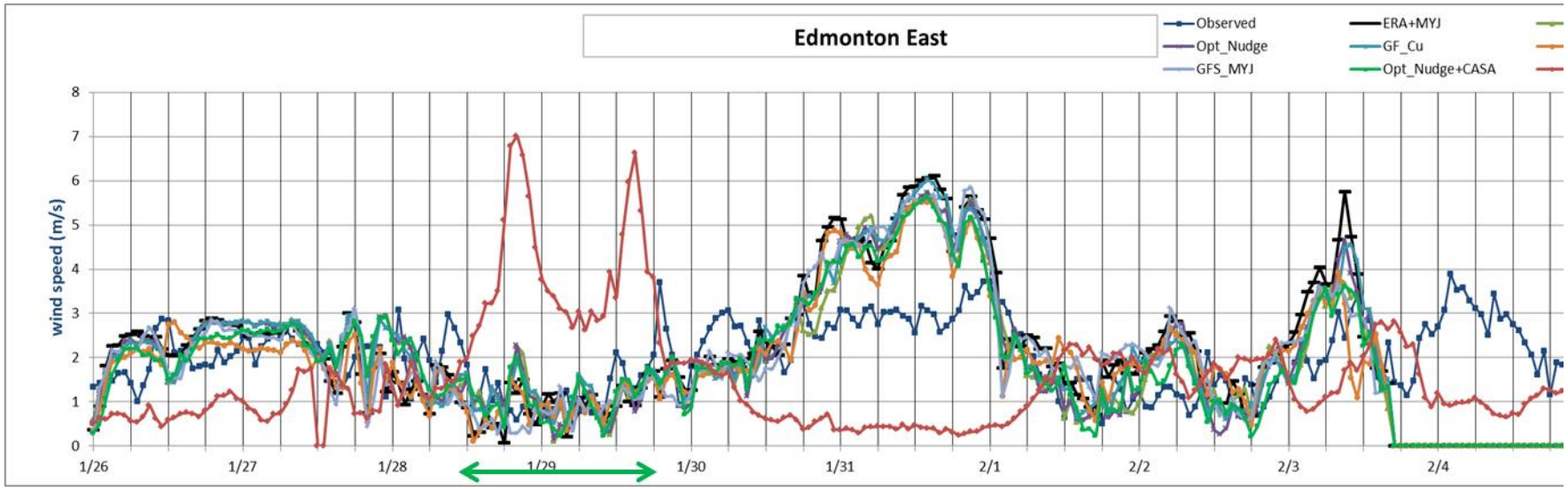

Figure 4-11. Observed and modeled hourly wind speed (primary axis) for ERA+MYJ and Phase II-B WRF simulations and observed $PM_{2.5}$ (secondary axis) time series at the Edmonton East CASA monitor for January 26-February 4, 2010. Green arrow highlights period of elevated $PM_{2.5}$ concentrations that coincides with stagnant conditions.

4.4 Summary

ENVIRON designed an initial set of WRF sensitivity simulations designed to improve meteorological performance over Phase I. We discovered that an overabundance of low-level cloudiness – caused by observation nudging artifacts – led to large sulphate over-predictions and therefore poor $PM_{2.5}$ performance in the CMAQ model. All Phase II-A WRF simulations improved upon Phase I by correcting these erroneous cloud cover fields. Although model performance was similar among the four Phase II-A WRF simulations, we selected the ERA+MYJ simulation due in part to better wind speed and temperature performance. This simulation also performed best in terms of $PM_{2.5}$ composition at the McIntyre monitor and total $PM_{2.5}$ concentrations.

We then designed a set of six WRF sensitivity tests to determine if model performance could be improved further. Using the Phase II-A ERA+MYJ simulation as a baseline configuration, we tested several configuration options: 1) Noah-MP LSM, 2) GFS analyses for IC/BC/analysis nudging dataset, 3) larger nudging coefficients, 4) observation nudging of moisture, 5) Grell-Freitas cumulus parameterization, and 6) observation nudging to CASA monitors.

Performance among the six WRF sensitivity tests in Phase II-B is very similar. The GFS simulation was the only run that differed slightly from the others during the stagnant period of January 28-29, which indicates that the coarse IC/BC dataset is difficult to overcome. Future WRF sensitivity simulations involving alternate observation nudging configuration options and coefficients could be explored with the goal of reducing wind speeds and increasing cloud cover in order to better simulate observed $PM_{2.5}$ concentrations and composition.

5.0 PHOTOCHEMICAL GRID MODELLING AND MODEL PERFORMANCE EVALUATION

5.1 CMAQ Model Configuration

CMAQ Version 5.0.2 (released May 2014) was exercised for the January-February, 2010, using the 2010 base case inputs developed under Tasks 1 and 2 that were discussed in Chapters 1 through 4. The CMAQ modelling domains are shown in Figure 1-1. Table 5-1 summarizes the CMAQ Chemical Transport Model (CTM) model configuration used in this study.

Table 5-1. CMAQ CTM model configuration.

Science Options	Configurations
Model Code	CMAQ Version 5.0.2 (May 2014)
Horizontal Grid Mesh	36/12/4 km
Vertical Grid Mesh	22 Layers up to 100 mb
Initial Conditions	15 days full spin-up
Boundary Conditions	MOZART(2010)
Emissions Processing	SMOKE Version 3.1
Gas-Phase Chemistry	CB05
Aerosol Chemistry	AE5 (With Sea Salt Emissions)
Secondary Organic Aerosols	SORGAM
Meteorological Processor	MCIP Version 4.1
Horizontal Transport	PPM
Horizontal Diffusion	K-theory spatially varying
Vertical Advection Scheme	Yamartino
Vertical Eddy Diffusivity Scheme	ACM2
Diffusivity Lower Limit	Kzmin = 0.01 to 1.0 m2/s (PURB option) (KZMIN set to true)
Deposition Scheme	M3dry

5.2 CMAQ Model Inputs

The CMAQ CTM (CCTM) meteorological inputs were generated by processing the WRF meteorological model output (discussed in Chapter 4) using the CMAQ Meteorological-Chemistry Interface Program (MCIP). The latest MCIP Version 4.2 (released December 2013) was used to extract 36/12/4 km fields from WRF simulation outputs. The 36/12/4 km WRF domains are shown in Figure 4-1. Table 4-1 shows the vertical layer mapping of the 39 WRF layers to 22 CMAQ layers.

The CCTM requires Boundary Conditions (BC) inputs to specify the assumed concentrations along the outer lateral edges of the 36 km modelling domain (see Figure 1-1) that are in the CCTM BCON input file. Initial Conditions (ICs) are also needed to be specified for the first day of the model simulation. The 12 km and 4 km domains are nested within the 36 km grid using one-way grid nesting, which means that the nested domain are run after the coarse domain and there is no feedback from the fine nest to the coarse domain. The BCs for the 12 km Alberta CMAQ modelling domain were obtained by processing the CCTM 36 km domain output using

the CMAQ BCON processor to generate an hourly 12 km BC input file. The ICs for the 12 km domain were obtained from the 36 km CCTM modelling results. Similarly, the BCs/ICs for the 4 km domain were obtained from the 12 km CCTM modelling results.

The BCs/ICs for the 36 km domain, photolysis tables, and ocean surface files were from the Phase I modelling study.

5.3 CMAQ MODEL EVALUATION

5.3.1 CMAQ Model Evaluation Methodology

The CMAQ evaluation conducted for the project focuses primarily on the operational and diagnostic model evaluation of the air quality model's performance with respect to fine particulate matter ($PM_{2.5}$).

5.3.1.1 Evaluation Approach

The U.S. EPA's integrated ozone, $PM_{2.5}$ and regional haze modelling guidance calls for a comprehensive, multi-layered approach to model performance testing, consisting of the four major components: operational, diagnostic, mechanistic (or scientific) and probabilistic (EPA, 2007). The Alberta Environment Air Quality Modelling Guideline references the EPA SCRAM website where EPA's modelling guidance resides (Idriss and Spurrell, 2009). The CMAQ model performance evaluation effort for $PM_{2.5}$ discussed in this task focused on the first two components of the EPA's recommended evaluation approach, namely:

- **Operational Evaluation**: Tests the ability of the model to estimate $PM_{2.5}$ mass concentrations and the components of $PM_{2.5}$, sulphate, nitrate, ammonium, organic aerosol, elemental carbon, and other inorganic $PM_{2.5}$. This evaluation examines whether the measurements are properly represented by the model predictions but does not necessarily ensure that the model is getting "the right answer for the right reason"; and

  Diagnostic Evaluation: Tests the ability of the model to predict visibility and extinction, PM chemical composition including ozone and PM precursors (e.g., SO_x, NO_x, VOC and NH_3) and associated oxidants (e.g., nitric acid); PM size distribution; temporal variation; spatial variation; mass fluxes; and components of light extinction (i.e., scattering and absorption).

The diagnostic evaluation also may include the performance of diagnostic sensitivity tests to better understand model performance and identify potential flaws in the modelling system that can be corrected. Such diagnostic sensitivity tests were conducted as part of this study.

As in any model performance evaluation, the evaluation is limited by the availability of observed concentration data that can be compared with the model estimates. For the model evaluation presented in this report, observed data for PM precursors and total $PM_{2.5}$ mass were available. Observed data for PM component species (e.g., sulphate, nitrate, organic aerosol, elemental carbon, etc.) were also available but limited. Specifically, 24-hour average speciated $PM_{2.5}$ concentrations are only collected at the McIntyre monitoring site on a 1:3 day sampling

frequency so are not as available on a spatial or temporal basis as the hourly total $PM_{2.5}$ mass measurements.

Ideally, the model should be separately evaluated for each component of $PM_{2.5}$ as the evaluation for just total $PM_{2.5}$ mass can be misleading due to the introduction of compensating errors. For example, a model could predict the same $PM_{2.5}$ mass as observed but over-predict the SO_4 component that is compensating an under-prediction of the OA component of the $PM_{2.5}$.

The mapping of the CMAQ modeled species versus those measured in the monitoring networks is fairly straight forward for the inorganic gaseous species. However, for the PM species the measured total $PM_{2.5}$ mass is composed of numerous CMAQ species. The following CMAQ species mapping for the $PM_{2.5}$ concentrations were used:

$$PM_{2.5} = ASO4J + ASO4I + ANO3J + ANO3I + ANH4J + ANH4I + AORGAT + AORGPAJ + AORGPAI + AORGBT + AORGCT + AECJ + AECI + A25 \quad \text{(Eq.2-1)}$$ [7]

The PM species size distribution in CMAQ is represented by three lognormally distributed modes: (I) Aitken ultrafine mode; (J) Accumulation fine mode; and (K) coarse mode. The CMAQ Operations Manual recommends when comparing CMAQ modelling results to $PM_{2.5}$ measurements that all of the PM mass below a 2.5 µ cut-point be included from all three modes as discussed by Jiang and co-workers (2006). However, the latest USEPA modelling guidance (USEPA, 2014b) recommends that all of the Aitken and Accumulation modes be included (i.e., the so called I+J approach) for comparison with $PM_{2.5}$ observations. Thus, we are using the I+J approach for defining CMAQ PM2.5 concentrations in this study.

5.3.1.2 Performance Statistics and Goals

To quantify model performance, several statistical measures were calculated and evaluated for all monitors and at individual monitors within the Capital Region. Table 5-2 lists the definitions of statistical performance measures that were used in model performance evaluation discussed below. The statistical measures selected were based on the recommendations outlined in Section 18.4 of the USEPA's Guidance on the Use of Models and Other Analyses for Demonstrating Attainment of Air Quality Goals for Ozone, $PM_{2.5}$, and Regional Haze[8] (USEPA, 2007).

[7] ASO_4=sulphate; ANO_3=nitrate; ANH_4=ammonium; AORGAT=anthropogenic organic aerosols; AORGPA=primary organic aerosols; AORGBT=biogenic organic aerosols; AEC=elemental carbon; A25=particulate others;I represents Aitken mode and J represents Accumulation mode. More specific listing can be found in spec_def.conc file that is part of the CMAQ evaluation utility package.

[8] http://www.epa.gov/scram001/guidance/guide/final-03-pm-rh-guidance.pdf

Table 5-2. Statistical model performance evaluation measure definitions.

Statistical Measure	Short hand Notation	Mathematical Expression	Units
Normalized Mean Bias	NMB	$\frac{\sum_{i=1}^{N}(P_i - O_i)}{\sum_{i=1}^{N} O_i}$	Percent
Normalized Mean Error	NME	$\frac{\sum_{i=1}^{N}\lvert P_i - O_i\rvert}{\sum_{i=1}^{N} O_i}$	Percent
Mean Normalized Bias	MNB	$\frac{1}{N}\sum_{i=1}^{N}\frac{(P_i - O_i)}{O_i}$	Reported as %
Mean Normalized Gross Error	MNE	$\frac{1}{N}\sum_{i=1}^{N}\frac{\lvert P_i - O_i\rvert}{O_i}$	Reported as %
Mean Fractionalized Bias (Fractional Bias)	MFB or FB	$\frac{2}{N}\sum_{i=1}^{N}\left(\frac{P_i - O_i}{P_i + O_i}\right)$	Reported as %
Mean Fractional Error	MFE or FE	$\frac{2}{N}\sum_{i=1}^{N}\left\lvert\frac{P_i - O_i}{P_i + O_i}\right\rvert$	Reported as %

The U.S. Regional Planning Organizations (RPOs) have established model performance goals and criteria for $PM_{2.5}$, PM_{10} and components of fine particle mass based on previous model performance for ozone and fine particles (e.g., Boylan and Russell, 2006; Morris et al., 2004a,b; 2009a,b). Table 5-3 summarizes EPA's ozone performance goals (EPA, 1991) and lists the model performance goals and criteria developed by the RPOs for PM to assist in interpreting the evaluating regional model performance for PM species.

Table 5-3. Model performance goals and criteria for PM.

Fractional Bias	Fractional Error	Comment
≤±15%	≤35%	Goal for PM model performance based on ozone model performance, considered excellent performance[1]
≤±30%	≤50%	Goal for PM model performance, considered good performance.[2]
≤±60%	≤75%	Criteria for PM model performance, considered average performance. Exceeding this level of performance indicates fundamental concerns with the modelling system and triggers diagnostic evaluation.[2]

[1]The ozone performance goals were originally developed for hourly ozone (EPA, 1991) but have also been shown to be useful for 8-hour ozone and 24-hour PM. Although we would not expect a model's PM performance to achieve this goal very often as measurement artifacts can be greater than this goal.

[2]The PM performance goals and criteria were developed for 24-hour PM concentrations.

5.4 Diagnostic Tests and Sensitivity Analyses

Episode #1 and #2 were selected for focused WRF/CMAQ 4 km domain sensitivity test modelling. The quality assurance of the McIntyre speciated $PM_{2.5}$ observations identified two of the samples during Episode#1 as being invalid due to discrepancies with the Dichot $PM_{2.5}$ measurements that limited its usefulness for evaluating the CMAQ diagnostic sensitivity tests.

CMAQ was first run for the 36/12 km domains using meteorological output from Phase I WRF-CFSR and the updated EC inventory (described in Section 3.1). The CMAQ 12 km outputs were processed using the BCON processor to generate BCs inputs for the 4 km domain that covers the Capital Region and vicinity. Model performance statistics for 24-hour $PM_{2.5}$ were computed for Episode#1 and #2. PM speciated data at McIntyre sites were not valid during Episode#1, thus model performance statistics for PM species were only calculated for Episode#2.

Although model performance statistics were calculated for three types of bias and error (fractional, normalized mean and mean normalized), we focus the discussion on the fractional bias and error (FB and FE) since that was the form that the PM Performance Goals and Criteria were developed for (Table 5-3). Furthermore, in a recent paper by USEPA (Simon, Philips and Baker, 2012) they preferred the FB/FE metrics because they were balanced treating high and low observations equally and bounded; FB by -200 to +200 percent and FE by 0 to 200 percent.

5.4.1 Test#1: Four WRF simulations from Phase II A

Given the importance of meteorology for simulating PM concentrations, the first sensitivity test compared PM model performance of the CMAQ model using the new four WRF meteorology outputs from Phase II A (Table 5-4) and WRF output from Phase I. This sensitivity test applied the updated EC 2010 emissions inventory (described in Section 3.1).

Table 5-4. Description of CMAQ scenarios in Test#1.

Scenario	Description		
	Meteorology	Emissions	CMAQ version
CFSR_MYJ	WRF IC/BCs = CFSR; PBL scheme = MYJ (Phase II-A)	Updated EC 2010	V 5.0.2
CFSR_YSU	WRF IC/BCs = CFSR; PBL scheme = YSU (Phase II-A)	Updated EC 2010	V 5.0.2
ERA_MYJ	WRF IC/BCs = ERA; PBL scheme = MYJ (Phase II-A)	Updated EC 2010	V 5.0.2
ERA_YSU	WRF IC/BCs = ERA; PBL scheme = YSU (Phase II-A)	Updated EC 2010	V 5.0.2
Phase I	WRF IC/BCs = CFSR; PBL scheme = YSU (Phase I)	Phase I with no updates	V 5.0.1
Phi-met	WRF IC/BCs = CFSR; PBL scheme = YSU (Phase I)	Updated EC 2010	V 5.0.2

A comparison of the CMAQ WRF sensitivity test results against the speciated $PM_{2.5}$ data at McIntyre site suggest that CMAQ results using Phase I WRF outputs exhibit high bias (i.e., FB and FE > 100%) of sulphate (SO_4; Figure 5-1,top). The sulphate performance only improves slightly when using an alternative emissions inventory (EC 2010) and a newer version of CMAQ (v5.0.2). All CMAQ simulations using Phase II-A WRF show significant sulphate improvement reducing fractional error down to the range of 52-72%. This improvement can be attributed to less cloud availability in all four Phase II-A WRF outputs compared to the Phase I WRF modelling.

Phase I CMAQ simulation underestimated nitrate (NO_3) by over a factor of 2 with average observed and predicted values for the four speciated $PM_{2.5}$ measurement during Episode#2 of 10.3 and 4.3 $\mu g/m^3$, respectively. Nitrate performance is improved with the Phase II-A WRF outputs, particularly CFSR_MYJ and ERA_MYJ. Average predicted nitrate increases to 6.6 and 6.8 $\mu g/m^3$ in CFSR_MYJ and ERA_MYJ, respectively.

Both elemental carbon (EC) and organic carbon (OC) are overestimated in all scenarios. In the four new WRF CMAQ simulations, EC is overestimated by a factor of 5.5 to 6.5 and OC is overestimated by a factor of 2.7 to 3.3. ERA_MYJ and ERA_YSU perform slightly better than other two WRF simulations. More than 90% of the predicted OC mass is primary, emitted directly from anthropogenic sources. The poor EC and OC performances are likely caused by overstated PM emissions.

With primary PM being highly overstated and the secondary PM being underestimated, it is not meaningful to examine $PM_{2.5}$ mass performance. Perhaps the conclusions that can be drawn from this test are:

- Phase I and updated EC 2010 inventories give comparable CMAQ MPE results
- Phase II-A WRF simulations significantly improve secondary PM performances
- Sulphate performance is improved significantly with the new WRF simulations due to less cloud availability but sulphate on the peak day is underestimated by a factor of 7
- Similar performances of primary PM among all WRF scenarios support that better sulphate improvement is driven by chemistry, not due to dispersion.
- Best overall CMAQ performance is seen from ERA_MYJ scenario

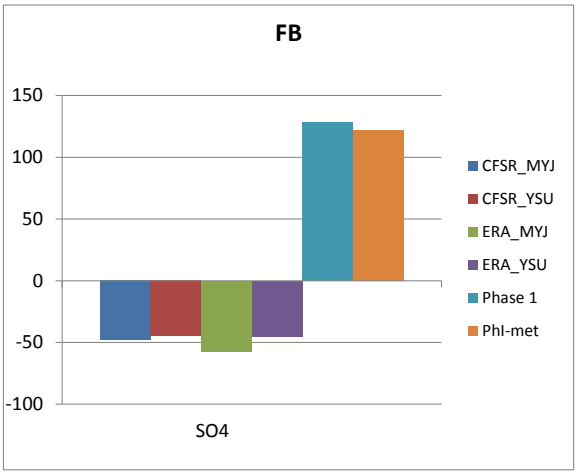
FB
150
100
50
0
-50
-100
SO4
CFSR_MYJ
CFSR_YSU
ERA_MYJ
ERA_YSU
Phase 1
PhI-met

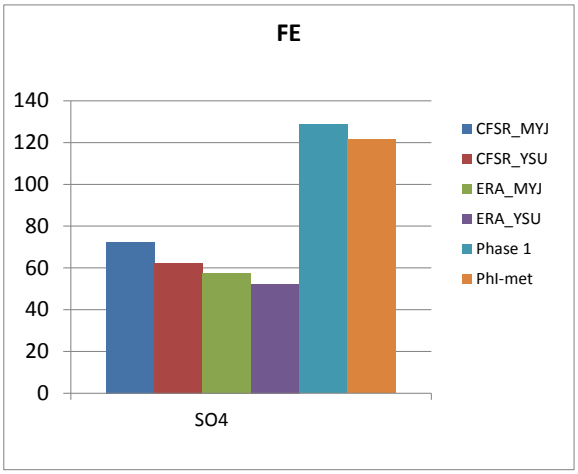
FE
140
120
100
80
60
40
20
0
SO4
CFSR_MYJ
CFSR_YSU
ERA_MYJ
ERA_YSU
Phase 1
PhI-met

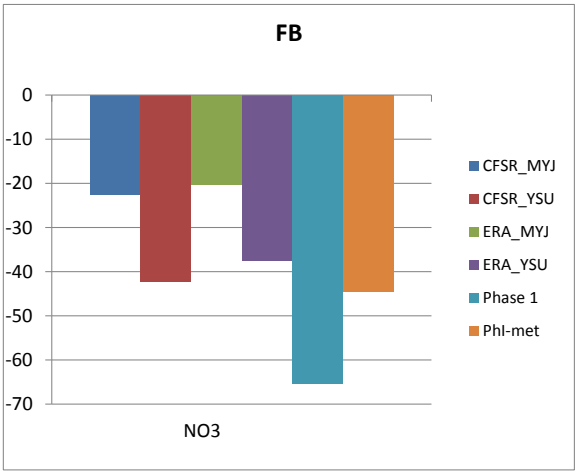
FB
0
-10
-20
-30
-40
-50
-60
-70
NO3
CFSR_MYJ
CFSR_YSU
ERA_MYJ
ERA_YSU
Phase 1
PhI-met

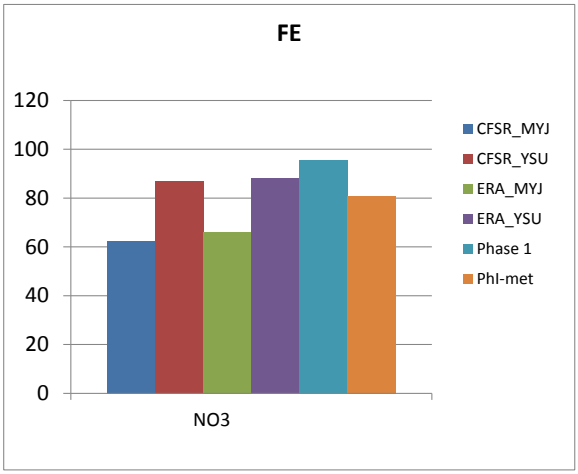
FE
120
100
80
60
40
20
0
NO3
CFSR_MYJ
CFSR_YSU
ERA_MYJ
ERA_YSU
Phase 1
PhI-met

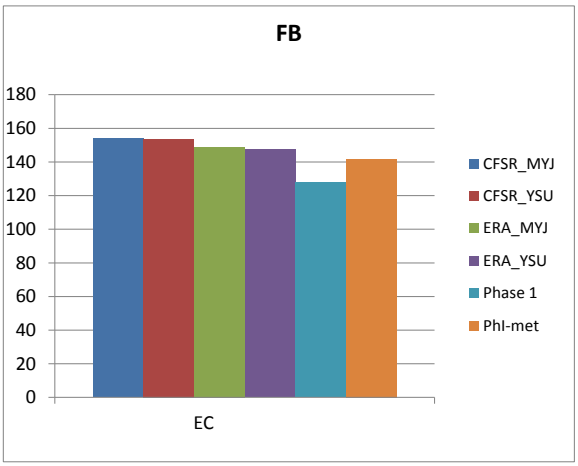
FB
180
160
140
120
100
80
60
40
20
0
EC
CFSR_MYJ
CFSR_YSU
ERA_MYJ
ERA_YSU
Phase 1
PhI-met

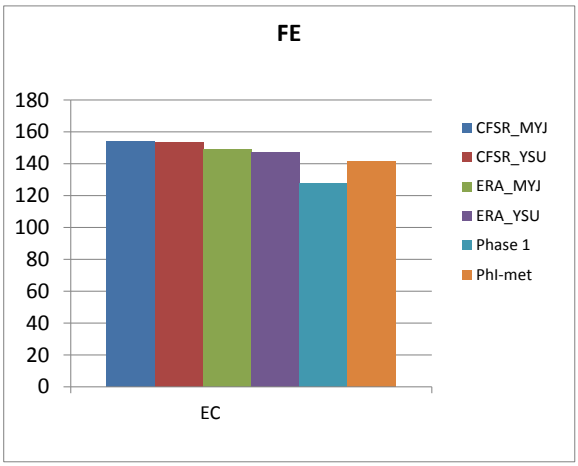
FE
180
160
140
120
100
80
60
40
20
0
EC
CFSR_MYJ
CFSR_YSU
ERA_MYJ
ERA_YSU
Phase 1
PhI-met

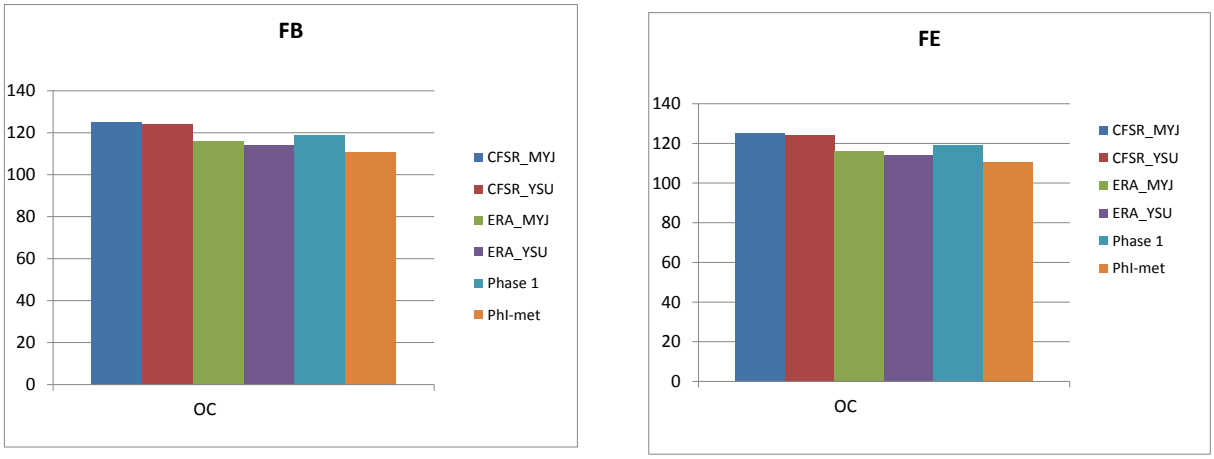

Figure 5-1. WRF Phase II A and WRF Phase I Episode#2 Fractional Bias and Error (%) model performance for 24-hour speciated $PM_{2.5}$ at the Edmonton McIntyre monitoring site.

5.4.2 Test#2: Heterogeneous N_2O_5 hydrolysis

In the ENVIRON Capital Region PM Modelling Study Phase I report, we recommended reducing the 15 minute coupling time step used in CMAQ. The reason behind this recommendation is to increase the frequency of the N_2O_5 formation in the gas-phase chemistry and the N_2O_5 hydrolysis reaction to form nitric acid in the aerosol chemistry that are coupled using the CMAQ default 15 minute coupling time step. The N_2O_5 hydrolysis is treated in aerosol/heterogeneous chemistry. The gas-phase is converting NO_2 to N_2O_5 using smaller time steps (~30 s), with part of the N_2O_5 disassociating back to NO_2. The gas-phase and aerosol-phase chemistry are coupled only every 15 minutes in CMAQ, and during the 15 minute-period N_2O_5 could be depleted by aerosol-phase chemistry even though it is continuously produced by the gas-phase chemistry. If these processes were allowed to interact more frequent, that could form more HNO_3 and NO_3. We considered lowering this coupling time step to increase NO_3 formation. However, CMAQ would run much slower because the aerosol-chemistry is called 30 times every 15 minute. In addition, the small time step would adversely introduce numerical diffusion due to more frequent advection calculations.

Alternatively, treating N_2O_5 hydrolysis and heterogeneous reactions in the gas-phase chemistry could potentially increase NO_3 formation while the efficiency of CMAQ remains intact. We contacted USEPA about this issue and it turned out they had already modified the CMAQ v5.0.2 codes to move the N_2O_5 hydrolysis reactions from the CMAQ aerosol chemistry module to gas-phase chemistry module. We obtained this modified CMAQ code and reviewed the implementation. We identified an error in the implementation of some of the rate constants that USEPA corrected and this modified CMAQ code was used for Test#2. Test#2 utilized CFSR_MYJ, CFSR_YSU, and ERA_MYJ as meteorology.

All CMAQ sensitivity tests after moving N_2O_5 hydrolysis to gas-phase module (labeled as 'WRF'_mod) show no improvement of nitrate performance (Figure 5-2). We found that gas-

phase and aerosol-phase chemistry time steps for the 4-km domain during Episode#2 are roughly the same (~2.5 minutes), so the modification was ineffective.

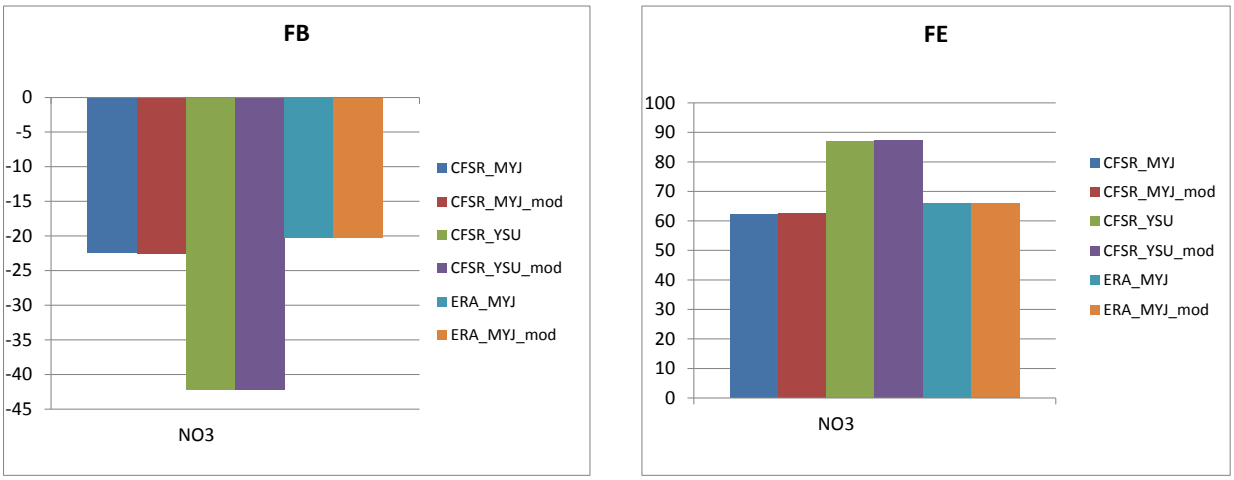

Figure 5-2. Before and after moving N_2O_5 hydrolysis to gas-phase module: Episode#2 Fractional Bias and Error model performance for 24-hour nitrate at the Edmonton McIntyre monitoring site.

5.4.3 Test#3: Off-Road Emissions

This test removed emissions related to off-road equipment that are not expected to operate in winter months (as described in Section 3.2.3). This test used the ERA_MYJ WRF outputs and the Phase I emissions inventory (with no CALMOB6 integration).

EC performance improves significantly when removing non-winter off-road emissions as shown in Figure 5-3 (most-left red bars) and Figure 5-4. Fractional error has gone down from 137% to 71%. Although this particular test targeted EC, other PM species were also affected because their emissions associated with this set of equipment were also removed. Specifically, FE and FB of OC are reduced by 8.5%. Primary sources of OC emissions are residential wood combustion so smaller impacts are as expected. Nitrate performance is also slightly better, most likely as a result of NO_X emissions reduction resulting in higher ozone concentrations (more testing on this topic in Test#5). Since sulphate was already underestimated, its performance was degraded slightly in this test.

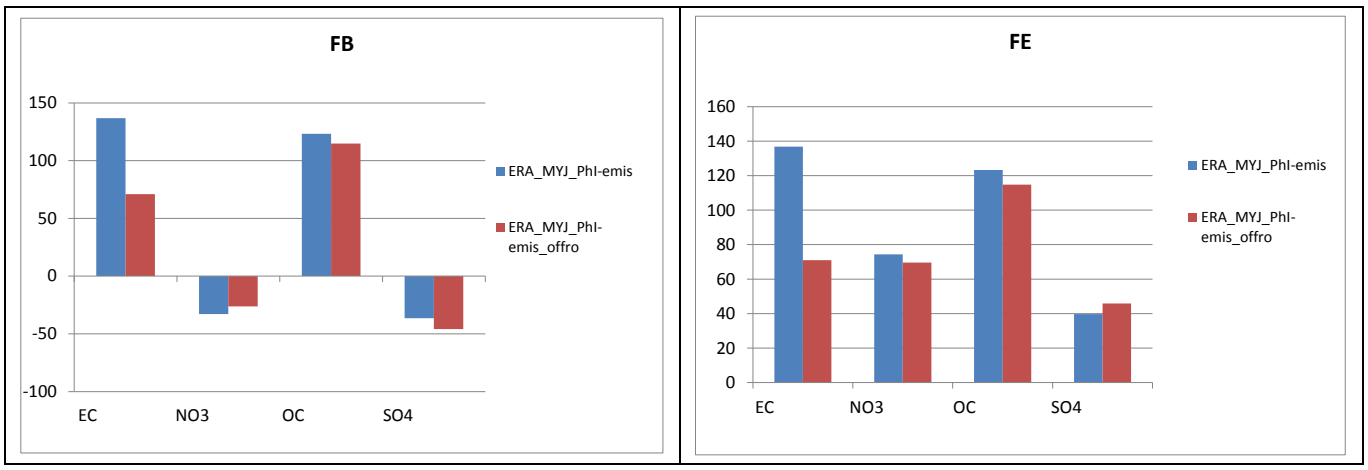

Figure 5-3. Before (blue bars) and after (red bars) removing off-road emissions not operating in winter: Episode#2 Fractional Bias and Error model performance for 24-hour nitrate at the Edmonton McIntyre monitoring site.

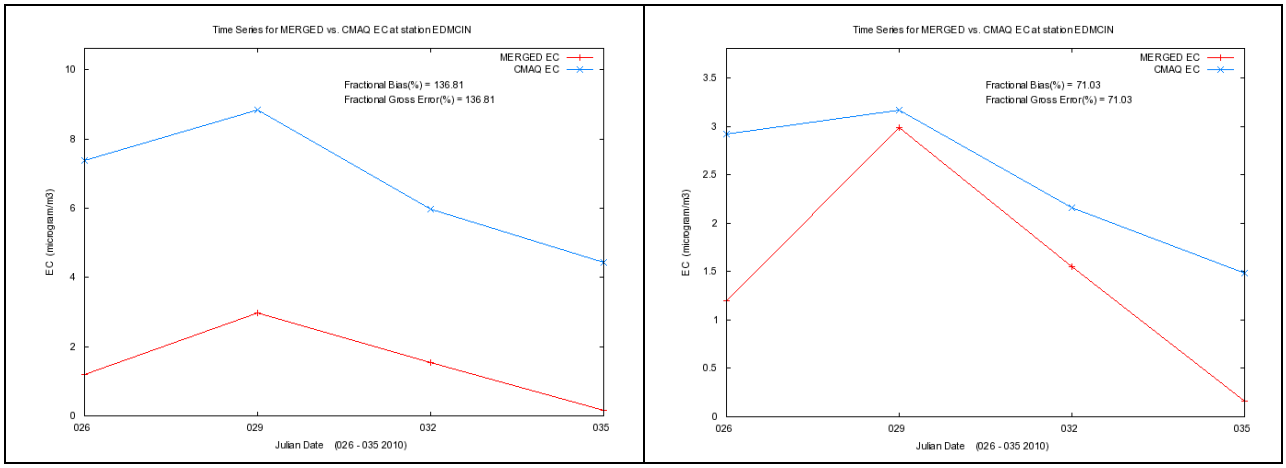

Figure 5-4. Time series of EC before (left) and after (right) removing off-road emissions not operating in winter

5.4.4 Test#4: Residential Wood Combustion (RWC) Emissions

Two CMAQ simulations were performed in this test: a) without RWC emissions and b) with reallocated RWC emissions following rural spatial distribution. We incorporated point source updates for the top 100 stacks (described in Section 3.2.1) to the emissions inventory used in Test#3 which excludes non-winter off-road emissions. WRF meteorology used in this test is ERA_MYJ.

The point source updates introduce minimal impacts to EC and OC performances (Figure 5-5, top compared to Figure 5-4). Specifically, OC is still largely overestimated on all four measurement days during Episode#2 and EC is overestimated on non-peak days. Reallocating RWC emissions to rural housing (Figure 5-5, bottom) reduces the 4-day average OC concentration from 8.9 to 6.9 µg/m^3 (22%). Removing all RWC emissions brings the 4-day

average OC concentration down to 3.7 µg/m^3 (58%) which is close to the average observation concentration of 3.1 µg/m^3. EC performance is also affected by adjusting RWC emissions, but to a lesser extent. Reallocating RWC emissions and removing these emissions reduce the 4-day average EC concentration from 2.4 to 2.0 and 1.5 µg/m^3, respectively.

There is not information to express whether removing all RWC emissions in the Capital region is appropriate. We merely conducted this sensitivity test to provide upper bound impacts from this source category (equivalent to zero-out approach). Reallocating RWC emissions to rural areas, however, deems appropriate. Future modeling exercise should examine the current rural housing spatial surrogate and determine whether Edmonton areas are defined appropriately.

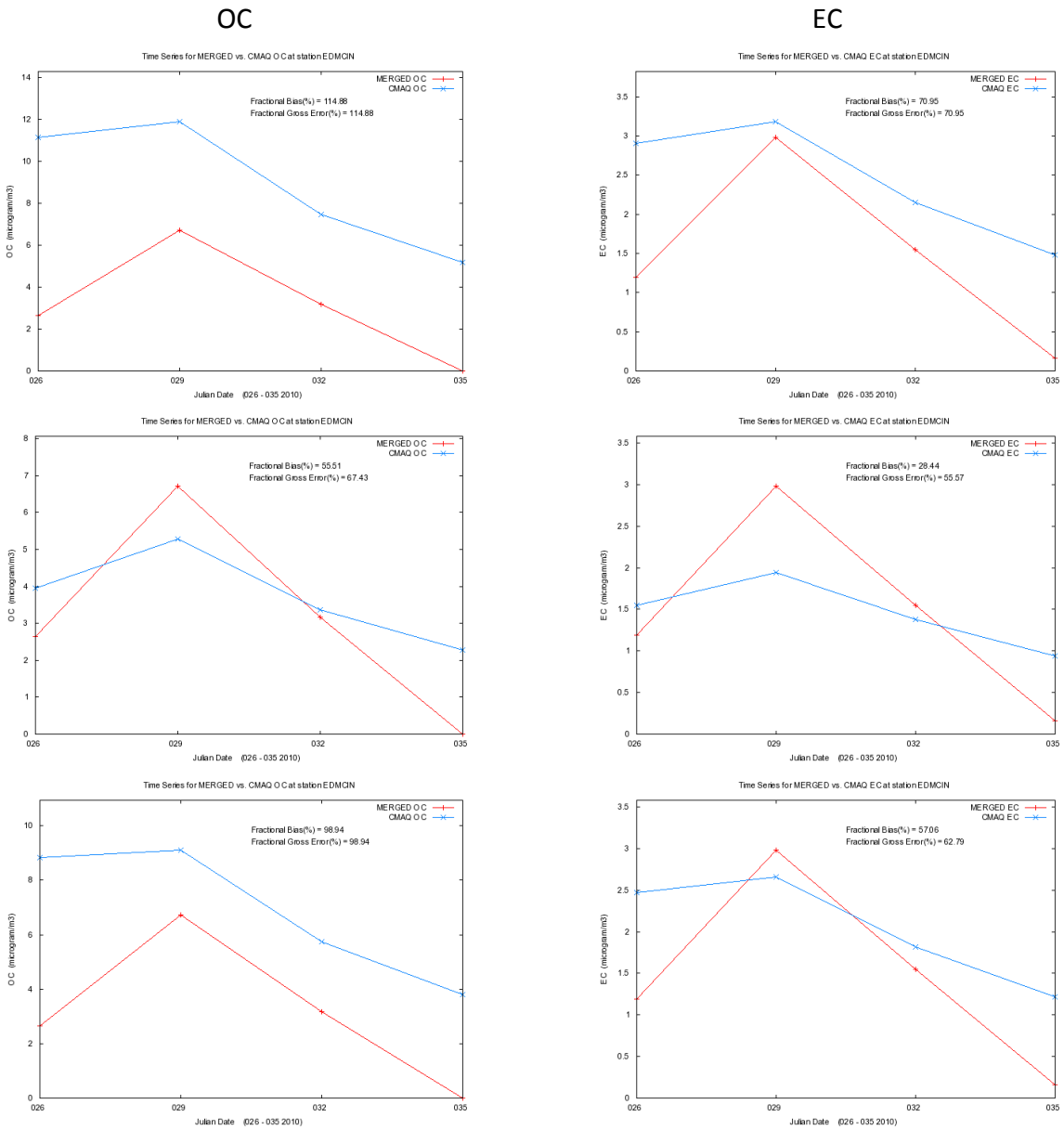

Figure 5-5. Time series of OC (left) and EC (right) before (top) and after adjusting RWC emissions by removing all (middle) or reallocating to rural areas (bottom)

5.4.5 Test#5: Reducing Surface NO_X Emissions

As discussed in Chapter 2, NO_3 formation via N_2O_5 depends on generation of radicals (e.g., NO_3^-) that will be highly dependent on ozone concentrations. Ozone is generally underestimated in the Capital Region for these winter periods that causes too few radicals to be available so understates the conversion of NO_X to HNO_3. Surface ozone can be depleted when there are excess NO_X emissions. This titration effect usually occurs at night in urban areas when VOC emissions are low and NO_X concentrations have built up. In the Phase I study, we found that better ozone performance is seen when the ozone BCs are increased by 20 ppb and increased ozone BCs also improve NO_3 model performance. Test#5 includes two CMAQ simulations that

were designed to promote local production of ozone by reducing surface NO_X emissions. The first CMAQ simulation reduces surface NO_X emissions in the Capital Region by 50%. The second simulation incorporated the CALMOB6 emissions (described in Section 3.2.2), reducing NO_X emissions in Edmonton by about 30%.

Nitrate time series at Edmonton McIntyre site and NO_X time series at Edmonton Central are shown in Figure 5-6 left and right, respectively. Reducing surface NO_X emissions by 50% (middle row) only increases ozone by about 4 ppb compared to the observed value of 7 ppb at the time $PM_{2.5}$ mass started to accumulate on Jan 28. Nitrate increases by 7% on the peak day (i.e., from 9.3 to 9.8 $\mu g/m^3$), while the NO_X performance is degraded considerably at Edmonton Central. This test suggests that ozone availability in Edmonton is insufficient to produce nitrate at the observed level even after removing a large amount of emitted NO_X.

The CMAQ simulation with CALMOB6 emissions sees about 3% increase of nitrate while NO_X performance is not degraded (bottom row). This result implies that across the board adjustment (e.g., 50% NO_X reduction across the Capital Region) will not be as effective as targeted adjustment.

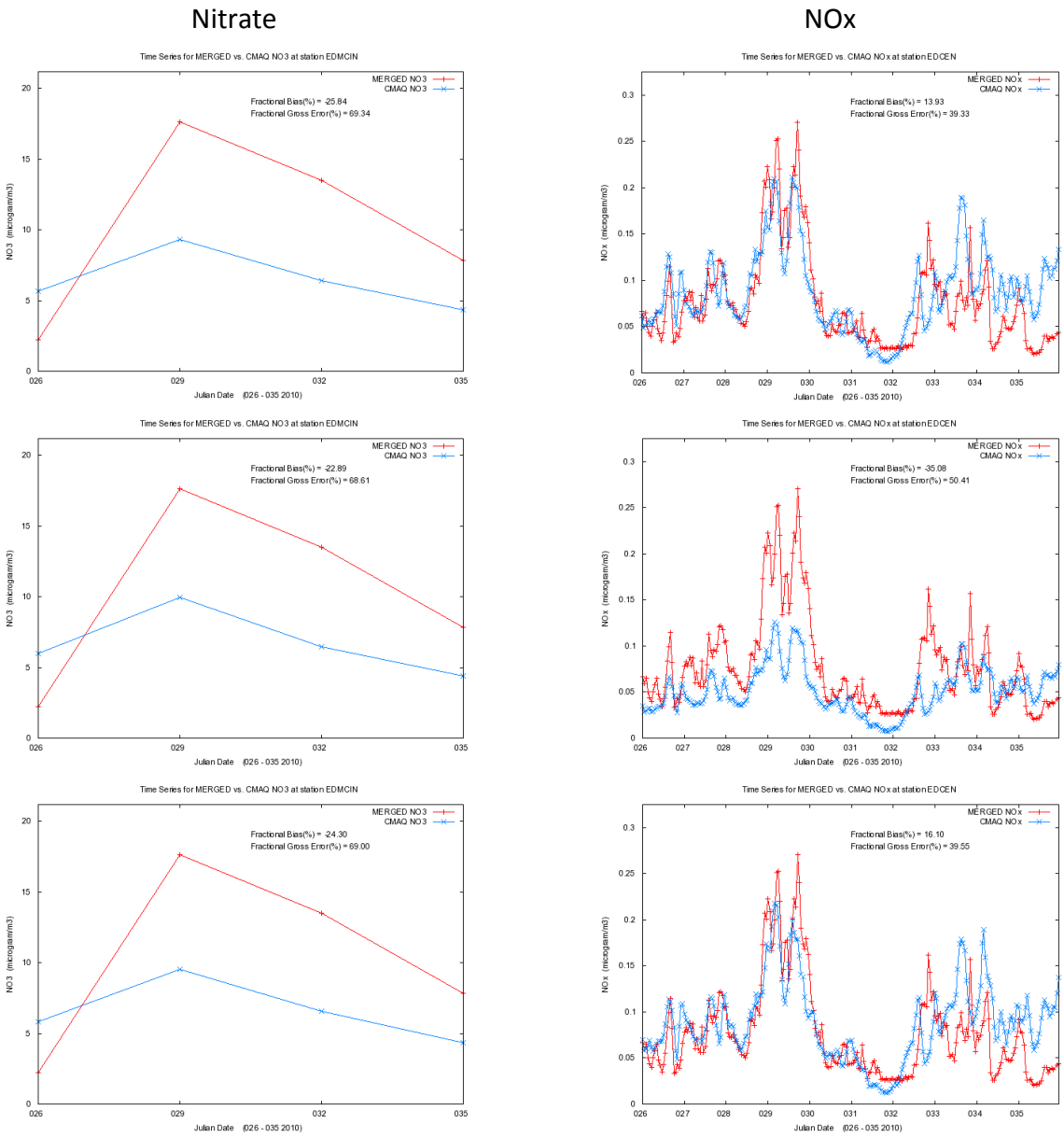

Figure 5-6. Time series of NO_3 at Edmonton McIntyre (left) and NO_X at Edmonton Central (right) before (top) and after reducing NO_X emissions by 50% (middle) or by integration of CALMOB6 emissions (bottom)

5.4.6 Test#6: Vertical Diffusion Sensitivity Test

One of the sensitivity tests conducted in the Phase I study limited vertical diffusion to reduce bringing down SO_2 concentrations from aloft plumes. By setting the vertical diffusion coefficient (K_v) to a low value (0.01 m^2/s), predicted concentrations of most PM species except nitrate more than double the base case concentrations. Test#6 was designed to perform additional vertical mixing tests.

CMAQ sets a minimum K_v ($K_{v,min}$) of 0.01 m^2/s to ensure enough mixing at night. This value can go up to 1 m^2/s in urban grid cells to take into account the effects of the urban heat island on vertical mixing. Three CMAQ sensitivity runs were conducted under this test (Table 5-5). The first simulation reduces maximum $K_{v,min}$ from 1 m^2/s to 0.5 m^2/s (scenario 'Kvmin_0p5'). The second simulation promotes more mixing by increasing $K_{v,min}$ from 1 m^2/s to 2 m^2/s (scenario 'Kvmin_2p0'). The third simulation further set $K_{v,min}$ to 2 m^2/s regardless of urban or non-urban grid cells (scenario 'Kvmin_2p0_allgrid').

Table 5-5. Description of CMAQ scenarios in Test#6.

Scenario	Description		
	Meteorology	Emissions	Kv,min
ERA_MYJ	WRF IC/BCs = ERA; PBL scheme = MYJ (Phase II-A)	Phase I with point source updates	maximum $K_{v,min}$ =1 m^2/s
Kvmin_0p5	Same as above	Same as above	maximum $K_{v,min}$ =0.5 m^2/s
Kvmin_2p0	Same as above	Same as above	maximum $K_{v,min}$ =2 m^2/s
Kvmin_2p0_allgrid	Same as above	Same as above	maximum $K_{v,min}$ =2 m^2/s for all grid cells

A comparison of the CMAQ K_v sensitivity test results against the speciated $PM_{2.5}$ data at McIntyre site suggest that primary species (i.e., OC and EC) are more sensitive to Kv than secondary species as shown in Figure 5-7 and Figure 5-8. Setting maximum $K_{v,min}$ to 0.5 or 2 m^2/s at urban grid cells introduces less than 2% change of nitrate average concentrations and less than 7% change of sulphate. Larger impacts are seen for OC and EC whose average concentrations change by 17-20%.

Allowing more mixing at all grid cells (non-urban and urban; scenario 'Kvmin_2p0_allgrid') broadly increases ozone in the 4km domain on Jan 28 with the maximum increase of 32 ppb (Figure 5-9). Although predicted ozone at the Edmonton McIntyre grid cell increases as high as 20 ppb, predicted nitrate only increases by 18% on Jan 29. The test implies that a lot more ozone is needed to produce the level of nitrate concentrations observed. In addition, the estimated ozone concentrations are already higher than observed ozone concentrations at Edmonton sites which are about generally less than 10 ppb. Adjusting vertical mixing appears to be ineffective to raise nitrate concentrations. Other radicals or reaction pathways that do not rely on ozone availability are likely contributing to high nitrate formation in the Capital Region during winter period.

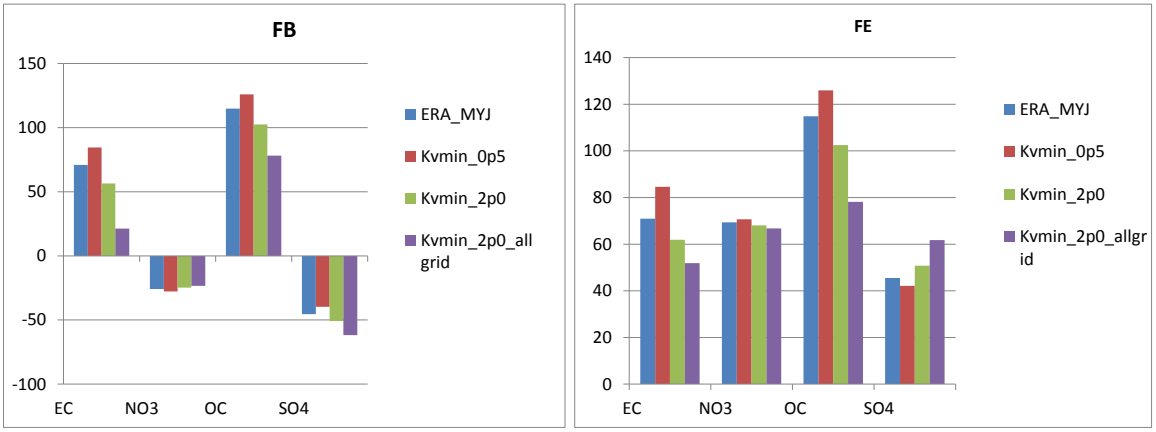

Figure 5-7. Kv sensitivity test: Fractional Bias and Error (%) model performance for 24-hour speciated $PM_{2.5}$ at the Edmonton McIntyre monitoring site.

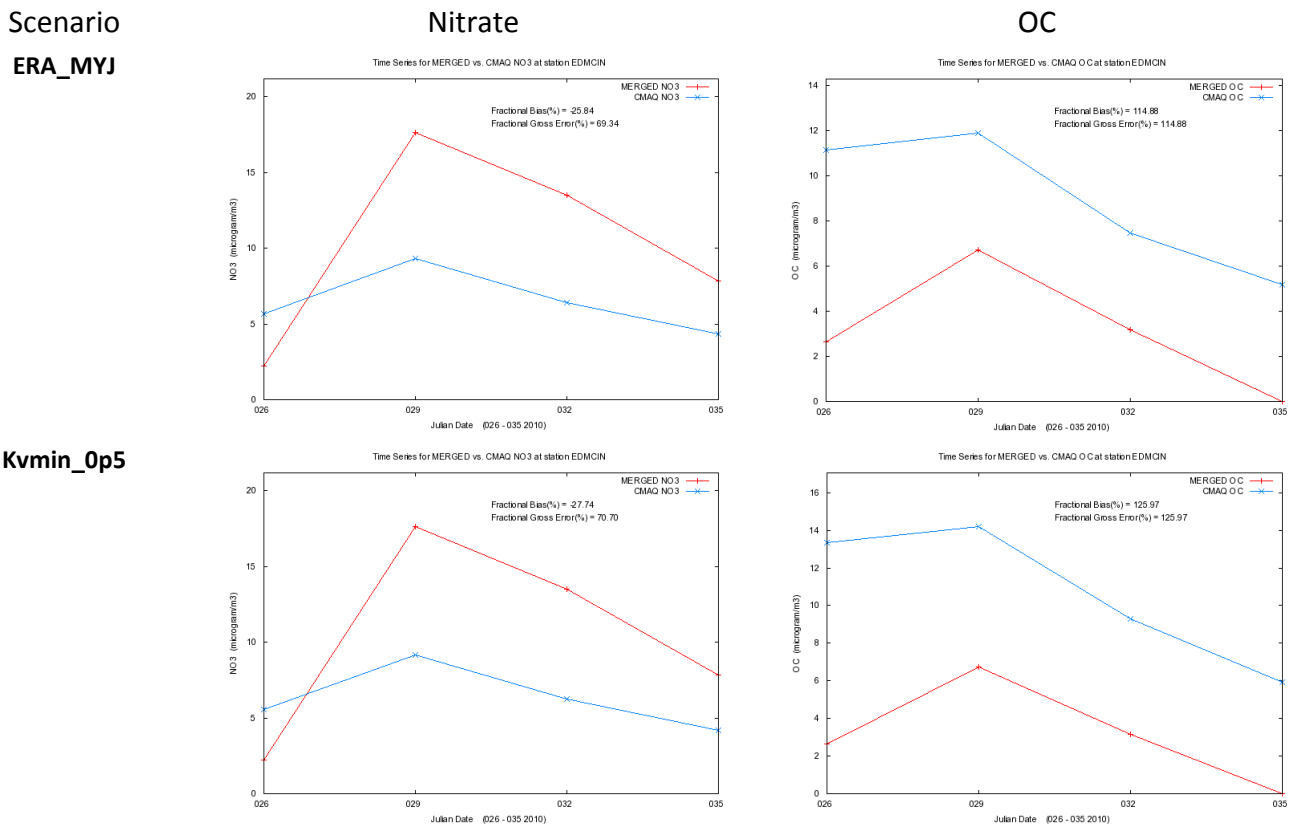

Scenario	Nitrate	OC
Kvmin_2p0	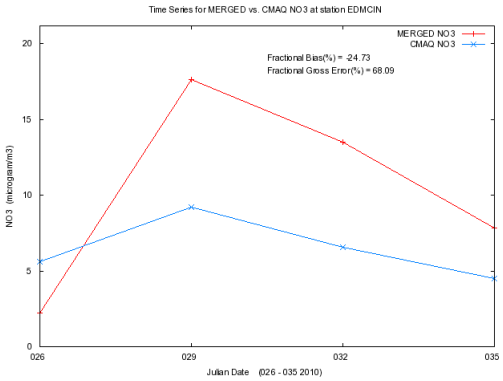	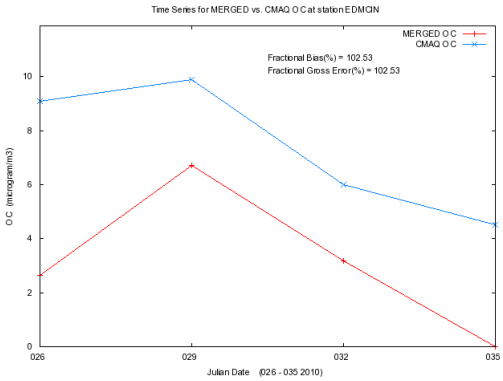
Kvmin_2p0_allgrid	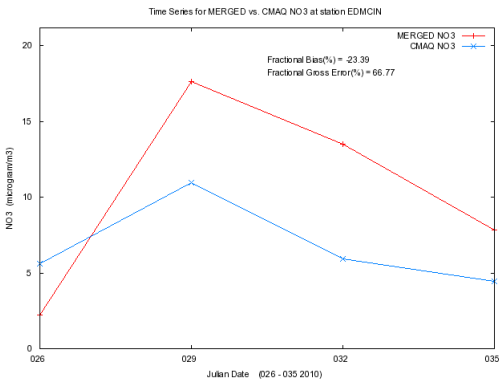	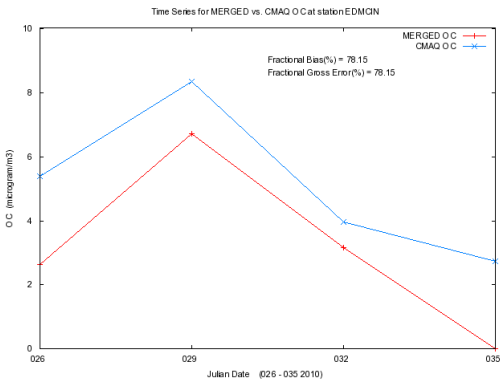

Figure 5-8. Time series of NO_3 (left) and OC (right) at Edmonton McIntyre before (top) and after adjusting minimum Kv to 0.5 m^2/s (2nd row), 2 m^2/s (3rd row), and 2 m^2/s at all grid cells (4th row)

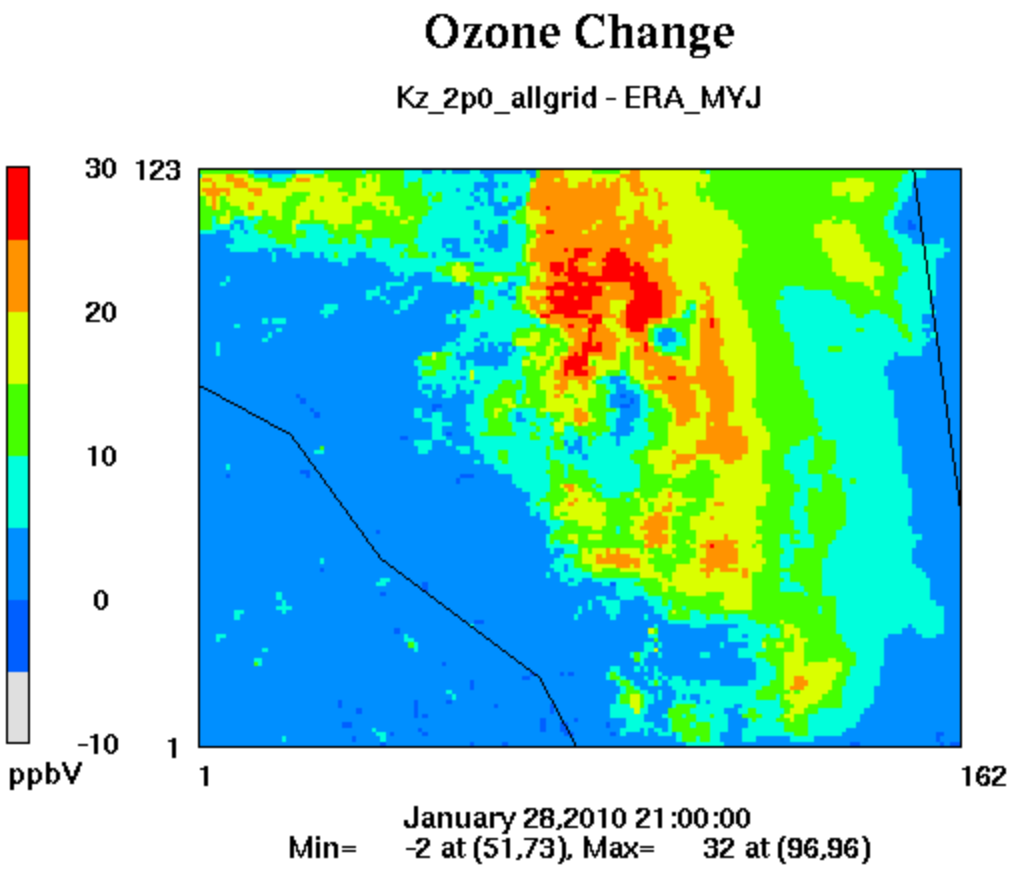

Figure 5-9. Difference in CMAQ-estimated ozone concentrations (ppb) in the 4 km domain on January 28 at 14:00 PM MST (when $PM_{2.5}$ mass started to accumulate) due to more mixing (i.e., maximum $K_{v,min}$ = 2 m^2/s) at urban and non-urban grid cells

5.4.7 Test#7: Heterogeneous Reaction Test

This sensitivity test was designed to examine nitrate formation via heterogeneous reactions. There are two heterogeneous reactions in CMAQ that form HNO_3:

A. N_2O_5 → 2.0 HNO_3

B. NO_2 → 0.5 HONO +0.5 HNO_3

One of the sensitivity tests conducted in the Phase I study increased the rate of reaction (A). This reaction rate is capped in CMAQ based on laboratory measurements at much warmer temperature and drier conditions than occurs during the Capital Region winter PM episodes. Raising this cap by a factor of three resulted in slightly more NO_3 formation. The overall process was limited by N_2O_5 availability which depended strongly on ozone concentrations.

Reaction (B) could be important because NO_X is abundant during high PM days in Edmonton. In addition, this pathway does not rely on an availability of radicals which appears limited in Edmonton. The reaction rate is expressed as pseudo first-order, independent of meteorology:

kNO_2 = 3.0e-3 [1/min] x [Surface to Volume ratio] Kurtenbach et al. (2001)

Test#7 increased this reaction rate by a factor of 10 (kNO_2x10) and 100 (kNO_2x100). Note that the heterogeneous reaction of NO_2 in CMAQ occurs in two places: aerosol surface and ground surface. The reaction on the ground surface is implemented in the deposition module and HNO_3 produced via this pathway is lost as they are assumed to stick to the ground surface. We only modified the rate occurring on aerosol surface.

Time series of nitrate at Edmonton McIntyre and NO_X at Edmonton Central are shown in Figure 5-10. The 24-hour average nitrate concentration on Jan 29 increases by 7% and 120% when the reaction rate (kNO_2) is increased by a factor of 10 and 100, respectively. The kNO_2x100 scenario is the only test in this study that the predicted average nitrate concentration on Jan 29 (20.5 $\mu g/m^3$) is higher than the observed value (17.7 $\mu g/m^3$). NO_X concentrations are reduced slightly in both tests, but the NO_X performance statistics at Edmonton Central are still comparable among all scenarios as shown in Figure 5-10 (right).

The results suggest that default kNO_2, may be too low for stagnant winter conditions. We are not suggesting that this rate should be increased by a factor of 100. The test merely implies that HNO_3 formation pathways that can convert NO_X directly to HNO_3 without relying on availability of radicals may be the key contributor to high nitrate in the Capital Region winter conditions and the magnitude of the rates may be comparable to 0.3 [1/min] x [Surface to Volume ratio] (i.e., 100 x kNO_2). These pathways are, perhaps, still missing in CMAQ.

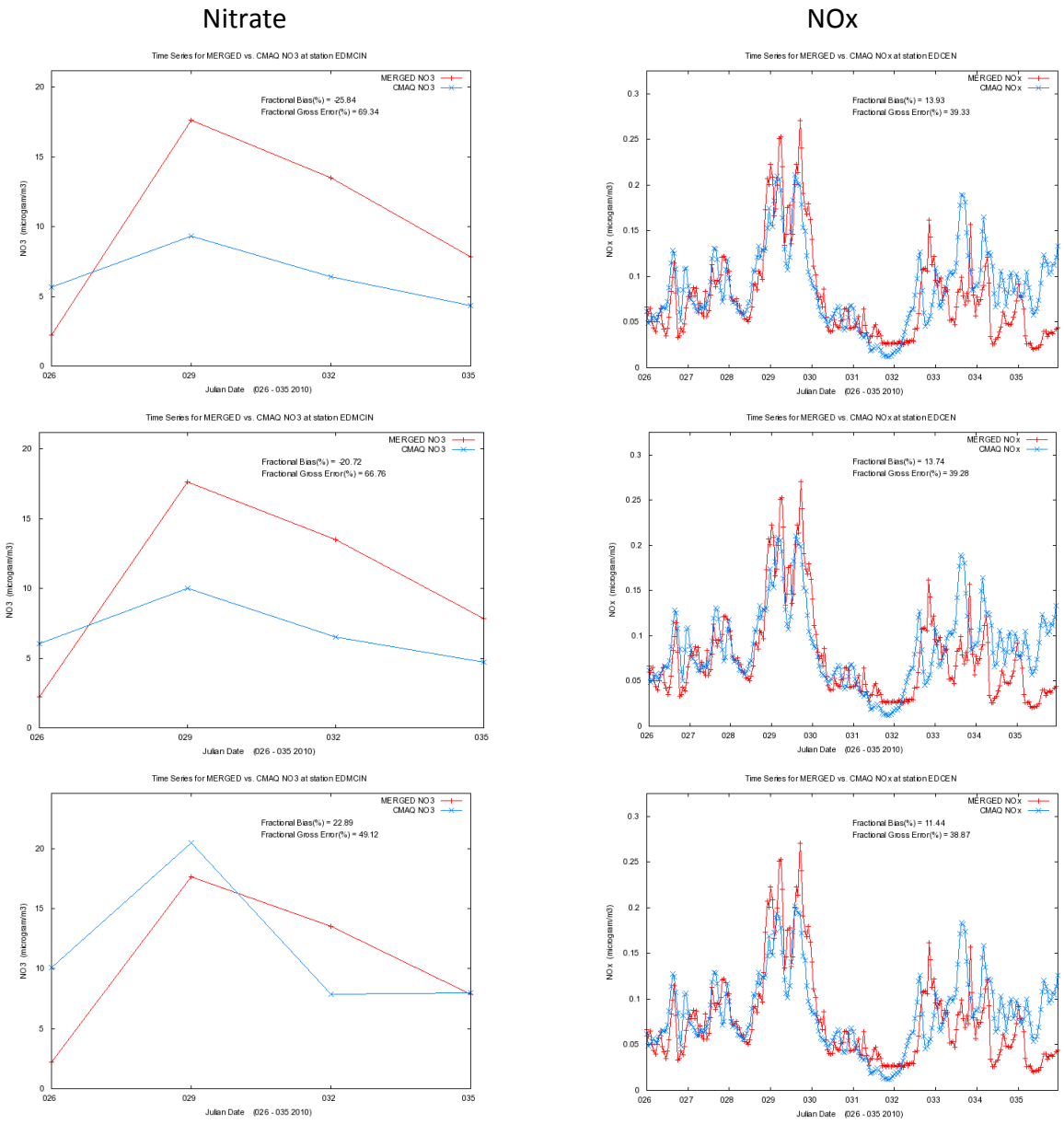

Figure 5-10. Time series of NO_3 at Edmonton McIntyre (left) and NO_X at Edmonton East (right) before (top) and after increasing $kNO_{2,heterogeneous}$ by a factor of 10 (middle) and a factor of 100 (bottom)

5.4.8 Test#8: 6 WRF Simulations from Phase II-B

After discussing the Phase II-A WRF performance with ESRD on February 20, 2015, ENVIRON were advised to have some continued scenarios with varied wind speed observational nudging and other alternative WRF setup that may improve wind and temperature performance. Test#8 compared PM model performance of the CMAQ model using the six new WRF meteorology outputs from Phase II B (Table 5-6) and ERA_MYJ WRF output from Phase II A. This sensitivity test applied the Phase I emissions inventory with all the updates introduced in this project (i.e., point sources, CALMOB6, no winter off-road, and revised RWC). Due to the time constraints, CMAQ was run for just Jan 25-Feb 3, covering three days of speciation measurements (instead of four).

Table 5-6. Description of CMAQ scenarios in Test#8.

Scenario	Description		
	Meteorology	Emissions	Note
ERA_MYJ	WRF IC/BCs = ERA; PBL scheme = MYJ	Updated Phase I EI	Phase II-A
NoahMP	WRF IC/BCs = ERA; PBL scheme = MYJ Use Noah MultiParameter LSM	Updated Phase I EI	Phase II-B
GFS_MYJ	WRF IC/BCs = GFS; PBL scheme = MYJ	Updated Phase I EI	Phase II-B
OptNudg	WRF IC/BCs = ERA; PBL scheme = MYJ Increase nudging coefficients of wind and temperature	Updated Phase I EI	Phase II-B
OptNudg+CASA	WRF IC/BCs = ERA; PBL scheme = MYJ Increase nudging coefficients of wind and temperature Add observational data from CASA website for nudging	Updated Phase I EI	Phase II-B
MoisNudg	WRF IC/BCs = ERA; PBL scheme = MYJ Increase nudging coefficients of wind and temperature Add moisture nudging	Updated Phase I EI	Phase II-B
GF_CU	WRF IC/BCs = ERA; PBL scheme = MYJ Increase nudging coefficients of wind and temperature Grell-Freitas cumulus parameterization	Updated Phase I EI	Phase II-B

All CMAQ simulations using Phase II-B WRF have very similar performances overall. Time series of EC (Figure 5-11) show consistent patterns with concentrations comparable with the observational data and most CMAQ runs except GF_CU, GFS_MYJ and Noah_MP. These three CMAQ runs show a large discrepancy of predicted EC from the observation on Jan 26, giving us some concerns that these three WRF simulations may provide less accurate mixing than other WRF setups. Time series of OC (not shown) show similar results to those of EC. There are minimal impacts to sulphate concentrations among all WRF simulations (Figure 5-12), although the OptNudg scenario predicted slightly higher sulphate concentrations than other scenarios.

Nitrate time series are presented in Figure 5-13. The ERA_MYJ CMAQ simulation underestimated nitrate by about 30% with average observed and predicted values for the three

speciated $PM_{2.5}$ measurement during Episode#2 of 11.1 and 7.7 µg/m^3, respectively. Four CMAQ simulations using WRF Phase II-B output increase this average value to 9.0, 9.1, 9.2 and 9.4 µg/m^3 using OptNudg+CASA, OptNudg, GF_CU, and MoisNudg, respectively.

The conclusions that can be drawn from this test are:

- Using local observations data from CASA website for nudging does not improve PM model performance
- GFS_MYJ, NoahMP, and GF_CU may provide less acute mixing based on CMAQ performance of primary PMs
- Best overall performance is seen from OptNudg scenario (Figure 5-14)

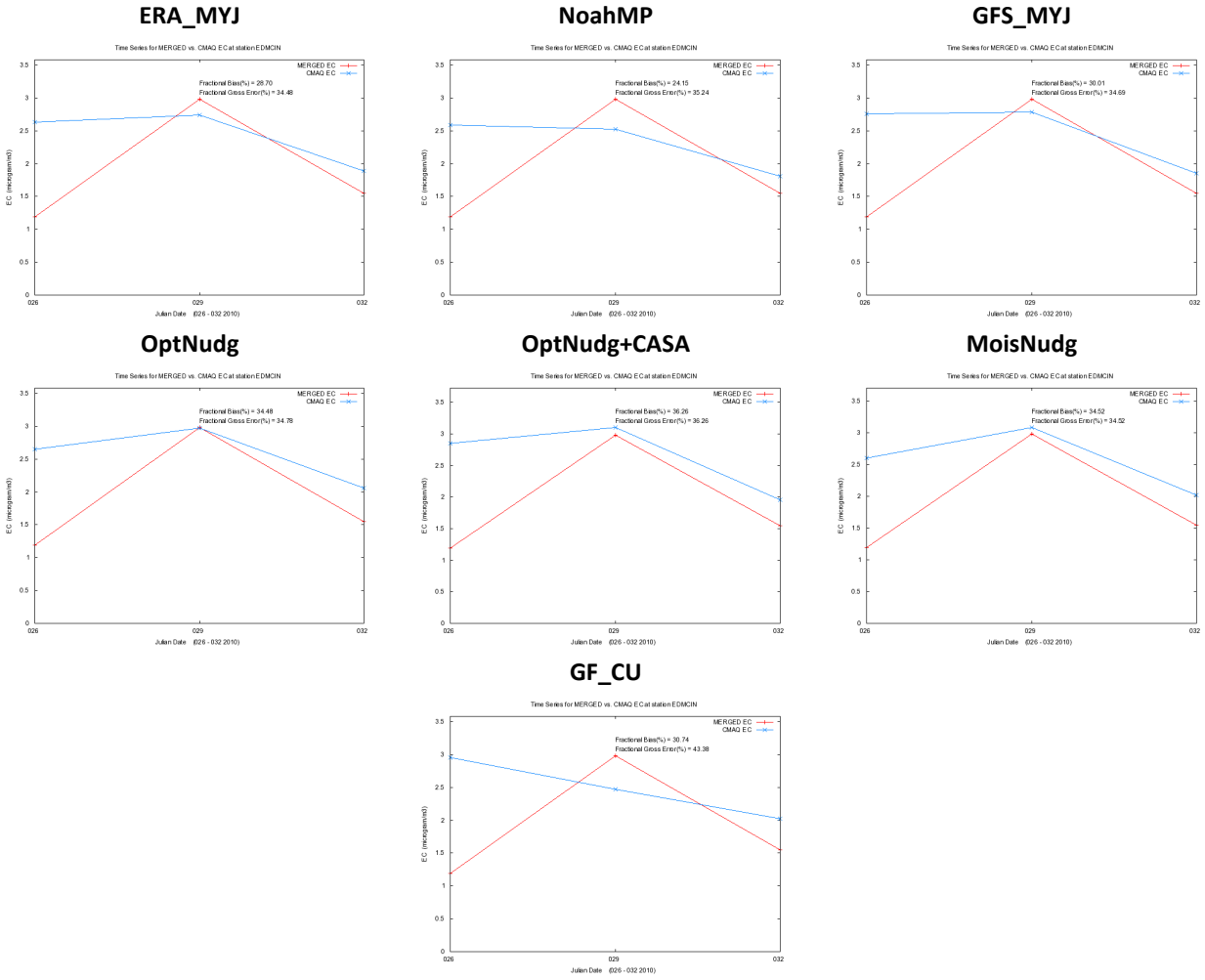

Figure 5-11. WRF Phase II A and WRF Phase II-B Episode#2 time series for 24-hour EC concentrations at the Edmonton McIntyre monitoring site

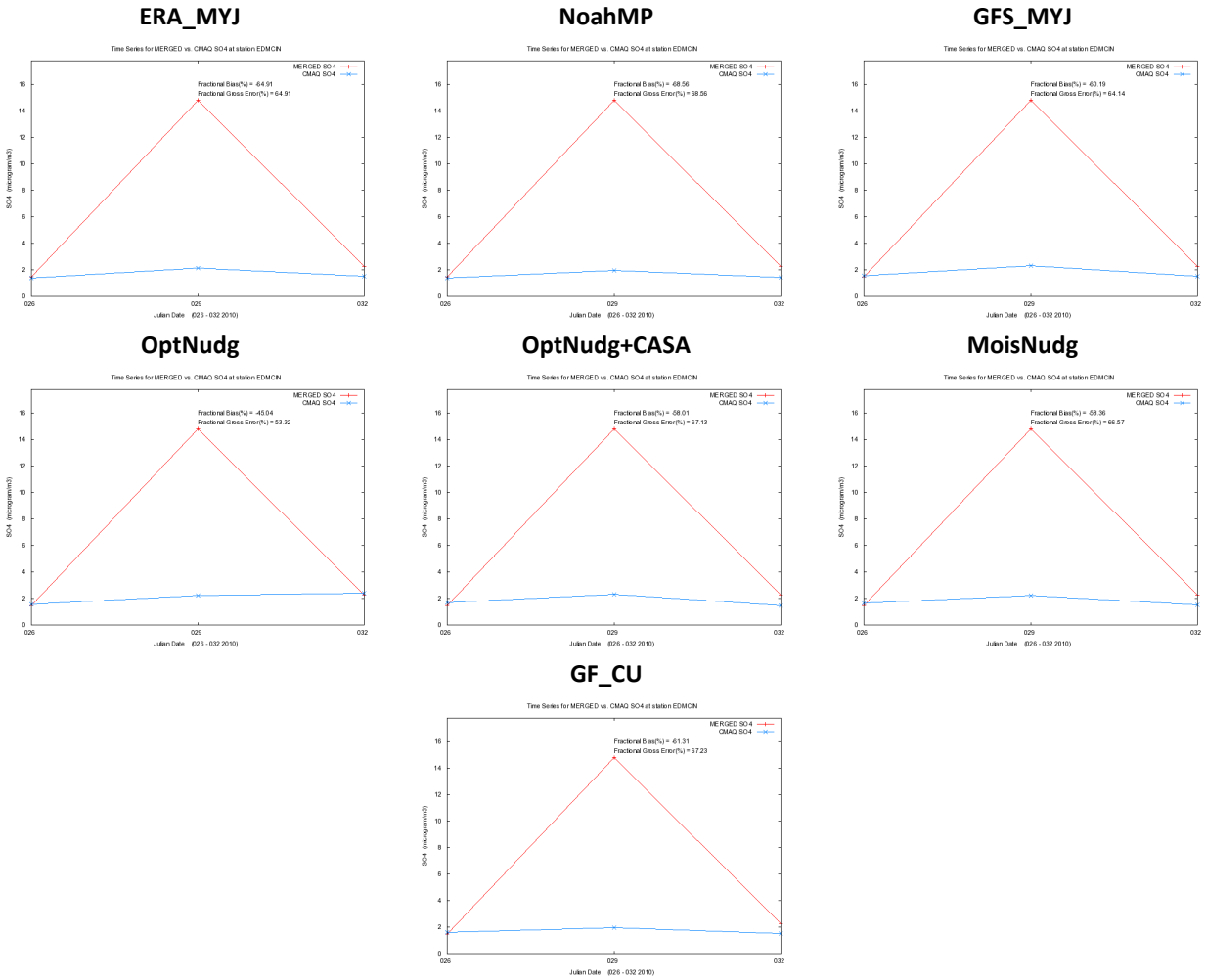

Figure 5-12. WRF Phase II A and WRF Phase II-B Episode#2 time series for 24-hour sulphate concentrations at the Edmonton McIntyre monitoring site

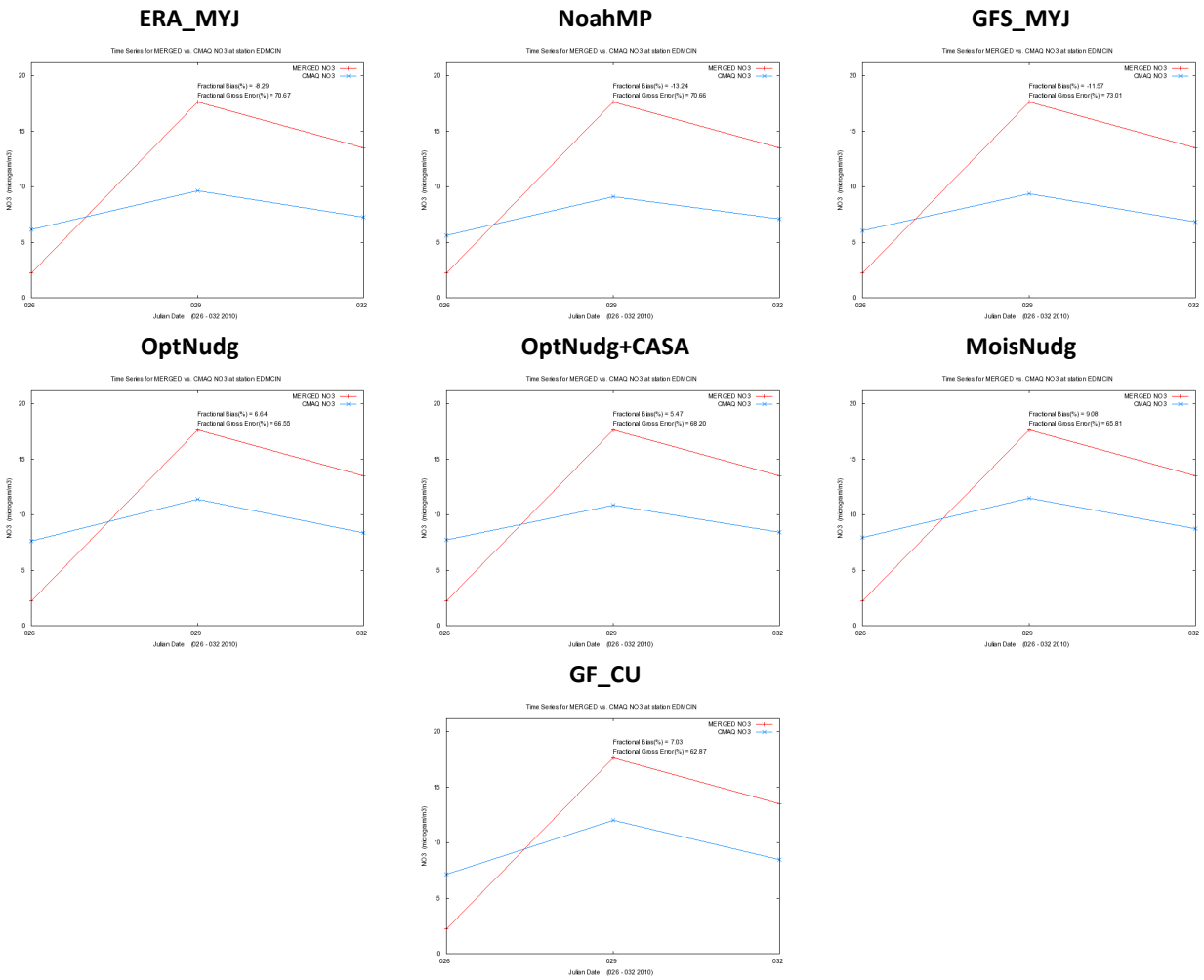

Figure 5-13. WRF Phase II A and WRF Phase II-B Episode#2 time series for 24-hour nitrate concentrations at the Edmonton McIntyre monitoring site.

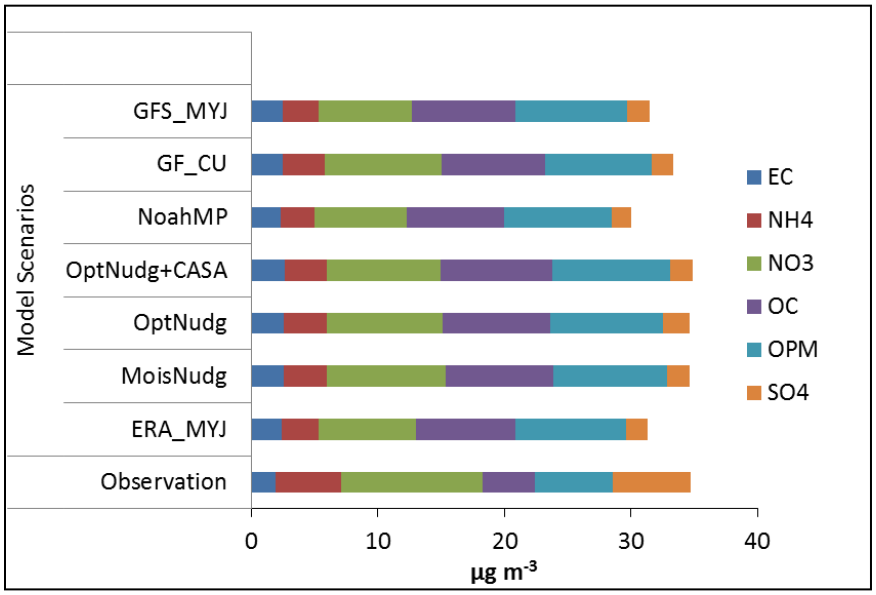

Figure 5-14. Comparisons of three-day average observations to CMAQ predictions using WRF Phase II-B output at the Edmonton McIntyre monitoring site during Episode#2.

5.5 Conclusion of Diagnostic Analyses

Phase I CMAQ setup showed some promise with elevated secondary $PM_{2.5}$ concentrations, but there were also several issues and concerns. Specifically, all PM species except nitrate were overstated.

In this Phase II study, we first revisit WRF setup with a major goal in improving moisture field performance. The WRF meteorological inputs were very important and sensitivity modeling using different analysis field for boundary conditions and PBL scheme identified the ERA-MYJ as performing better than other alternative setup. Sulphate performance is improved significantly due to less cloud availability from all four WRF simulations (Phase II-A).

As we progressed through the diagnostic tests, it was clear that key contributors to each PM species were disconnected and each diagnostic test would need to target individual species. OC and EC performances are driven by surface emissions, although by different source sectors. Specifically, removing off-road equipment emissions not expected to operate in winter improves EC performance dramatically. Revising allocation methodology of residential wood combustion emissions improves OC performance throughout Episode#2. In addition to the surface emissions, vertical diffusion can also impact accuracy of OC and EC (and other primary PMs) predictions.

Nitrate predictions are improved, although they are still understated. The conditions during winter (e.g., stagnant, temperature below zero degree Celsius) in the Capital Region make it difficult to have sufficient radicals for the conversion of NO_X to N_2O_5 which can further convert to nitrate. During Episode#2, ozone in the City of Edmonton was less than 10 ppb, mostly less than 5 ppb, due to excess NO_X that titrates ozone. We confirmed our finding from Phase I that

nitrate formation conditions in the Capital Region during high PM episodes is HNO_3-limited, not ammonia-limited. We believe that pathways that can covert NO_X directly to HNO_3 without relying on availability of radicals are important in the Capital Region winter conditions. The pathways are likely not important in summer because of lower NO_X concentrations and abundant availability of radicals. The current heterogeneous reaction of NO_2 to HNO_3 in CMAQ could be understated but there may be other pathways that are missing in CMAQ.

Ammonium performance was not discussed but we expect its performance to follow that of nitrate.

6.0 SUMMARY AND RECOMMENDATIONS

ENVIRON International Corporation and Stantec (ENVIRON/Stantec) performed the Formation of Secondary $PM_{2.5}$ in the Capital Region during winter months for the Alberta Environmental and Sustainable Resources Development (ESRD). The objective of the study is to develop a Photochemical Grid Model (PGM) modelling database for the Capital Region, which includes Edmonton and surrounding communities, that reproduces the observed winter elevated $PM_{2.5}$ concentrations sufficiently well that it can be a reliable tool for analyzing source contributions to elevated $PM_{2.5}$ concentrations. This is a follow-on study to the Capital Region Particulate Matter Air Modelling Assessment study led by ENVIRON (Phase I) and is based in a large part on the Phase I modelling database and the recommendations in the final report (Nopmongcol et al., 2014). Modelling inputs developed in the Phase I were for the Community Multiscale Air Quality (CMAQ) modelling system. We used this CMAQ input database to conduct air quality model simulations.

Several sensitivity tests were performed to determine the optimal modelling configuration by evaluating the results against measurement data. We revisit two key components of the modeling inputs – meteorology and emissions. Several updates were identified and the CMAQ model was applied to determine contributing factors of high PM concentrations in the Capital Region. The resultant modelling technology will be provided to Alberta Environment for use in assisting them in air quality management.

6.1 Revision of Modelling Inputs

6.1.1 Emissions Inputs

The study also introduced improvements to the Phase I emissions inventory including: (1) updates of 2010 emissions to large point sources in the Capital Region, (2) refinement of Edmonton on-road mobile emissions based on information provided by the City of Edmonton (CALMOB6 data) with ammonia emissions in the 4 km domain, (3) removal of off-road equipment emissions not expected to operate in winter, and (4) improvement of spatial distributions of residential wood combustion emissions.

The SMOKE emissions modelling system was used to generate the hourly, gridded, speciated CMAQ model-ready emissions inputs for January-February, 2010 period

6.1.2 Meteorological Inputs

This study revisit the WRF meteorology used in the Phase I modeling and applied the WRF meteorological model using alternative setups. An initial set of WRF sensitivity simulations was designed to improve meteorological performance over Phase I. We discovered that an overabundance of low-level cloudiness – caused by observation nudging artifacts – led to large sulphate over-predictions and therefore poor $PM_{2.5}$ performance in the CMAQ model. All Phase II-A WRF simulations improved upon Phase I by correcting these erroneous cloud cover fields. Although model performance was similar among the four Phase II-A WRF simulations, we selected the ERA+MYJ simulation due in part to better wind speed and temperature

performance. This simulation also performed best in terms of $PM_{2.5}$ composition at the McIntyre monitor and total $PM_{2.5}$ concentrations.

Using the Phase II-A ERA+MYJ simulation as a baseline configuration, we further tested additional six configuration options: 1) Noah-MP LSM, 2) GFS analyses for IC/BC/analysis nudging dataset, 3) larger nudging coefficients, 4) observation nudging of moisture, 5) Grell-Freitas cumulus parameterization, and 6) observation nudging to CASA monitors. Performance among the six WRF sensitivity tests in Phase II-B is very similar. The GFS simulation was the only run that differed slightly from the others during the stagnant period of January 28-29, which indicates that the coarse IC/BC dataset is difficult to overcome.

6.2 Diagnostic Evaluation

Our initial CMAQ simulations based on the new WRF meteorology conditions showed some promise with significant improvements of sulphate predictions, but there were also several issues and concerns. We discussed the initial CMAQ results with the ESRD and agreed to focus on diagnostic evaluation to improve CMAQ model performance rather than performing extended base case simulations with questionable model performance results. We performed several sensitivity tests to determine the optimal modelling configuration by evaluating the results against measurement data. The sensitivity tests focus primarily on the model performance based on Episode #2 covering January 26-February 4, 2010 that included the multiple days with exceedances of the $PM_{2.5}$ CWS.

6.2.1 Sensitivity Test Results

Multiple sensitivity simulations were conducted to find an optimal CMAQ setup for winter PM modelling. These sensitivity tests were designed to investigate specific issues associated with the CMAQ model performance from the Phase I base case simulation. In the Phase I, the CMAQ model performance during the winter PM episodes in the Capital Region was characterized by an underestimation of nitrate (NO_3) and an overestimate of other species, especially sulphate (SO_4). The Phase II study improves model performance of all major PM species (i.e., NO_3, SO_4, OC and EC) via targeted sensitivity tests:

<u>WRF</u>

- The WRF meteorological inputs were very important and sensitivity modeling using different analysis field for boundary conditions, PBL scheme, and nudging strength identified the ERA_MYJ with strong nudging coefficients as performing slightly better than other nine WRF simulations performed.
- Both sulphate and nitrate performances are improved with the new WRF outputs.

<u>Sulphate</u>

- Sulphate performance is improved significantly with the new WRF simulations due to less cloud availability but sulphate on the peak day is underestimated by a factor of 7.

- CMAQ-predicted sulphate concentrations are in agreement with observations on non-peak days.
- Similar performances of primary PMs among all WRF scenarios support that better sulphate improvement is driven by chemistry, not due to dispersion.

Nitrate

- Moving N_2O_5 hydrolysis to gas-phase module is not effective because the time steps of gas-phase and aerosol-phase are similar at the 4 km resolution.
- Nitrate is less responsive to changes in vertical mixing than OC and EC.
- Abundant NO_X during high PM episodes in Edmonton limits ozone availability during the same period, hence limits reactions that rely on availability of radicals.
- Pathways that can convert NO_X to HNO_3 without relying on availability of radicals will be important in the Capital Region winter conditions. These pathways are likely not important in summer because of lower NO_X concentrations and abundant availability of radicals.
- The current heterogeneous reaction of NO_2 to HNO_3 in CMAQ could be understated but there may be other pathways that are missing in CMAQ.

EC

- EC emissions were overstated in the initial CMAQ runs. We would expect very little off-road equipment emissions related to agriculture, lawn & garden, and mining & constructions during these winter episodes so they were set to zero. This emissions update improves EC performance significantly.
- Increasing or reducing the maximum $K_{v,min}$ that aims to promote night-time mixing by a factor of two changes EC four-day average concentrations by 17-20%.

OC

- OC emissions were overstated in the initial CMAQ runs. Residential Wood Combustion (RWC) is the main source of primary OC in the Capital Region; however, we would expect these emissions to be dominated in the rural areas. Reallocating these emissions based on rural housing spatial distribution improves the four-day average concentration by about 22%.
- OC and EC show a similar response to the maximum $K_{v,min}$.

6.2.2 Phase I versus Phase II

The Phase II study designed several diagnostic tests that target individual PM species. By doing so, we were able to improve CMAQ PM performance significantly and effectively. Figure 6-1 presents PM speciation contributions by specie as predicted by the CMAQ model in Phase I and Phase II[9] and compares to the observations during the same period at the Edmonton McIntyre

[9] Based on the CMAQ results from OptNudg simulation described in Section 5.4.8

site. All species except other PM (OPM)[10] see positive improvements. CMAQ performances of OPM as well as NH_4 are expected to improve when CMAQ can better replicate nitrate and sulphate concentrations during these high PM episodes.

With the primary PM being overstated and the secondary PM being underestimated, it is less meaningful to examine $PM_{2.5}$ mass performance due to compensation effects among PM species. However, it is important to note that $PM_{2.5}$ performance during Episode#2 from the Phase II CMAQ simulation is improved and the improvements are for appropriate reasons (Figure 6-2).

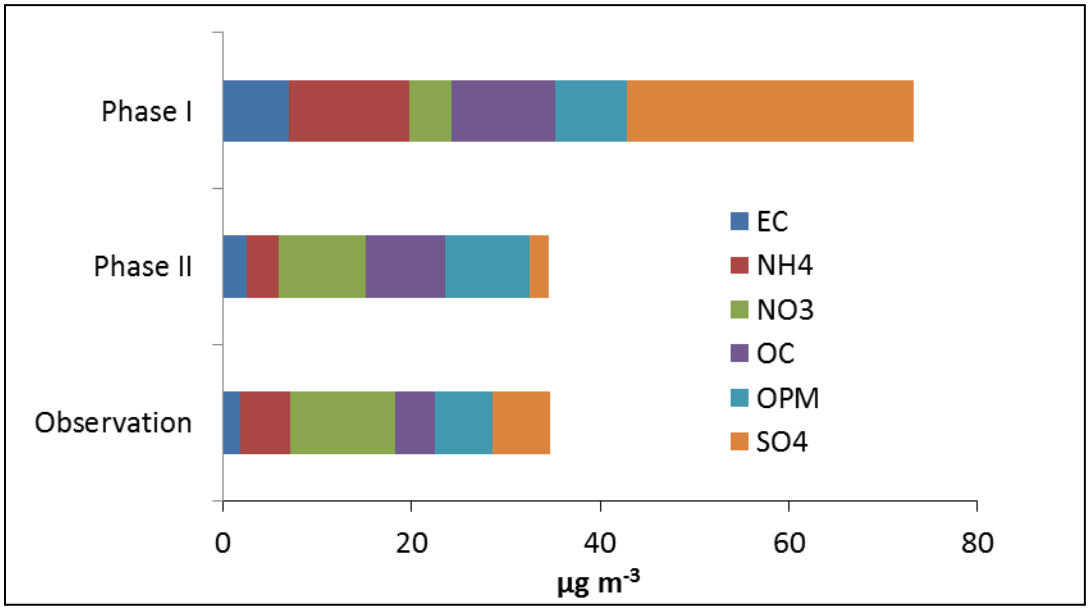

Figure 6-1. Comparisons of three-day average observations to CMAQ predictions in Phase I and Phase II at the Edmonton McIntyre monitoring site during Episode#2.

[10] OPM = Total $PM_{2.5}$ – NO_3 – SO_4 – NH_4 – EC - OC

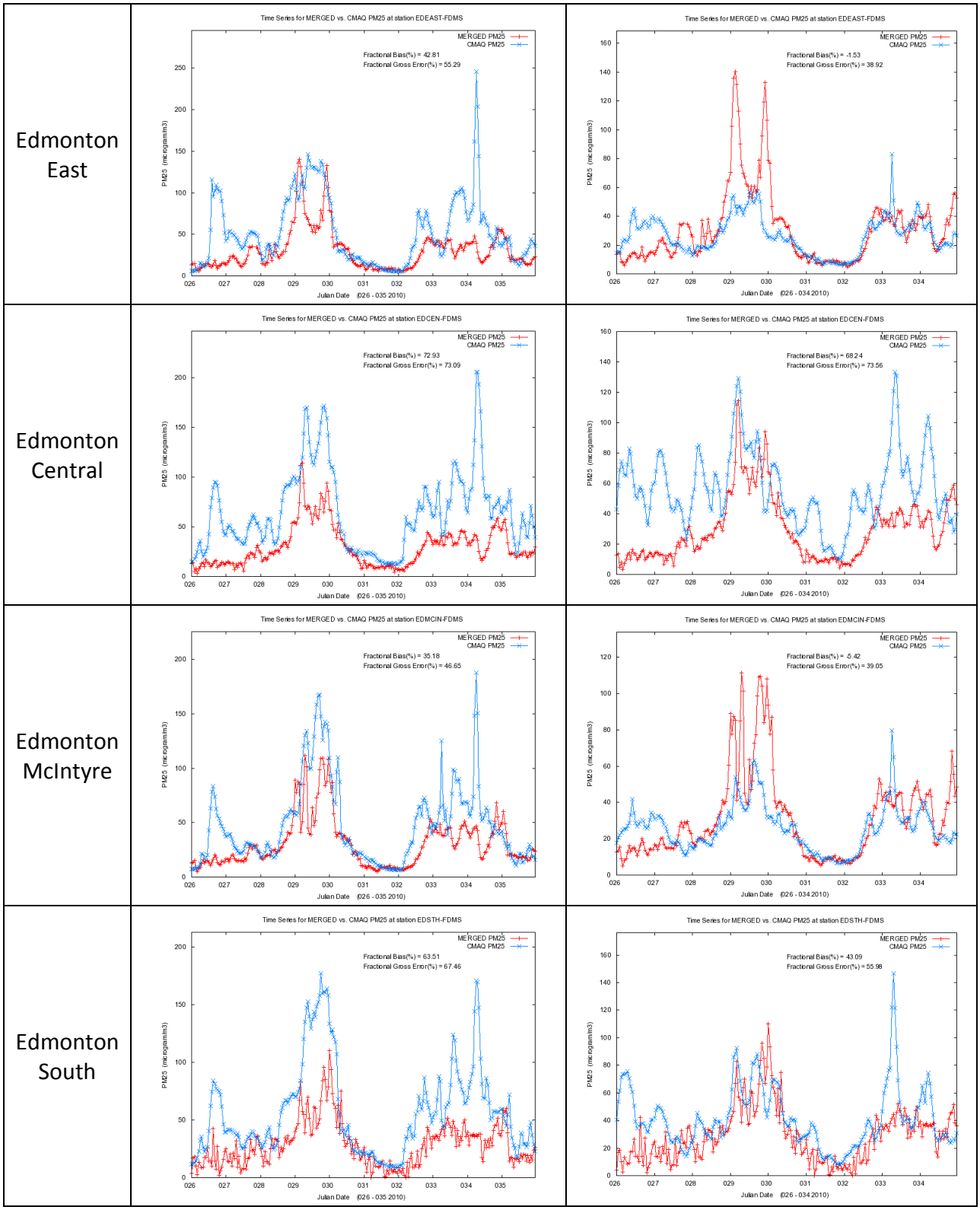

Figure 6-2. Comparisons of $PM_{2.5}$ observations to CMAQ predictions in Phase I and Phase II at the Edmonton McIntyre monitoring site during Episode#2.

6.3 Uncertainties and Limitations

There are several limitations and sources of uncertainties associated with the modelling results of this study, including the meteorology, the emission inventory estimates and the air quality modelling.

Regarding the meteorology, while the overall 2010 WRF model performance conducted in Phase II appears reasonable and shows major improvement of moisture field compared to the Phase I WRF performance, the model could not replicate low wind speed (approaching zero) especially during PM episode days.

Emissions are a critical component of the air quality modelling. We highlight some of the key limitations and uncertainties with regards to the emission inputs including the following:

- Emission inventory development – Emission inputs used in this study were based on the Phase I Capital Region emissions inventory with several updates. Revision of RWC emissions provides promising results but the RWC emissions are still likely overstated.
- Emission modelling – Uncertainties and limitations in the emissions modelling for the study include the speciation of VOC emissions as well as the temporal and spatial allocation of the emission inventory. In particular, the spatial allocation of regional emission estimates introduces additional limitations with respect to the modelling inventories used for the study. In the non-stationary sources, estimates at the Provincial level were allocated to grid cells using spatial surrogates developed for the entire province. For certain emission source sectors, this could result in allocation of these emissions to erroneous areas of the modelling domain and/or artificially spreading these emissions across for broader regions than is realistic. There are also uncertainties related to the Shapefiles used in developing these spatial surrogates.
- Some of the industrial point sources will have episodic emissions (e.g., fugitives) that are not captured by the average emissions used in the modelling

As is true for any grid-based chemical transport model, such as CMAQ used in the current study, a number of inherent limitations and uncertainties are present. These include uncertainties in the chemical speciation of input data and inherent assumptions with respect to the chemical mechanism implementation in the model, as well as uncertainties and biases associated with meteorology, transport and deposition of modelled pollutants. Moreover, there remains uncertainty in the treatment of aqueous chemistry, aerosol thermodynamics, and rates of removal of PM and gaseous species by wet and dry deposition. The winter PM episode temperature conditions fall outside of the range that the CMAQ parameterization of HNO_3 formation through heterogeneous N_2O_5 reactions were developed for. Due to limited radicals available and access NO_X, HNO_3 formation through heterogeneous reactions is dominated by NO_2 reaction over N_2O_5 reaction in CMAQ. CMAQ may be missing similar pathways that can similarly convert NO_X directly to HNO_3 without relying on radical availability. There are also errors and biases in the monitoring data that were used in the MPE, which in some cases may be as large as, or larger than, the modelled biases for certain species, particularly PM species.

6.4 Conclusions and Recommendations

The development of a photochemical modelling database usually involves the performance of diagnostic model simulations designed to refine the model inputs and configuration to improve model performance. The Phase II study designed several diagnostic tests that target individual PM species. By doing so, we were able to improve CMAQ PM performance significantly and effectively. However, the CMAQ PM model performance still shows over-prediction of primary PM species such as EC and OC but under-prediction of secondary PM such as nitrate and sulphate.

The following recommendations are made with respect to improvements to the CMAQ 2010 January-February modelling database.

6.4.1 Meteorological Inputs

WRF meteorological performance could be further improved by reducing wind speed bias during stagnant periods and increasing cloud cover. Future WRF sensitivity tests designed to address these issues could include:

- Removing analysis and observation nudging selectively to determine their individual effects on wind speed.
- Investigating use of Environment Canada observation data for nudging, possibly through ESRD.
- Further changes to observation nudging parameters (radius of influence, nudging time window, etc.)

6.4.2 Emission Inventory

- Conversion of the primary emitted NO_X to gaseous nitric acid (HNO_3) relies on reactivity of the atmosphere. Specifically, the model will need more active radicals from VOC and/or background ozone. VOC speciation profiles from on-road mobile and refinery should be reviewed to ensure proper allocation of VOC to model species.
- Hot spots generally occur near emitting sources such as high SO_2 concentrations occurring near refineries sources. Emissions of these facilities should be reviewed to ensure correctness of the emissions inputs.
- Primary PM emissions and their spatial/temporal allocations should also be reviewed. Despite reallocating residential wood combustion to rural housing spatial distribution, the model still over-estimated OC. We note that several grid cells in the city of Edmonton were designated as having partly rural housing. The rural housing spatial surrogate should be reviewed and corrected if necessary.
- High ambient NO_X concentrations (particularly NO) on high PM days at multiple Edmonton monitors suggest that the stagnant air trapped surface NO_X emissions at ground level. It may also suggest that the cold temperature effect on light-duty vehicle emissions is significant because the catalyst needs time to heat up and will cool off quickly. Figure 6-3 below demonstrates that start NO_X emissions are approximately 10

times higher with winter conditions for new vehicles. Similar temperature effect may be applicable to particulate nitrate. On-road emissions should be revisit to ensure that the cold temperature effects are sufficiently accounted for.

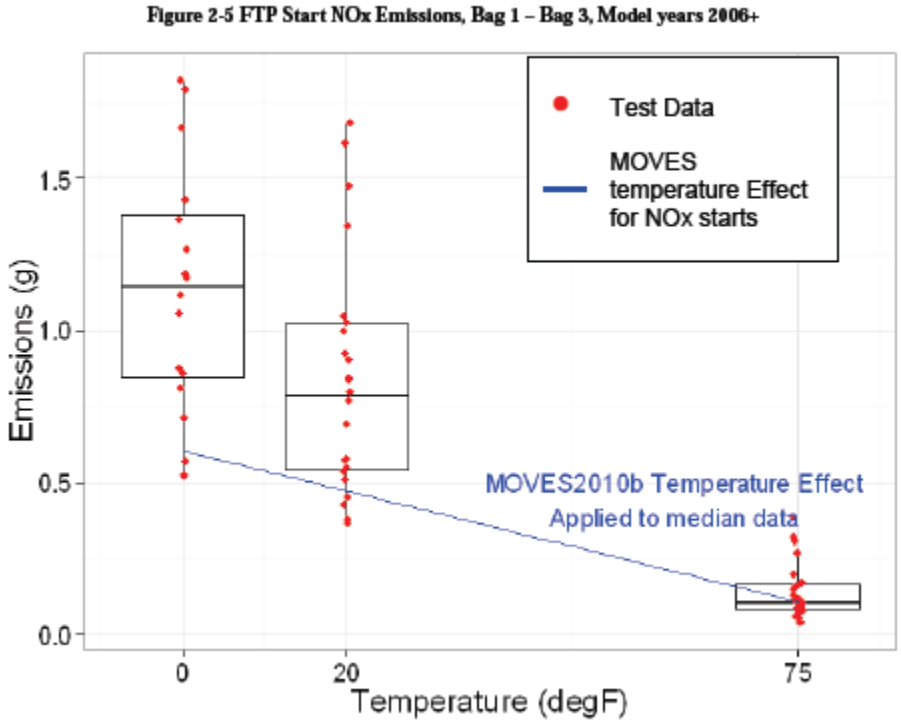

Figure 6-3. Temperature effects of start NO_X emissions in MOVES2010b model (Source: USEPA, 2014a)

6.4.3 Diagnostic Sensitivity Tests

The same winter period should be investigated further through PGM to identify model options that could improve PM model performance, such as:

- Emission sensitivity tests, such as increasing anthropogenic VOC emissions.
- Sulphate under-estimation may be related to model resolution. Unlike nitrate, there were not many days during January-March, 2010, period that sulphate was elevated. High sulphate events may be associated with SO_2 plumes from industrial sources transported over Edmonton McIntyre site. The Phase II simulations were run at 4 km resolution which could artificially dilute SO_2 emissions from elevated sources. Increase the resolution to 1.33 km may help address this issue.
- Additional vertical mixing tests are recommended as the primary PMs are sensitive to the vertical mixing. The overestimation of primary emitted species (e.g., EC and OC), may indicate insufficient vertical mixing. As shown in Figure 6-4, the vertical diffusion

coefficient at Edmonton East on January 28 is set to 0.01 m^2/s at night because the relevant grid cell is designated as 100% rural area. The effects of the urban heat island on vertical mixing in Edmonton are likely not fully accounted for in the WRF/CMAQ modelling and the landuse data used by CMAQ should be reviewed.

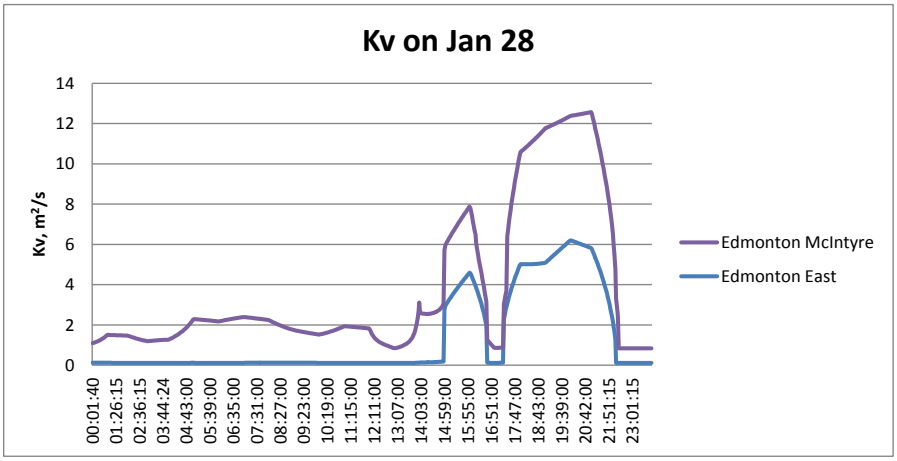

Figure 6-4. CMAQ-estimated vertical diffusion coefficient (m^2/s) at two Edmonton sites on January 28, 2010

- The CMAQ default heterogeneous chemistry rate of NO_2 maybe under-estimated. Further literature review on the effects of meteorology to this reaction is recommended.
- Further literature review on alternative pathways that can convert NO_X to HNO_3 without relying on availability of radicals is recommended. These pathways are likely not important in summer because of lower NO_X concentrations and abundant availability of radicals.
- Deposition process removes HNO_3 and its pre-cursors from the ambient air. If CMAQ overstates deposition velocities of these pollutants, then their predicted ambient concentrations can be underestimated. CMAQ should be run with in-line deposition velocity diagnostic file option turned on and deposition velocities of relevant species should be examined.

Finally, future modelling exercise should expand to cover more PM episodes. With the primary PMs being highly overstated and the secondary PMs being underestimated, it is less meaningful to examine $PM_{2.5}$ mass performance in the current study. We believe that the overestimation of OC and EC is related to overstated emissions and diagnostic tests suggested above will help address the issue. Then, $PM_{2.5}$ mass performance evaluation will be helpful because there are more data points (i.e., hourly resolution, multiple monitors) than the speciation measurements.

7.0 REFERENCES

Boylan, J.W. and A.G. Russell. 2006. PM and Light Extinction Model Performance Metrics, goals and Criteria for Three-Dimensional Air Quality Models. Atmos. Env. 40:4946-4959.

Davis, J.M., P.V., Bhave, and K.M., Foley. 2008. Parameterization of N2O5 Reaction Probabilities on the Surface of Particles Containing Ammonium, Sulphate and Nitrate. Atmos. Chem. Phys., 8, 5295-5311. http://www.atmos-chem-phys.net/8/5295/2008/acp-8-5295-2008.html

Environment Canada (EC). 2014. Documentation for SMOKE-Ready 2010 Canadian CAC Emissions Inventory Package - Version1, REPORT # AQSC-14-007. July.

Idriss, A. and F. Spurrell. 2009. Air Quality Model Guideline. Alberta Environment, Climate Change, Air and Land Policy Branch, Edmonton, Alberta. (http://environment.gov.ab.ca/info/library/8151.pdf). May.

Jiang, W., S. Smyth, E. Giroux, H. Roth and D. Yin. 2006. Differences between CMAQ Fine Mode Particle and $PM_{2.5}$ Concentrations and their Impact on Model Performance Evaluation in the Lower Fraser Valley. *Atmos. Env.* 40 (2006) 4973-4985.

Kurtenbach, R., Becker, K.H., Gomes, J.A.G., Kleffmann, J.,L. Orzer, J.C., Spittler, M., Wiesen, P., Ackermann, R.,Geyer, A., Platt, U. 2001. Investigations of emissions and heterogeneous formation of HONO in a road traffic tunnel. Atmospheric Environment 35, 3385–3394.

Morris, R.E., B. Koo, B. Wang, G. Stella, D. McNally and C. Loomis. 2009a. Technical Support Document for VISTAS Emissions and Air Quality Modelling to Support Regional Haze State Implementation Plans ENVIRON International Corporation, Novato, CA and Alpine Geophysics, LLC, Arvada, CO. March.

Morris, R.E., B. Koo, S. Lau, D. McNally, T.W. Tesche, C. Loomis, G. Stella, G. Tonnesen and C-J. Chien. 2004b. VISTAS Phase II Emissions and Air Quality Modelling – Task 4a Report: Evaluation of the Initial CMAQ 2002 Annual Simulation. Prepared by ENVIRON International Corporation, Alpine Geophysics, LLC, and the University of California, Riverside (CE-CERT). Prepared for the VISTAS Technical Analysis Committee. September.

Morris, R.E., B. Koo, S. Lau, T.W. Tesche, D. McNally, C. Loomis, G. Stella, G. Tonnesen and Z. Wang. 2004a. VISTAS Emissions and Air Quality Modelling – Phase I Task 4cd Report: Model Performance Evaluation and Model Sensitivity Tests for Three Phase I Episodes. Prepared by ENVIRON International Corporation, Alpine Geophysics, LLC, and the University of California, Riverside (CE-CERT). Prepared for the VISTAS Technical Analysis Committee.

Morris, R.E., B. Koo, T. Sakulyanontvittaya, G. Stella, D. McNally, C. Loomis and T.W. Tesche. 2009b. Technical Support Document for the Association for Southeastern Integrated Planning (ASIP) Emissions and Air Quality Modelling to Support PM2.5 and 8-Hour Ozone State Implementation Plans. ENVIRON International Corporation, Novato, CA and Alpine Geophysics, LLC, Arvada, CO. March 24.

Nopmongcol, U., J. Jung, J. Zagunis, T. Shah, R. Morris, T. Pollack, W. Allan, X. Qiu, N. Walters and F. Yang. 2014. Capital Regional Particulate Matter Air Modeling Assessment – Final Report. Prepared for David Lyder, Alberta Environment and Sustainable Resources Development. Prepared by ENVIRON (EC) Canada, Inc., Mississauga, ON and ENVIRON International Corporation, Novato, CA.

Simon, H., K.R. Baker and S. Phillips. 2012. Compilation and interpretation of photochemical model performance statistics published between 2006 and 2012, *Atmos. Environ.*, 61, 124-139.Skamarock, W.C., J.B. Klemp, J. Dudhia, D.O. Gill, D.M. Barker, M.G. Duda, X-Y Huang, W. Wang, J.G. Powers. 2008. "A Description of the Advanced Research WRF Version 3." NCAR Technical Note, NCAR/TN-45+STR (June 2008). http://www.mmm.ucar.edu/wrf/users/.

USEPA. 1991. Guidance for Regulatory Application of the Urban Airshed Model (UAM). Office of Air Quality Planning and Standards, U.S. Environmental Protection Agency, Research Triangle Park, NC.

USEPA. 2007. Guidance on the Use of Models and Other Analyses for Demonstrating Attainment of Air Quality Goals for Ozone, PM2.5 and Regional Haze. U.S. Environmental Protection Agency, Research Triangle Park, NC. EPA-454/B-07-002. April.

USEPA. 2014a. Emission Adjustments for Temperature, Humidity, Air Conditioning, and Inspection and Maintenance for On-road Vehicles in MOVES2014. U.S. Environmental Protection Agency, Research Triangle Park, NC. EPA-420-R-14-012. December.

USEPA. 2014b. Draft Guidance on the Use of Models and Other Analyses for Demonstrating Attainment of Air Quality Goals for Ozone, PM2.5 and Regional Haze. U.S. Environmental Protection Agency, Research Triangle Park, NC. December. (http://www.epa.gov/ttn/scram/guidance/guide/Draft_O3-PM-RH_Modeling_Guidance-2014.pdf).

ENVIRON

APPENDIX A

Review and Updates to Industrial Point Source Emission Inventory

Appendix A. Review and Updates to Industrial Point Source Emission Inventory

Stantec completed a review of industrial point source emissions in the 2010 EC emission inventory to determine completeness and accuracy of the inventory compared to other available data sources. The review was focused on industrial emission sources within Alberta and included comparing inventory data with facility stack and emission information obtained from Environmental Impact Assessments (EIAs), emission inventories developed for industry groups (e.g., CEMA) and government data sources such as facility approvals (Environmental Protection and Enhancement Act Approvals) and facility emission totals reported to NPRI.

A number of QA/QC checks were undertaken for all significant industrial emission sources within the inventory; however, the primary focus was on reviewing and correcting stack and emission parameters for industrial facilities located in and near the Capital Region. These include:

- Reviewing emission rates for all of the significant industrial and UOG oil and gas facilities with large emission rates and comparing with emission data reported to NPRI for 2010.
- Reviewing the locations of the emission sources were confirmed using mapping tools such as latitudes and longitudes of facilities reporting to NPRI, locations of facilities noted in EPEA approvals, satellite imagery to confirm project locations, and stack locations obtained from EIAs.
- The emission inventory was reviewed for logical consistency to ensure values such as stack heights, diameters, exhaust temperatures, and velocities were within the range of typical values for each source type.
- A review of SCC codes for major industrial facilities to ensure that the SCC code is consistent with the type of facility.

The review indicated that the point source emission inventory was deficient in a number of areas including incorrect facility locations, missing and incorrect stack and exhaust parameters, and emission rates inconsistent with NPRI. Enhancements to the industrial emission inventory were made to correct errors and fill information gaps. These enhancements include:

- There were significant errors and omissions to the 2010 EC inventory for the entire oil sands component of the emission inventory. For example, the inventory contained emission data for oil sands projects that do not exist such as the Synenco Northern Lights Mine, the Suncor Fort Hills Mine, the Total Joslyn Mine and the Imperial Oil Kearl Mine. While the Kearl Project does exist, it did not in 2010. It was determined that it was necessary to remove the oil sands sector sources from the 2010 EC inventory and replace it with the oil sands sector emission inventory prepared for CEMA, consistent with the Capital Region PM Modelling Study Phase 1 Inventory.
- For the non UOG emission sources in and near the Capital Region, the review indicated a need to correct a few facility locations including the ATCO Battle River Generating Station and Shell Scotford Upgrader.

- For many of the significant non UOG emission sources, stack height, diameter, exhaust flow rate and temperature were missing or were incorrect. Based upon highly detailed emission inventories prepared for EIA and based upon facility EPEA approvals, missing stack details were added or corrected in the 2010 EC inventory for approximately 100 facilities.
- Facilities with major shutdowns or temporal variation in emissions during 2010 were identified so that emissions could be apportioned to only the months the facility operated. These included the permanent shutdown of the Transalta Wabamun Power Station in April of 2010 and the shutdown of the Shell Scotford Upgrader from mid-March to end of May during a major maintenance turnaround.
- All of the natural gas, coal and diesel fuel fired power generating facilities in Alberta were identified and correct SCC codes for these sources were applied.
- For the UOG sources, the emission inventory was reviewed to first identify major emission sources. All of the large sour gas plants with high SO_2 emissions were identified and compared against emissions reported to NPRI for 2010. Substantial differences were noted requiring that emission rates for SO_2 be updated for all major sour gas processing facilities.
- The entire UOG emission inventory did not include any stack parameters. For large sour gas plants, generic stack parameters were included to represent a typical tail gas thermal oxidizer stack. For combustion source emissions at the remaining UOG facilities including compressor stations, small gas plants and battery facilities, generic stack parameters were applied typical of small heaters and reciprocating engines. No stack parameters were applied for SCC codes associated with fugitive emission including well casing vents, production tanks, leaking components, crude oil loading, tank venting and storage and transport of hydrocarbons.